

Aus der Abteilung Anatomie und Embryologie  
(Prof. Dr. med. C. Viebahn)  
im Zentrum Anatomie  
der Medizinischen Fakultät der Universität Göttingen

---

# **Morphological and molecular studies of germ layer differentiation in the early mammalian embryo**

INAUGURAL – DISSERTATION  
zur Erlangung des Doktorgrades

der Medizinischen Fakultät  
der Georg-August-Universität zu Göttingen

vorgelegt von

**Romia Hassoun**

aus

Latakia-Syrien

**Göttingen 2009**

Dekan: Prof. Dr. med. C. Frömmel

I. Berichterstatter: Prof. Dr. med. C. Viebahn

II. Berichterstatter/in:

III. Berichterstatter/in:

Tag der mündlichen Prüfung:

## Contents

<b>1. Introduction</b> .....	1- 4
<b>2. Summarised representation of the material and methods</b> .....	5- 6
2.1 Animal tissue.....	5
2.2 Fixation for morphological and molecular analysis .....	5
2.3 Morphological analysis.....	6
2.4 Molecular analysis.....	6
<b>3. Summarised representation of the results</b> .....	7- 10
<b>4. References</b> .....	11- 14
<b>5. Copies of the publications</b> .....	15
5.1 The first publication: Axial differentiation and early gastrulation stages of the pig embryo.....	16- 26
5.2 The second publication: Sox17 expression patterns during gastrulation and early neurulation in the rabbit suggest two sources of endoderm formation. ....	27- 43
<b>6. The manuscript: Germ layer differentiation during early hindgut formation in the rabbit and pig embryo</b> .....	44- 66
<b>7. Acknowledgements</b> .....	67
<b>8. Curriculum Vitae</b> .....	68

## 1. Introduction

Human prenatal development is divided arbitrarily into two periods. During the embryonic period, which lasts from fertilisation until the end of the 8th week of development, the conceptus develops through specific stages such as blastocyst formation, gastrulation, neurulation and organogenesis. During the fetal period, which lasts from the end of 8th week of development until the birth, the organs that appeared in the preceding embryonic period develop further, structurally and functionally, following markedly different time schedules. Both the embryonic and fetal periods of development are accomplished by basic developmental processes such as cell proliferation, cell differentiation, coordinated (morphogenetic) cell movement, as well as programmed cell death (apoptosis). During the cell differentiation process the cell's size, shape, biochemistry and, subsequently, the cell function change largely due to a highly-controlled gene regulatory network. Thus, each specialised cell type expresses a subset of the genes that constitute the genome of that species i.e., each cell type is defined by its particular pattern of regulated genes. The morphological differentiation of cells during early embryonic development is the subject of many publications (in mouse; Tam et al. 1993; Downs and Davies 1993, in rabbit; Viebahn 1999 and in pig Barends et al. 1989). On the other hand, defining the signaling pathways involved in regulating cell differentiation (s. Ang and Constam 2004; Tam et al. 2006 for reviews) is important for understanding the mechanisms that lead to the findings observed in the morphological studies.

A common characteristic in early development of many animal species is the generation of germ layers, a typical example of forming early embryonic compartments, during the gastrulation phase. In principle, the gastrulation process follows three major aims: (1) establishing of the internal milieu of the early vertebrate embryo by formation of three germ layers (ectoderm, mesoderm and endoderm); (2) definition of the main body axes, namely the anterior-posterior (head-tail) and, consequently, the left-right axes; and (3) laying down the arrangement of the organ anlagen and thus the construction of the principal body plan. In amniotes the origin of the germ layers goes back to the epiblast, which is itself one of the two cell layers (the

epiblast and the hypoblast) originating from the so called inner cell mass (Gardner and Rossant 1979). The epiblast is, thus, the sole source of the germ layers (and hence of all fetal tissues both somatic and germline) and, also, forms the amnion epithelium and most of the extraembryonic mesoderm (Rossant et al. 1978; Gardner 1985; Beddington RS et al. 1989; Lawson and Pedersen 1992). Experiments in which murine epiblasts were transferred to ectopic sites demonstrated the potency of the epiblast to form derivatives of all three germ layers around which the body plan is constructed (Beddington RS 1985; Svajger et al. 1986), this capacity being present in gastrulating (Levak- Svajger and Svajger 1974; Beddington SP 1981) as well as pre-primitive streak stage embryos (Diwan and Stevens 1976; Levak-Svajger and Svajger 1971).

In the mammalian embryo, too, germ layers and their precursors are useful for sorting the multitude of cells of the early embryo into well defined compartments and for tracing cell and tissue fates destined for specific organs or tissue compartments. However, many gaps in the picture of morphological and molecular germ layer differentiation still exist and require to be studied in order to understand the mechanisms involved in early development of mammalian embryo which, in turn, may form the basis for new medical treatment in reproduction and pathology. Initial and further germ layer differentiation, therefore, forms the main focal points of the two publications as well as the submitted manuscript which are assembled in this doctoral thesis.

In the paper entitled 'axial differentiation and early gastrulation stages of the pig embryo' morphological and molecular characteristics of the hypoblast, the early ventral layer of the embryo, are used to answer the question as to whether the mammalian anterior pregastrulation differentiation (APD) i.e., anterior visceral endoderm (AVE) of the mouse (Rosenquist and Martin 1995) or the anterior marginal crescent (AMC), which is hithero fully described in the rabbit embryonic disc only (Viebahn et al. 1995), exists also in the early gastrulating pig embryo. Because the mouse egg-cylinder and the rabbit flat embryonic disc have distinct structural differences in the APD and in the molecular blueprint of the body plan prior to gastrulation, the pig with its mammotypical flat embryonic disc and its late

implantation schedule (Heuser and Streeter 1929; Patten 1948; Perry and Rowlands 1962) was chosen as a new model organism for laying down general rules in mammalian gastrulation development. Indeed, an anterior axial structure was characterised for the early gastrulating pig embryo, similar to the AMC in the rabbit, and called in this publication the anterior hypoblast (AHB). *Sox17*, an early axis differentiation gene in the mouse, was found to be expressed strongly in the AHB of early pig embryo, too. These results support the data obtained in chick, mouse and in the disc-shaped rabbit embryo that the anterior hypoblast has a central role in development of the anterior structures of the embryo.

Apart from being an anterior marker *sox17* is well known as an important molecule in the signaling pathway involved in regulating endoderm formation, the endoderm being the precursor of the primitive gut tube, which, during organogenesis, gives rise to the epithelia of the gastrointestinal tract, the respiratory tract and associated organs. The role of *sox17* in endoderm differentiation was determined in *Xenopus* (Hudson et al. 1997), zebrafish (Alexander and Stainier 1999) and the mouse (Kinder et al. 2001; Kanai-Azuma et al. 2002). The recent surge in stem cells concepts revived interest in the findings obtained by Gardner and co-workers (Gardner and Rossant 1979; Gardner 1985) that the endoderm itself originates entirely from the epiblast, which since Pander's time (1817) had been held to be the forerunner of the ectoderm and mesoderm layers only. However, the question as to which parts of the mammalian gastrulation-stage embryonic disc generate endoderm cells is still unresolved. The paper entitled '*sox17* expression patterns during gastrulation and early neurulation in the rabbit suggest two sources of endoderm formation', therefore, analyses the question where there are molecular signs of endoderm differentiation along the anterior-posterior axis and uses whole-mount in situ hybridisation and high-resolution histological analysis of the topographic distribution of *sox17* in the rabbit at around gastrulation stages. Whereas *sox17* mRNA was expressed in the one region already known for endoderm formation i.e., in the anterior extremity of the primitive streak, it was, also, found in the posterior extremity of the primitive streak. This suggests a second source, which is described here for the first time, of endoderm formation.

Furthermore and in support of our data obtained in the pig and the data obtained in the mouse, *sox17* was also found in the anterior margin of early rabbit embryonic disc.

The fact that *sox17* is expressed in the posterior end of the primitive streak has drawn attention to the differentiation of the germ layers at the posterior pole of the embryo. The manuscript to be submitted in an international scientific journal entitled ‘Germ layer differentiation during early hindgut formation in the rabbit and pig embryo’, therefore, describes cellular and subcellular characteristics of the germ layers at the posterior pole of mammalian embryos at the light and electron microscopical levels. Such description could help to find out which parts of the endoderm could be populated by the putative posterior source of the endoderm. On the other hand, our description of the topographic rearrangement of the germ layers at the posterior pole of the embryo could be important for the analysis of the intercellular interactions and, thus, the signaling cascades which are responsible to induce the principal differentiation steps in this part of embryo, including cloacal membrane formation. Moreover, explaining the pathogenesis of congenital malformations in the caudal part of the embryo such as anal atresia and cloacal exstrophy that have been studied in mouse (Kluth et al. 1995), chick (Maenner and Kluth 2005) and human (Nievelstein et al. 1998) embryos still requires precise definition of the posterior endoderm differentiation, including the cloacal membrane, which antedates the formation of the external cloaca at early stages of development. This study, therefore, draws up the schedule for cloacal membrane formation in pig and rabbit as mammotypical organisms. Our analysis shows that cloacal membrane formation seems to be similar in morphology but widely divergent with regard to the time of its initiation amongst mammals.

## **2. Summarised representation of the material and methods**

### **2.1 Animal tissues**

Gastrulation and neurulation stages of pig and rabbit embryos were used in this doctoral thesis for a morphological and molecular analysis of germ layer differentiation in mammary typical flat embryonic discs. Late pre-pubertal gilts (German Landrace x Large White) were stimulated using pregnant mare serum gonadotropin, superovulated using human chorionic gonadotropin (hCG) and mated twice with Piétrain boars at the Institute of Animal Science and Behaviour, Mariensee, Germany. The time of the first mating was taken to be the coital time from which embryonic age was calculated. Uteri were removed after slaughter. For obtaining rabbit embryos, uteri of New Zealand White rabbits (Lammers, Euskirchen, Germany) stimulated and naturally mated at the Zentrale Tierexperimentelle Einrichtung der Universitätsmedizin Göttingen were removed through cesarean section after injecting an overdose of a barbiturat anaesthetic agent intravenously. All blastocysts of the pig (between 8.0 and 13.0 days post coitum, d.p.c.) and the young blastocysts of the rabbit (between 6.25 and 6.75 d. p. c.) were flushed from the uterine horns using warm and sterile phosphate buffered saline (PBS). The older embryos of the rabbit, i.e. embryos between 7.0 and 9.5 d.p.c. were dissected from their endometrial attachment in sterile PBS using iridectomy scissors and tungsten needles after opening the uterine wall antimesometrially.

### **2.2 Fixation for morphological and molecular analysis**

For light and transmission electron-microscopical analysis, blastocysts of pig and rabbit were prefixed in a mixture of paraformaldehyde (PFA) and glutaraldehyde (GA) in phosphate buffer followed by postfixation in osmium tetroxide (OsO<sub>4</sub>) in phosphate buffer and embedding in Araldite® (Schwartz et al. 1984). For in situ hybridisation analysis, the blastocysts were fixed at room temperature in (PFA) in phosphate buffer and microdissected as necessary to eliminate most of extraembryonic tissue. The specimens were dehydrated in a graded series of ethanol, frozen in ethanol and stored at -20° C for up to one year or used for in situ hybridisation immediately.



### 2.3 Morphological analysis

OsO<sub>4</sub>-fixed pig and rabbit embryos were photographed as whole-mounts prior to embedding in Araldite® for exact correlation of sections and gross morphology. Complete series of semithin (1 µm) sections were cut using a diamond knife either in the transverse or sagittal plane and stained with methylene blue (Schwartz et al. 1984). At suitable intervals 70 nm sections were cut for transmission-electron-microscopical analysis of regions defined in semithin sections and dorsal views of whole blastocysts taken prior to sectioning. If necessary, selected semithin sections were re-embedded (Viebahn et al. 1995) and sectioned at 70 nm.

### 2.4 Molecular analysis

A digoxigenin-labelled *sox17* mRNA probe used in the two papers was generated from a mouse *sox17* cDNA (GenBank Accession number NM\_011441). The digoxigenin-labelled *brachyury* mRNA probe used to mark the mesoderm formation at the posterior pole of the early pig embryo was generated from a mouse *brachyury* cDNA (GenBank Accession no NM 009309). The *nodal* mRNA probe used to define anterior-posterior axial differentiation in the early pig embryo was generated from pig genomic DNA. In situ hybridisation was carried out for all three genes at 70°C using standard protocols adapted for early rabbit embryonic discs (Weisheit et al. 2002). Hybridised RNA was visualised using anti-digoxigenin antibody coupled to alkaline phosphatase and BM-purple substrate. After staining in BM-purple embryos were photographed and then embedded in Technovit 8100®. The embedded embryos were serially sectioned using glass knives at 5µm in the sagittal or the transverse plane. The reaction product of the in situ hybridisation procedure was analysed using differential interference contrast or, if necessary, with the help of neighbouring methylene blue stained Technovit® sections. Sense cRNA probe were generated as negative controls and used under the same conditions as the antisense probes described above in at least one specimen for every stage and gene examined

### 3. Summarised representation of the results

The first publication entitled ‘axial differentiation and early gastrulation stages of the pig embryo’ used high-resolution light microscopy and transmission electron microscopy as well as in situ hybridisation for analysing the expression patterns of three key genes involved in the early development; *sox17* (Kanai-Azuma et al. 2002; Pfister et al. 2007), *nodal* (Lu and Robertson 2004; Mesnard et al. 2006; Liguori et al. 2008) and the key mesoderm marker *brachyury* (Herrmann 1991, Arnold and Robertson 2009). In this way, two new axial features were identified in the early pig embryo: (1) the anterior hypoblast (AHB) characterised by increased cellular height and density and by *sox17* expression, and (2) mesoderm precursors existed in the epiblast prior to primitive streak formation. The primitive streak itself was found to be characterised by a high pseudostratified epithelium in the posterior epiblast with an unusually thick basement membrane, by localised epithelial–mesenchymal transition, and molecularly by *brachyury* expression. The stepwise appearance of the AHB and the primitive streak and their molecular features was used to define three stages at the start of gastrulation, which may be applicable to mammals in general. The discussion of this paper covers as a main aspect that the anterior pre-gastrulation differentiation (APD) presently known in the mammalian embryo draws its significance from the fact that the transient structures (AVE in the mouse, AMC in the rabbit and AHB in the pig) fix principal body axes by establishing structural cell shape changes at the anterior border of a seemingly symmetrical round embryonic disc early in development. However, the round shape and gradual posterior displacement of the AHB in the pig is different from APD in mouse and rabbit and appears to be species-specific. Moreover, correlation of AHB shape with distribution of early mesoderm in the pig suggests that the APD may be functionally involved in shaping extraembryonic tissues and, possibly, the specific adult body form. Indeed, the signals residing in the APD may inhibit dissolution of the basement membrane required for epithelial-mesenchymal transition and, subsequently, mesoderm and endoderm formation in the anterior part of the embryo (Rowe and Weiss 2008; Nakaya et al. 2008). *Sox17* mRNA appearing in the AHB serves as an additional marker involved in anterior-posterior axis differentiation (cf. the co-localisation with several other anteriorizing genes such as *DKK1* and *Cer1*, Idkowiak

et al. 2004). The functional activity of these molecules at early stages of development may set up germ layer differentiation by, for example, suppressing mesoderm formation (see above) and inducing neuroectoderm identity in the anterior epiblast (Knoetgen et al. 1999; Kimura C et al. 2000; Idkowiak et al. 2004; Perea-Gomez et al. 2007; Egea et al. 2008). Thus, the anterior pole of the early mammalian embryo has a developmental importance similar to the well-described primitive streak. With these results the study established the basis for using the pig as a further mammalian species in experimental gastrulation analysis.

The second publication entitled ‘*sox17* expression patterns during gastrulation and early neurulation in the rabbit suggest two sources of endoderm formation’ used whole-mount in situ hybridisation and high-resolution histological analysis to define the topographic distribution of *sox17* within the tissue compartments of the rabbit embryo throughout gastrulation and early neurulation stages. The rabbit provides the tissue resolution necessary for analysis the complex topography of gene expression and, thus, the principles of analysis endoderm differentiation in mammals. This gene expression study showed that *sox17* displays several distinct expression patterns in different regions throughout the early phases of laying down the body plan. *Sox17* was found: (1) in prospective endoderm cells of the central epiblast at the early streak stage, (2) adjacent to the anterior segment of the stage 3 and 4 primitive streak in mesoderm cells and in prospective endoderm cells inserted into the ventral layer, (3) bilateral to the notochordal process during early neurulation stages, again in both mesoderm and ventral layer. These expression patterns confirmed the validity of this approach, as these anterior regions had previously been shown to generate endoderm in mouse (Kinder et al. 2001; Kanai-Azuma et al. 2002; Chapman et al. 2007; Pfister et al. 2007; Tam et al. 2007) and chick (Kimura W et al. 2007). In addition, and described for the first time in a mammalian embryo, *sox17* mRNA was also found in a mosaic-like distribution in the epiblast at the posterior pole of the embryonic disc immediately prior to the appearance of mesoderm cells in the primitive streak. This *Sox17* expression in the posterior epiblast together with its transient expression at the posterior extremity of the primitive streak suggested that the endoderm (possibly hindgut) may be formed close to the emerging cloacal membrane. The main

topics of discussion in this paper are whether the identity of different parts of gut endoderm is defined by the two expression domains in the pre-gastrulation epiblast. As a first step towards revealing the answer to this question, fate map studies could be designed to compare directly the tissue potency in the anterior and posterior extremities of the primitive streak. With regard to endoderm formation and, possibly, endoderm differentiation towards specific organs such as pancreas (anterior) or colon (posterior) fate map as well as the molecular studies could help to explain the background of many disorders such as familial adenomatous polyposis (FAP).

The manuscript to be submitted in an international scientific journal entitled 'Germ layer differentiation during early hindgut formation in the rabbit and pig embryo' attempts to draw up the schedule for formal endoderm differentiation at the posterior pole of pig and rabbit embryos. The presence of mesoderm cells in the posterior pole of the embryonic disc up to the stage preceding cloacal membrane formation emphasizes the fact that the cloacal membrane, in contrast to many textbook descriptions, does not form as early as primitive streak formation. Therefore, the analysis of mesoderm elimination as an initial step for cloacal membrane formation is now open for further analysis. Also in contrast to common text books descriptions, the cloacal membrane position was not found at the posterior border of the embryo but rather further anteriorly between the posterior end of the primitive streak and the surface destined to form the infraumbilical abdominal wall ectoderm. Electron microscopical analysis of the cloacal membrane area shows both patches electron-dense extracellular material and discontinuous basement membrane between the ectoderm and the endoderm. However, germ layer rearrangement (and, thus, cloacal membrane formation) at the posterior pole of the embryo seems to be similar in morphology but differs markedly with regard of its timing amongst the two species examined. While the mesoderm cells between ectoderm and endoderm at the future cloacal membrane area begin to disappear at early neurulation stages of pig (between stages 4 and 5), this was found much later in the rabbit (stage 8 to a stage with about 13 pairs of somites). The morphological similarity of pig and rabbit with most other mammalian groups during axial differentiation including endoderm and cloacal membrane

formation makes the integration of the results into the concepts of early human development and the frequent anorectal malformations an intriguing proposition.

#### 4. References

- Alexander J, Stainier DY (1999): A molecular pathway leading to endoderm formation in zebrafish. *Curr Biol* 9, 1147-1157.
- Ang S.L, Constam DB (2004): A gene network establishing polarity in the early mouse embryo. *Semin Cell Dev Biol* 15, 555–561.
- Arnold SJ, Robertson EJ (2009): Making a commitment: cell lineage allocation and axis patterning in the early mouse embryo. *Nat Rev Mol Cell Biol* 10, 91–103.
- Barends PM, Stroband HW, Taverne N, te Kronnie G, Leen MP, Blommers PC (1989): Morphology of the preimplantation pig blastocyst during expansion and loss of polar trophoderm (Raubert cells) and the morphology of the embryoblast as an indicator for developmental stage. *J Reprod Fertil* 87, 715–726.
- Beddington RS (1985): The development of 12th to 14th day foetuses following reimplantation of pre- and early-primitive-streak-stage mouse embryos. *J Embryol Exp Morphol* 88, 281-291.
- Beddington RS, Morgernstern J, Land H, Hogan A (1989): An in situ transgenic enzyme marker for the midgestation mouse embryo and the visualization of inner cell mass clones during early organogenesis. *Development* 106, 37-46.
- Beddington SP (1981): An autoradiographic analysis of the potency of embryonic ectoderm in the 8th day postimplantation mouse embryo. *J Embryol Exp Morphol* 64, 87–104
- Chapman SC, Matsumoto K, Cai Q, Schoenwolf GC: (2007) Specification of germ layer identity in the chick gastrula. *BMC Dev Biol* 7: 91.
- Diwan SB, Stevens LC (1976): Development of teratomas from the ectoderm of mouse egg cylinders. *J Natl Cancer Inst* 57, 937-942.
- Downs KM, Davies T (1993): Staging of gastrulating mouse embryos by morphological landmarks in the dissecting microscope. *Development* 118, 1255–1266.
- Egea J, Erlacher C, Montanez E, Burtscher I, Yamagishi S, Hess M, Hampel F, Sanchez R, Rodriguez-Manzaneque MT, Boesl MR, Faessler R, Lickert H, Klein R (2008): Genetic ablation of FLRT3 reveals a novel morphogenetic function for the anterior visceral endoderm in suppressing mesoderm differentiation. *Genes Dev* 22, 3349–3362.
- Gardner RL (1985): Clonal analysis of early mammalian development. *Philos Trans R Soc Lond B Biol Sci* 312, 163-178.

- Gardner RL, Rossant J (1979): Investigation of the fate of 4.5 day post-coitum mouse inner cell mass cells by blastocyst injection. *J Embryol Exp Morphol* 52, 141–152.
- Herrmann BG (1991): Expression pattern of the Brachyury gene in whole mount TWis/TWis mutant embryos. *Development* 113, 913–917.
- Heuser, CH, Streeter GL (1929): Early stages in the development of pig embryos, from the period of initial cleavage to the time of appearance of limb-buds. Carnegie Inst Pub No. 394. *Contrib Embryol* 20, 1–30.
- Hudson C, Clements D, Friday RV, Stott D, Woodland HR (1997): Xsox17alpha and -beta mediate endoderm formation in *Xenopus*. *Cell* 91, 397–405.
- Idkowiak J, Weisheit G, Plitzner J, Viebahn C (2004): Hypoblast controls mesoderm generation and axial patterning in the gastrulating rabbit embryo. *Dev Genes Evol* 214, 591–605.
- Kanai-Azuma M, Kanai Y, Gad JM., Tajima Y, Taya C, Kurohmaru M, Sanai Y, Yonekawa H, Yazaki K, Tam PP, Hayashi Y (2002): Depletion of definitive gut endoderm in Sox17-null mutant mice. *Development* 129, 2367–2379.
- Kimura C, Yoshinaga K, Tian E, Suzuki M, Aizawa S, Matsuo I (2000): Visceral endoderm mediates forebrain development by suppressing posteriorizing signals. *Dev Biol* 225, 304–321.
- Kimura W, Yasugi S, Fukuda K (2007): Regional specification of the endoderm in the early chick embryo. *Dev Growth Differ* 49, 365–372.
- Kinder SJ, Tsang TE, Ang SL, Behringer RR, Tam PP (2001): Defects of the body plan of mutant embryos lacking Lim1, Otx2 or Hnf3beta activity. *Int J Dev Biol* 45, 347–355.
- Kluth D, Hillen M, Lambrecht W (1995): The principles of normal and abnormal hindgut development. *J Pediatr Surg* 30, 1143-1147
- Knoetgen H, Viebahn C, Kessel M (1999): Head induction in the chick by primitive endoderm of mammalian, but not avian origin. *Development* 126, 815–825.
- Lawson KA, Pedersen RA (1992): Clonal analysis of cell fate during gastrulation and early neurulation in the mouse. *Ciba Found Symp* 165, 3–21.
- Levak-Svajger B, Svajger A (1971): Differentiation of endodermal tissues in homografts of primitive ectoderm from 2-layered rat embryonic shields. *Experientia* 27, 683-4.
- Levak-Svajger B, Svajger A (1974): Investigation on the origin of the definitive endoderm in the rat embryo. *J Embryol Exp Morphol* 32, 445-459.

- Liguori GL, Borges AC, D'Andrea D, Liguoro A, Goncalves L, Salgueiro AM, Persico MG, Belo JA (2008): Cripto-independent nodal signaling promotes positioning of the A–P axis in the early mouse embryo. *Dev Biol* 315, 280–289.
- Lu CC, Robertson EJ (2004) : Multiple roles for nodal in the epiblast of the mouse embryo in the establishment of anterior–posterior patterning. *Dev Biol* 273, 149–159.
- Maenner J, Kluth D (2005): The morphogenesis of the exstrophy-epispadias complex: a new concept based on observations made in early embryonic cases of cloacal exstrophy. *Anat Embryol (Berl)* 210, 51-57.
- Mesnard D, Guzman-Ayala M, Constam DB (2006): Nodal specifies embryonic visceral endoderm and sustains pluripotent cells in the epiblast before overt axial patterning. *Development* 133, 2497–2505.
- Nakaya Y, Sukowati EW, Wu Y, Sheng G (2008) : RhoA and microtubule dynamics control cell–basement membrane interaction in EMT during gastrulation. *Nat Cell Biol* 10, 765–775.
- Nievelstein RA, Vos A, Valk J (1998): MR imaging of anorectal malformations and associated anomalies. *Eur Radiol* 8, 573-581.
- Pander CH: Beiträge zur Entwicklungsgeschichte des Hühnchens im Eye. Brönnner, Würzburg (1817).
- Patten BM: Embryology of the Pig. McGraw-Hill, New York (1948).
- Perea-Gomez A, Meilhac SM, Piotrowska-Nitsche K, Gray D, Collignon J, Zernicka-Goetz M (2007): Regionalization of the mouse visceral endoderm as the blastocyst transforms into the egg cylinder. *BMC Dev Biol* 7, 96.
- Perry JS, Rowlands IW (1962): Early pregnancy in the pig. *J Reprod Fertil* 4, 175–188.
- Pfister S, Steiner KA, Tam PP (2007): Gene expression pattern and progression of embryogenesis in the immediate post-implantation period of mouse development. *Gene Expr Patterns* 7, 558–573.
- Rosenquist TA, Martin GR (1995): Visceral endoderm-1 (VE-1): an antigen marker that distinguishes anterior from posterior embryonic visceral endoderm in the early post-implantation mouse embryo. *Mech Dev* 49, 117–121.
- Rossant J, Gardner RL, Alexandre HL (1978): Investigation of the potency of cells from the postimplantation mouse embryo by blastocyst injection: a preliminary report. *J Embryol Exp Morphol* 48, 239-247.



- Rowe RG, Weiss SJ (2008): Breaching the basement membrane: who, when and how?. *Trends Cell Biol* 18, 560–574.
- Schwartz P, Piper HM, Spahr R, Spieckermann PG (1984): Ultrastructure of cultured adult myocardial cells during anoxia and reoxygenation. *Am J Pathol* 115, 349–361.
- Svajger A, Levak-Svajger B, Skreb N (1986): Rat embryonic ectoderm as renal isograft. *J Embryol Exp Morphol* 94, 1-27.
- Tam PP, Williams EA, Chan WY (1993): Gastrulation in the mouse embryo: ultrastructural and molecular aspects of germ layer morphogenesis. *Microsc Res Tech* 26, 301–328.
- Tam PP, Loebel DA, Tanaka SS (2006): Building the mouse gastrula: signals, asymmetry and lineages. *Curr Opin Genet Dev* 16, 419-425.
- Tam PP, Khoo PL, Lewis SL, Bildsoe H, Wong N, Tsang TE, Gad JM, Robb L (2007): Sequential allocation and global pattern of movement of the definitive endoderm in the mouse embryo during gastrulation. *Development* 134, 251–260.
- Viebahn C (1999): The anterior margin of the mammalian gastrula: comparative and phylogenetic aspects of its role in axis formation and head induction. *Curr Top Dev Biol* 46, 63–103.
- Viebahn C, Mayer B, Miething A (1995): Morphology of incipient mesoderm formation in the rabbit embryo: a light- and retrospective electron- microscopic study. *Acta Anat* 154, 99–110.
- Weisheit G, Mertz KD, Schilling K, Viebahn C (2002): An efficient in situ hybridisation protocol for multiple tissues sections and probes on miniaturized slides. *Dev Genes Evol* 212, 403–406.

## **5. Copies of the publications**

### **5.1 The first publication**

Hassoun R, Schwartz P, Feistel K, Blum M, Viebahn C (2009): Axial differentiation and early gastrulation stages of the pig embryo. *Differentiation*. In press



Contents lists available at ScienceDirect

## Differentiation

journal homepage: [www.elsevier.com/locate/diff](http://www.elsevier.com/locate/diff)Axial differentiation and early gastrulation stages of the pig embryo<sup>☆</sup>Romia Hassoun<sup>a</sup>, Peter Schwartz<sup>a</sup>, Kerstin Feistel<sup>b</sup>, Martin Blum<sup>b</sup>, Christoph Viebahn<sup>a,\*</sup><sup>a</sup> Department of Anatomy and Embryology, Göttingen University, Kreuzberggring 36, 37075 Göttingen, Germany<sup>b</sup> Institute of Zoology, Hohenheim University, Stuttgart, Germany

## ARTICLE INFO

## Article history:

Received 4 March 2009

Received in revised form

20 July 2009

Accepted 23 July 2009

## Keywords:

Hypoblast/visceral endoderm

Epiblast

Mesoderm

Epithelial–mesenchymal transformation

Amnion

Trophoblast

## ABSTRACT

Differentiation of the principal body axes in the early vertebrate embryo is based on a specific blueprint of gene expression and a series of transient axial structures such as Hensen's node and the notochord of the late gastrulation phase. Prior to gastrulation, the anterior visceral endoderm (AVE) of the mouse egg-cylinder or the anterior marginal crescent (AMC) of the rabbit embryonic disc marks the anterior pole of the embryo. For phylogenetic and functional reasons both these entities are addressed here as the mammalian anterior pregastrulation differentiation (APD). However, mouse and rabbit show distinct structural differences in APD and the molecular blueprint, making the search of general rules for axial differentiation in mammals difficult. Therefore, the pig was analysed here as a further species with a mammotypical flat embryonic disc. Using light and electron microscopy and in situ hybridisation for three key genes involved in early development (*sox17*, *nodal* and *brachyury*), two axial structures of early gastrulation in the pig were identified: (1) the anterior hypoblast (AHB) characterised by increased cellular height and density and by *sox17* expression, and (2) the early primitive streak characterised by a high pseudostratified epithelium with an almost continuous but unusually thick basement membrane, by localised epithelial–mesenchymal transition, and by *brachyury* expression in the epiblast. The stepwise appearance of these two axial structures was used to define three stages typical for mammals at the start of gastrulation. Intriguingly, the round shape and gradual posterior displacement of the APD in the pig appear to be species-specific (differing from all other mammals studied in detail to date) but correlate with ensuing specific primitive streak and extraembryonic mesoderm development. APD and, hence, the earliest axial structure presently known in the mammalian embryo may thus be functionally involved in shaping extraembryonic membranes and, possibly, the specific adult body form.

© 2009 International Society of Differentiation. Published by Elsevier Ltd. All rights reserved.

## 1. Introduction

One of the earliest axial structures in the mammalian embryo is an inconspicuous cellular differentiation at the anterior pole of the embryonic disc during the start of the gastrulation phase. Known as the anterior visceral endoderm (AVE) in the mouse (Rosenquist and Martin, 1995; Thomas and Beddington, 1996) or the anterior marginal crescent (AMC) in the rabbit (Viebahn et al., 1995a; cf. Kölliker, 1879), it is only transiently present (similar to other axial structures of gastrulation such as Hensen's node or the notochord) but draws its significance for development at least from the following three features: (1) AVE or AMC fixes two principal body axes (longitudinal and transversal) simultaneously by establishing structural cell shape changes at the (anterior) border of an embryonic disc, which is polarised along its dorsal–ventral (sagittal) axis only; (2) signaling potency residing

in the AVE/AMC seems to be responsible for suppressing mesoderm formation and for inducing neuroectoderm or head identity in the epiblast (Knoetgen et al., 1999; Kimura et al., 2000; Idkowiak et al., 2004; Perea-Gomez et al., 2007; Egea et al., 2008), the latter function being suggestive of a Spemann type organiser (Beddington and Robertson, 1998; Hallonet et al., 2002; del Barco Barrantes et al., 2003, but s.a. Albazerchi and Stern, 2007); and (3) AVE/AMC cells appear to belong to the extraembryonic tissues that are shed after birth but, during early development, set up the basic body plan and the germ line using a complex expression pattern ("blue print") of signaling molecules (cf. Ang and Constam, 2004; Georgiades and Rossant, 2006; Chuva de Sousa Lopes et al., 2007). As these features touch several essential processes of gastrulation and embryonic development as a whole, the anterior pole of the early mammalian embryo may have a developmental significance similar to the well-described primitive streak, with its morphogenetic potential and capacity to form mesoderm by epithelial–mesenchymal transition (EMT, cf. Voiculescu et al., 2007; Yang and Weinberg, 2008). Therefore and for the purpose of the present report, we subsume the different designations for the early anterior lower layer differentiation in

<sup>☆</sup>Join the International Society for Differentiation ([www.isdifferentiation.org](http://www.isdifferentiation.org)).

\* Corresponding author. Tel.: +49 551 39 7000; fax: +49 551 39 7043.

E-mail address: [cviebah@gwdg.de](mailto:cviebah@gwdg.de) (C. Viebahn).

the mammalian embryo (see also Viebahn, 1999) under the heading of anterior pregastrulation differentiation (APD).

Mammalian species show surprising differences with respect to the topographical arrangement of the (relatively few) tissues involved in the start of gastrulation (see Behringer et al., 2006; Selwood and Johnson, 2006; Blomberg et al., 2008). As a consequence, size and mutual contact areas of (polar or mural) trophoblast, epiblast and hypoblast, for example, vary considerably; however, these characteristics correlate to some extent with the extraembryonic differentiation and the implantation schedule, which may start well ahead of gastrulation (mouse, higher primates and man) or may be delayed until the late gastrulation phase (rabbit) or advanced neurulation stages (ruminants, ungulates). Even within one of these groups the relative size of tissues may vary, too, the epiblast being rather large and “forced” into a cylinder shape (the “egg-cylinder”) in the mouse (Tam and Gad, 2004), or being small and representing a flat disc as in higher primates including man. Mouse and rabbit are two popular laboratory species recently used for analysis of mammalian gastrulation as they represent opposite ends of this topography spectrum between egg-cylinder (mouse) and the mammary typical flat disc (rabbit). Importantly, both these species are amenable to experimentation (cf. Rossant and Tam, 2009; Reupke et al., 2009) during this phase of development, which, in mammals, has so far been impossible to observe directly in the secluded environment of the uterus. By comparison of results obtained in these two species, it can be assumed that general rules for the mechanisms running mammalian gastrulation may be derived. However, even if careful approximations are taken into account to project the complex topography and expression patterns of the rodent egg-cylinder onto the mammary typical embryonic disc (cf. Behringer et al., 2000), topographical and molecular results can be matched only partially between these two species (cf. Blomberg et al., 2008), making it impossible to decide which results may be generally applicable to mammals and which may be species-specific.

In search of general rules for axial differentiation at the start of mammalian gastrulation, the present study intends to establish the basis for using the pig as a third mammalian species in experimental gastrulation analysis. The pig has the mammary typical flat disc (Fléchon, 1978; Barends et al., 1989; Vejlsted et al., 2006) but a (late) implantation schedule (Heuser and Streeter, 1929; Patten, 1948; Perry and Rowlands, 1962) differing distinctly from that of the rabbit; the pig may therefore have to accommodate extraembryonic signaling for setting up the body plan in a yet again different topographical arrangement. Not least because of its late implantation, the pig seems also well suited for experimental analysis of this phase of development (Papaioannou and Ebert, 1988; Fléchon et al., 1995; Wianny et al., 1997). However, it is presently not clear how initial axial differentiation or early and pregastrulation stages can be defined in the pig, because a systematic comparison of standard dorsal (orthogonal) views of the embryonic disc is lacking at these early stages. Also, EMT which is the hallmark of mesoderm formation, has not been defined or correlated with the gross morphology of primitive streak formation (Fléchon et al., 2004). Therefore, high-resolution morphological analysis as well as in situ hybridisation for the expression of the axial differentiation and patterning genes *sox17* (cf. Pfister et al., 2007; Hassoun et al., 2009), *nodal* (cf. Lu and Robertson, 2004; Mesnard et al., 2006; Liguori et al., 2008) and the key mesoderm marker gene *brachyury* (Herrmann, 1991, cf. Arnold and Robertson, 2009) are applied here to closely spaced pre- and early gastrulation stages of the pig (between 8 and 10 days post conception, d.p.c.). In this way we find typical signs of APD in the hypoblast, mesoderm precursors in the epiblast and the EMT as the hallmark of initiating overt primitive streak

formation. On the basis of these structural and molecular features three stages can be defined at the start of gastrulation, which may well be applicable to mammals in general and helps to clarify differences and similarities between mammals during this crucial period of development.

## 2. Methods

### 2.1. Animal tissues

Late pre pubertal gilts (Landrace × Large White, Institute of Animal Science and Behaviour, 31535 Mariensee, Germany) were stimulated using 5 ml equine Regumate<sup>®</sup> (2.2 mg/ml, Intervet, Unterschleißheim, Germany) per os once daily for 10–18 days and using 1500 IU pregnant mare serum gonadotropin (Integonan<sup>®</sup>, Intervet) i.m. 72 h prior to mating with Piétrain boars; on the day before starting the mating schedule, gilts were superovulated using 500 IU chorionic gonadotropin (Ovogest<sup>®</sup>, Intervet) i.v. Each gilt was mated (or artificially inseminated) twice, the first time 24 h after hCG treatment and a second time 36 or 48 h after hCG treatment. The time of the first mating or insemination was taken to be the time of conception from which embryonic age was calculated, i.e. embryos designated to be recovered at 8.0 days post conception (d.p.c.) had an embryonic age of minimally 7.0 and maximally 8.0 days. Uteri were removed after slaughter between 8.0 and 10.0 d.p.c. (2 litters with a total of 32 embryos at 8 d.p.c., 3 litters with a total of 70 embryos at 9 d.p.c., and 2 litters with a total of 61 embryos at 10 d.p.c.).

Uterine horns were flushed twice with 20 ml warm (37 °C) phosphate-buffered saline (PBS) containing 2% polyvinyl alcohol (PVA). For in situ hybridisation blastocysts were fixed in 4% paraformaldehyde (PFA) in phosphate buffer for 2–3 h at room temperature; after microdissection using iridectomy scissors and tungsten needles, specimens were dehydrated in a graded series of ethanol and frozen in 100% ethanol at –20 °C until used for in situ hybridisation. For high-resolution light and transmission electron-microscopical analysis, blastocysts were prefixed for 2–3 h in 1.5% PFA and 1.5% glutaraldehyde (GA) in phosphate buffer followed by microdissection as above, postfixation in 1% OsO<sub>4</sub> in phosphate buffer and embedding in Araldite<sup>®</sup> (Schwartz et al., 1984).

### 2.2. Morphological analysis

OsO<sub>4</sub>-fixed embryos were photographed as whole -mounts from their ventral and dorsal sides prior to embedding in Araldite<sup>®</sup> (Plano, Wetzlar, Germany), i.e. while suspended in phosphate buffer, and again after embedding, for faithful topographical correlation of structures observed in the serial sections obtained in the following step. Complete series of semithin (1 µm) sections were cut from a total of 11 Araldite<sup>®</sup>-embedded embryos either in the transverse or in the sagittal plane (determined with the help of the whole-mount photographs) and stained with methylene blue (Schwartz et al., 1984). Peripheral tissue borders created in the blastocyst wall by microdissection were traced back to the edges of the stained semithin sections and used to define the angle and position of individual serial sections within the whole-mount photographs taken prior to and after embedding. At suitable intervals 70 nm sections were cut for transmission electron-microscopical analysis of regions defined to be of interest in semithin sections and dorsal views of whole blastocysts. If necessary, selected semithin sections were re-embedded in Araldite<sup>®</sup> (Viebahn et al., 1995b) and sectioned at 70 nm.

### 2.3. Molecular analysis

A digoxigenin-labelled *sox17* mRNA probe was generated from a mouse *sox17* cDNA (kind gift of Dr. H. Lickert), which spans 707bp of the coding region from nucleotides no. 1102 through to 1808 of the mouse *sox17* gene (GenBank NM\_011441). Similarly, a digoxigenin-labelled *brachyury* mRNA probe was generated from a mouse *brachyury* cDNA (1760 bp, GenBank NM009309), which spans the open reading frame and 5' and 3' UTR sequences of mouse *brachyury* (Herrmann et al., 1990, kind gift of Dr. Bernhard Herrmann, Berlin). The *nodal* mRNA probe, however, was generated from pig genomic DNA (primers 5' CAG AAC TGG ACI TTC ACI TTT GAC TT 3' and 5' TAI GCA TTG TAC TGC TTI GGG TA 3' resulting in a 611 bp fragment corresponding to nucleotides 214–842 of the mouse cDNA and spanning most of mouse exon 2). In situ hybridisation was carried out at 70 °C using standard protocols adapted for early rabbit embryonic discs (Weisheit et al., 2002). After staining in BM-purple (Roche, Mannheim, Germany) embryos were photographed in Mowiol4-88 (Hoechst, Frankfurt, Germany) and prior to embedding in Technovit 8100<sup>®</sup> (Heraeus-Kulzer, Werheim, Germany) as described (Idkowiak et al., 2004). Embryos were serially sectioned at 5 µm in sagittal or transverse planes. Gene expression was analysed using differential interference contrast (DIC, Axioskop, Zeiss, Göttingen, Germany) or, if necessary, with the help of neighbouring methylene blue stained

Technovit<sup>®</sup> sections. Sense cRNA probes were generated as negative controls and used under the same conditions as the antisense probes described above in at least one specimen for every stage and gene examined.

### 3. Results

All blastocysts investigated in the present study had hatched from their zona pellucida and neozona – the remnants of which were still found in the flushing fluid at the earliest day of development investigated (8.0 d.p.c.) – and blastocysts had not yet started the marked elongation phase typical for the pig embryo (cf. Geisert et al., 1982), i.e. overall blastocyst shape varied between round or slightly oblong (Fig. 1A). In contrast and as could be expected from the double mating schedule applied, the morphology of the embryo proper (which in pig as in ruminants and lower primates is disc-shaped and integrated into the blastocyst wall, Fig. 1A–D) varied markedly amongst embryos from the same litter. The primitive streak or Hensen's node of early gastrulation stages could be clearly distinguished under the stereomicroscope but, importantly, two separate stages prior to the primitive streak stage could be identified as well: (1) an early pregastrulation stage in which the embryonic disc was small and round, but in most cases completely covered by polar trophoblast

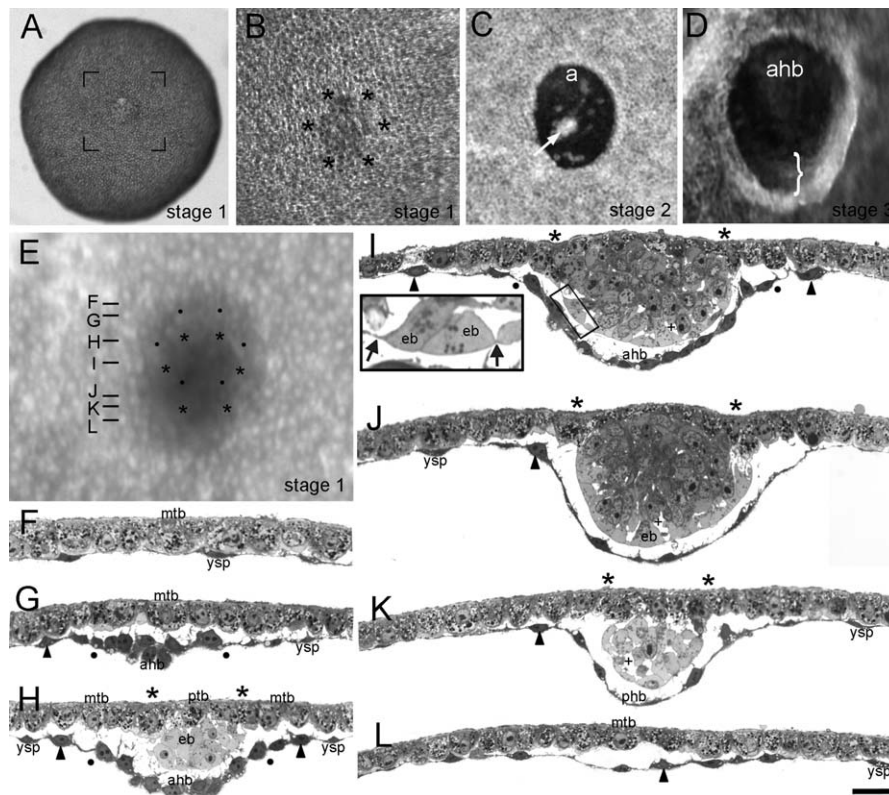


**Fig. 1.** Pig embryos at the start of gastrulation. Dorsal views (A–E) and semithin histological sections (F–L) of paraformaldehyde-fixed embryos (shown in Fig. 4) prior to in situ hybridisation (A–D) or of an OsO<sub>4</sub>-fixed embryo (E) using brightfield (A, E) or darkfield (B–D) illumination. (A, B) blastocyst (A) and embryonic disc area (B, position marked in A) of the 8 d.p.c. embryo shown after gene expression analysis in Fig. 4A; asterisks are placed just peripheral to the embryonic disc border. (C) Embryonic disc area of the stage 2 (9 d.p.c.) embryo shown after gene expression analysis in Fig. 4N; arrow points to some of the remnants of polar trophoblast (Raubers cells); a, anterior pole of embryonic disc. (D) Embryonic disc area of the stage 3 (10 d.p.c.) embryo shown after gene expression analysis in Fig. 4I; bracket delineates length of primitive streak; ahb, region of increased density in anterior hypoblast. (E–L) Stage 1 embryo obtained at 9.0 d.p.c. with axial differentiation marked in the overview (E) and transverse 1 µm sections (F–L) as follows: Asterisks mark embryonic/extraembryonic borders determined in the epiblast/trophoblast layer. Dots delineate the area of the anterior pregastrulation differentiation (APD) as determined by the high-columnar and dense region of hypoblast epithelium. Arrowheads mark yolk sac precursor cells which are higher and more numerous close to the embryonic disc than in the rest of the blastocyst. Arrows point to position of continuous basement membrane on the ventral surface of organelle-free basal cytoplasmic regions of the epiblast cells facing the hypoblast. Crosses indicate widened extracellular spaces between ventral epiblast cells. ysp, yolk sac precursors; mtb, mural trophoblast; ptb, polar trophoblast; eb, epiblast; ahb, anterior hypoblast; phb, posterior hypoblast Scale bar: (A) 160 µm, (B–E) 100 µm, (F–L) 40 µm, (insert in I) 18 µm.

(Raubers layer) and therefore difficult to identify in the living or paraformaldehyde-fixed whole-mount embryo (cf. Fig. 1A and B), and (2) a late pregastrulation stage in which the polar trophoblast was either partially or completely lost and the embryonic disc showed an oval outline (Fig. 1C) but, in contrast to gastrulation stages (cf. Fig. 1D), a primitive streak was not yet visible. Embryos with only few remnants of polar trophoblast revealed, however, a localised patch of increased tissue density (Fig. 1C); in histological sections, this was shown to be caused by morphological differentiation of the hypoblast near one pole of the embryonic disc (see below) and could be found similarly at early primitive streak stages (Fig. 1D). Molecular markers indeed provided evidence for the anterior identity of this pole (cf. *sox17* expression in Fig. 4B with dorsal view in Fig. 1C, see also *brachyury* expression in Fig. 4N showing the same embryo as in Fig. 1C), and this anterior identity was subsequently also found in embryos prior to the loss of polar trophoblast (see below). To arrive at definitions for pre- and early gastrulation stages of the pig, which could be easily compared in the staging system of other mammals (Theiler, 1989; Kaufman, 1992; Viebahn, 2004) and birds (Hamburger and Hamilton, 1992), and to obtain reliable information on the shape and the molecular constitution of APD in the pig, 30 pre- and early gastrulation embryos (of the total of 163 embryos generated) were analysed by high-resolution light microscopy and in situ hybridisation in this study. The specimens were grouped into three stages according to the morphology and molecular constitution they had in common, rather than according to their calculated range of embryonic age, number of embryos per stage or method of analysis.

### 3.1. Anterior differentiation in the hypoblast (stage 1)

Blastocysts at stage 1 are in most of the 8 serially sectioned specimens included in this stage still spherical and measure about 800  $\mu\text{m}$  in the longest diameter (Fig. 1A). The embryonic disc is a small, roughly circular area of high cellular density in the wall of the blastocyst and measures 130–140  $\mu\text{m}$  in diameter; it is surrounded by less dense extraembryonic tissue and also covered completely by the polar trophoblast (Raubers layer, see below) and is, therefore, easily detected only after fixation with  $\text{OsO}_4$  (cf. Fig. 1B and E). When the polar trophoblast begins to recede, brightfield illumination helps to reveal the embryonic disc (Fig. 1A); however, the exact position of the border between embryo (epiblast) and surrounding extraembryonic tissues (e.g. trophoblast) can be distinguished in histological sections only (see below).

Histological sections also reveal axial differentiation at the earliest stages investigated here, when the orientation of the embryonic disc is still difficult to ascertain in dorsal views even after  $\text{OsO}_4$  fixation (Fig. 1E), and concerns the hypoblast rather than the epiblast. The latter lies between the polar trophoblast (dorsal) and the hypoblast (ventral), forms a more or less dense globe, which bulges into the blastocyst cavity (Fig. 1H–K), and its cells show different constitutions depending on their position within the globe: epiblast cells close to the hypoblast layer have nuclei positioned towards the dorsal part of the cells leaving the parts of the cytoplasm facing the continuous basement membrane (see arrows in Fig. 1I; electron microscopic data not shown, cf. Fig. 3M and N) largely free of organelles (Fig. 1I and J); also, rather large extracellular spaces are dispersed mainly between ventral epiblast cells (Fig. 1I–K). Towards the overlying polar trophoblast and in the centre of the epiblast layer fewer nuclei are found (Fig. 1J), producing a radial arrangement of epiblast cells in the dorsal part of the globe-like cellular arrangement. At this stage, trophoblast cells are easily distinguished from all other cell types

by their high content of intracytoplasmic coarse granules; the polar part of the trophoblast covers the epiblast completely but is thinner than the adjacent mural trophoblast (Fig. 1F–L).

In contrast to the epiblast there is a clear axial differentiation in the continuous layer of hypoblast cells underlying the epiblast at this stage: On one side of the embryo there is a stretch of near-cuboidal hypoblast epithelium with numerous cells that lie close together, have round nuclei and extend many thin finger- or sheet-like cellular processes towards the epiblast (Fig. 1H and I); on the opposite side of the embryo hypoblast cells are fewer, have flat nuclei and are connected to each other with thin sheet-like cytoplasmic processes but extend only few or no cellular processes towards the epiblast (Fig. 1J and K). These variations between different parts of the hypoblast fit the description of anterior–posterior differentiation in the lower layer of other mammals (e.g. rabbit, mouse) at pregastrulation stages, and similar histological characteristics in the hypoblast are, indeed, also found in older pig embryos, which have a primitive streak at the posterior pole (cf. Fig. 3). Together with the molecular analyses (see below and Fig. 4) these characteristics are considered to represent a sign of early APD in the pig, as in other mammals. The near-cuboidal stretch of hypoblast epithelium will, therefore, be called “anterior hypoblast” (AHB) and used as an anterior landmark in the following two stages, also.

The histological properties of the AHB at stage 1 cover more than the anterior half of the embryo (see Fig. 1E) and, in addition, reach beyond the anterior border of the embryonic disc (cf. Fig. 1G); here, AHB touches a region of flat (extraembryonic) yolk sac precursor cells that underlie the mural trophoblast (cf. Fig. 1F and G) and which are higher and more numerous close to the embryonic disc than in the rest of the blastocyst (arrowheads in Fig. 1G–L). Taken together, the extra- and intraembryonic regions of the AHB produce an overall disc-like shape whose centre is markedly offset towards the anterior pole when compared with the embryonic disc borders represented by the outlines of the epiblast (cf. asterisks marking embryonic disc borders and dots marking the outlines of the dense hypoblast differentiation in Fig. 1E).

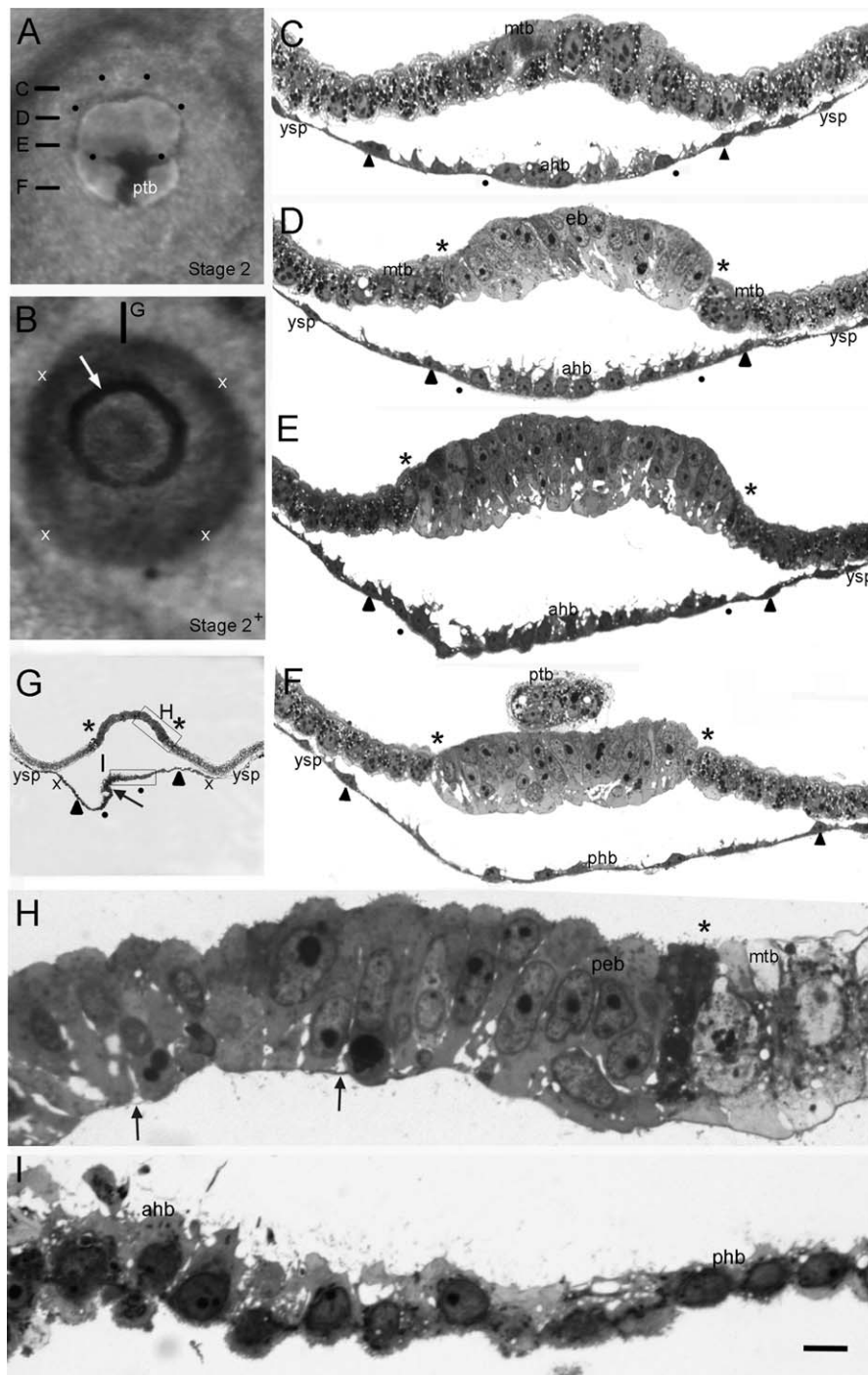
*Sox17* is already differentially expressed in the embryonic disc at stage 1 ( $n = 3$  embryos), in that its expression is stronger towards the anterior half than in the posterior half (Fig. 4A). Sections show stronger expression in the AHB than in the posterior hypoblast and similarly strong expression also in the small region of the AHB, just outside the anterior border of the embryo (Fig. 4D and E). In addition, weak *sox17* expression is also found in a few posterior epiblast cells and in small granules of the mural trophoblast (Fig. 4D and E); the latter intracellular distribution is similarly found at older stages (Fig. 4F) and with *nodal* expression (see below, Fig. 4J). *Nodal* is evenly expressed throughout the embryonic disc (in epiblast and hypoblast) and, in some (late) stage 1 embryos, also in coarse granules in the basal compartments of a few trophoblast cells next to the embryonic disc (Fig. 4J,  $n = 3$  embryos). No expression of *brachyury* can be found at this stage (Fig. 4M,  $n = 2$  embryos).

### 3.2. Mesoderm precursors in the posterior epiblast (stage 2)

The blastocyst as a whole still has a spherical or oblong shape in the 17 serially sectioned embryos included in stage 2 while the embryonic disc, now oval and with its longer diameter lying parallel to the anterior–posterior axis, has increased in size and measures between 200 and 250  $\mu\text{m}$ . The border of the embryonic disc is clearly delineated in dorsal or ventral views as the polar trophoblast, previously covering the embryonic disc, is either partially (Fig. 2A) or completely (Fig. 2B) lost (cf. Barends et al.,

1989; Prele et al. 2001, Fig. 5; Fléchon et al., 2004, Fig. 6b; Vejlsted et al., 2006, Fig. 1b). The epiblast has changed from a globe-like into a disc-like shape, a configuration that is apparently more difficult to preserve using glutaraldehyde fixation (necessary for high-resolution light and electron microscopy, cf. Fig. 2C) than with paraformaldehyde (used for whole-mount gene expression analysis, cf. Fig. 4F and K). Without the support of an

overlying polar trophoblast the single high-columnar epithelial layer of the epiblast regularly buckles dorsally into a dome-like shape while the flat epithelium of the underlying hypoblast shrinks in a planar fashion, with the effect that both layers are widely separated (Fig. 2C–G). As a result of epiblast (and in some cases also hypoblast) folding, dense areas appear in overviews, which represent tangential views of tissue folds (cf. arrows in



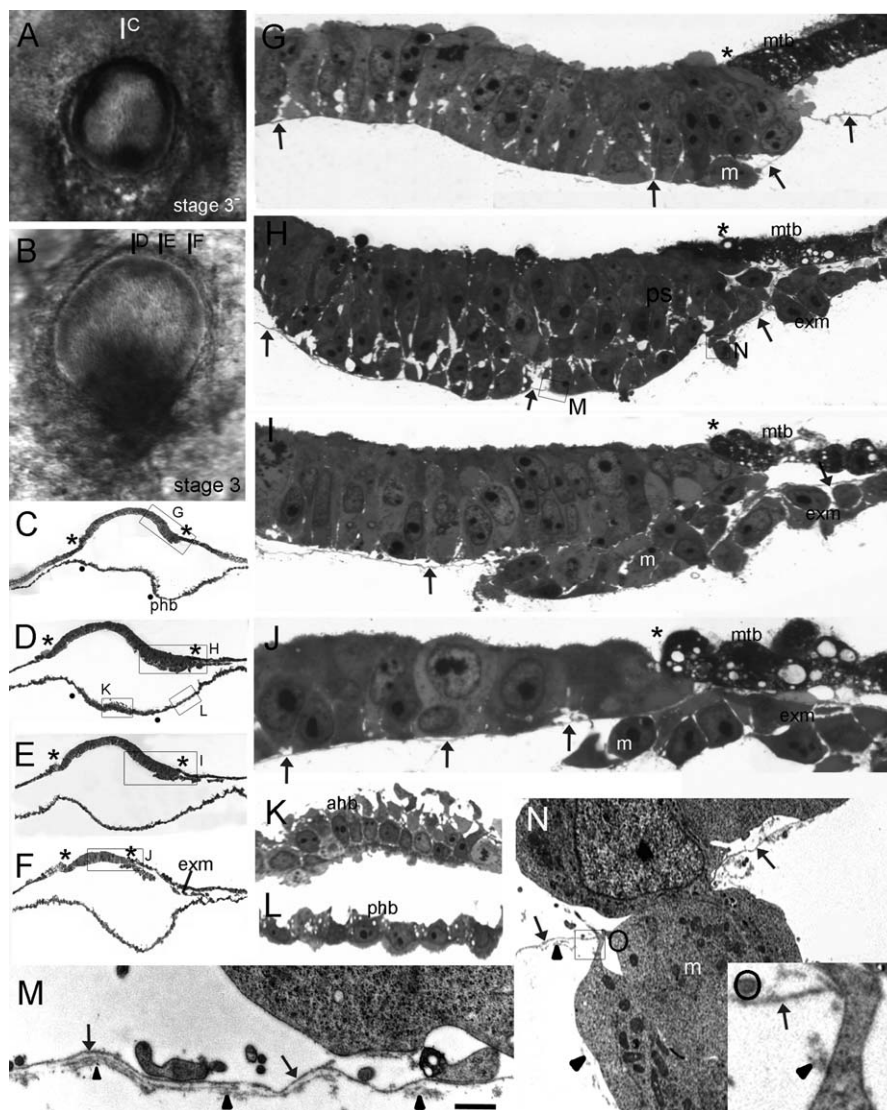
**Fig. 2.** Morphology of stage 2 in the pig embryo. (A, B) Dorsal views of a 9.0 and a 10.0 d.p.c. embryo, respectively. (C–I) Transverse (C–F) and sagittal (G–I) 1  $\mu$ m sections from the embryos shown in A and B, respectively. Position and the orientation of the sections are indicated with bars in A and B. Labeling by asterisks, dots and arrowheads is as in Fig. 1. Arrows refer to dense areas in the overview (B) caused by artifactual folds (seen in G) which lie tangentially in the light path. X labels the peripheral border of the area containing higher and more densely populated yolk sac precursor cells (ysp) than the rest of the blastocyst. Boxes in G mark higher power views of posterior epiblast and central hypoblast shown in H and I, respectively. mtb, mural trophoblast; ptb, polar trophoblast; eb, epiblast; ahh, anterior hypoblast; phb, posterior hypoblast; peb, posterior epiblast. Scale bar: (A–B) 100  $\mu$ m, (G) 130  $\mu$ m, (C–F) 30  $\mu$ m, (H–I) 10  $\mu$ m.

Fig. 2B and G). Nevertheless, sections confirm the absence or the remnants of polar trophoblast and, interestingly, show increased thickness of the epiblast in the centre at early stage 2 (Fig. 2E) and at the posterior pole at late stage 2 (Fig. 2H) as compared with the anterior pole (Fig. 2D, cf. Fig. 2G); in this area of the higher epiblast epithelium cell nuclei lie more frequently in the basal compartments. A thick basement membrane covering the basal epiblast surface is visible in the light microscope (arrows in Fig. 2H) and is continuous throughout between dorsal and ventral cell layers, i.e. it separates epiblast and hypoblast, and mural trophoblast and yolk sac precursors, respectively (cf. Fig. 3M and N).

Sections also show that the AHB has concentrically enlarged at stage 2. Below the anterior and central epiblast hypoblast cells have increased in height, forming a high-columnar epithelium (Fig. 2D, E; I to the left). This central AHB area is surrounded by a ring-like domain of cuboidal hypoblast cells (e.g. Fig. 2I to the

right) that occupy an almost round but larger part of the hypoblast than at stage 1. As a result, the AHB reaches both well beyond the anterior border of the embryonic disc as is the case at stage 1 (Fig. 2C) and beyond the centre of the disc posteriorly (see Fig. 2G). AHB cells still extend many thin cytoplasmic processes towards the basal surface of the epiblast.

*Sox17* expression is found in the whole region of the concentrically enlarged AHB and is strongest in the high-columnar, central part of it (Fig. 4B and F); its expression decreases towards the posterior hypoblast but, interestingly, in the (extraembryonic) mural trophoblast the *sox17* expression domain has markedly increased in size as compared to stage 1 and shows a differential distribution: *Sox17* mRNA is found in fine granules apically and in broader patches basally, whereby the basal patch-like distribution is found mainly in trophoblast cells close to the anterior circumference of the embryonic disc (Fig. 2F,  $n = 7$  embryos). This extraembryonic expression pattern applies



**Fig. 3.** Morphology of stage 3 in the pig embryo. (A, B) Dorsal views of two 10.0 d.p.c. embryos. (C–O) Sagittal light-microscopical 1  $\mu$ m (C–L) and neighbouring electron-microscopical 70 nm (M–O) sections from the embryos shown in A and B, respectively. Position and the orientation of the sections are indicated with bars in A and B and with boxes in C–F, H and N. Labeling by asterisks and dots is as in Fig. 1. The first mesoderm cell ingressing from the primitive streak (ps) at stage 3 – is marked m in (G). Arrows point to basement membrane underlying the epiblast and trophoblast seen at the light-microscopical (G–J) and electron-microscopical (M–O) level. Arrowheads in M–O point to electron-dense extracellular matrix material on the hypoblast surface of the basement membrane (M, N) and on the free surface of ingressing mesoderm cells (O). mtb, mural trophoblast; ahb, anterior hypoblast; phb, posterior hypoblast; m, mesoderm; exm, extraembryonic mesoderm. Scale bar: (A–F) 200  $\mu$ m, (G–L) 30  $\mu$ m, (M,N) 4  $\mu$ m, (O) 1  $\mu$ m.



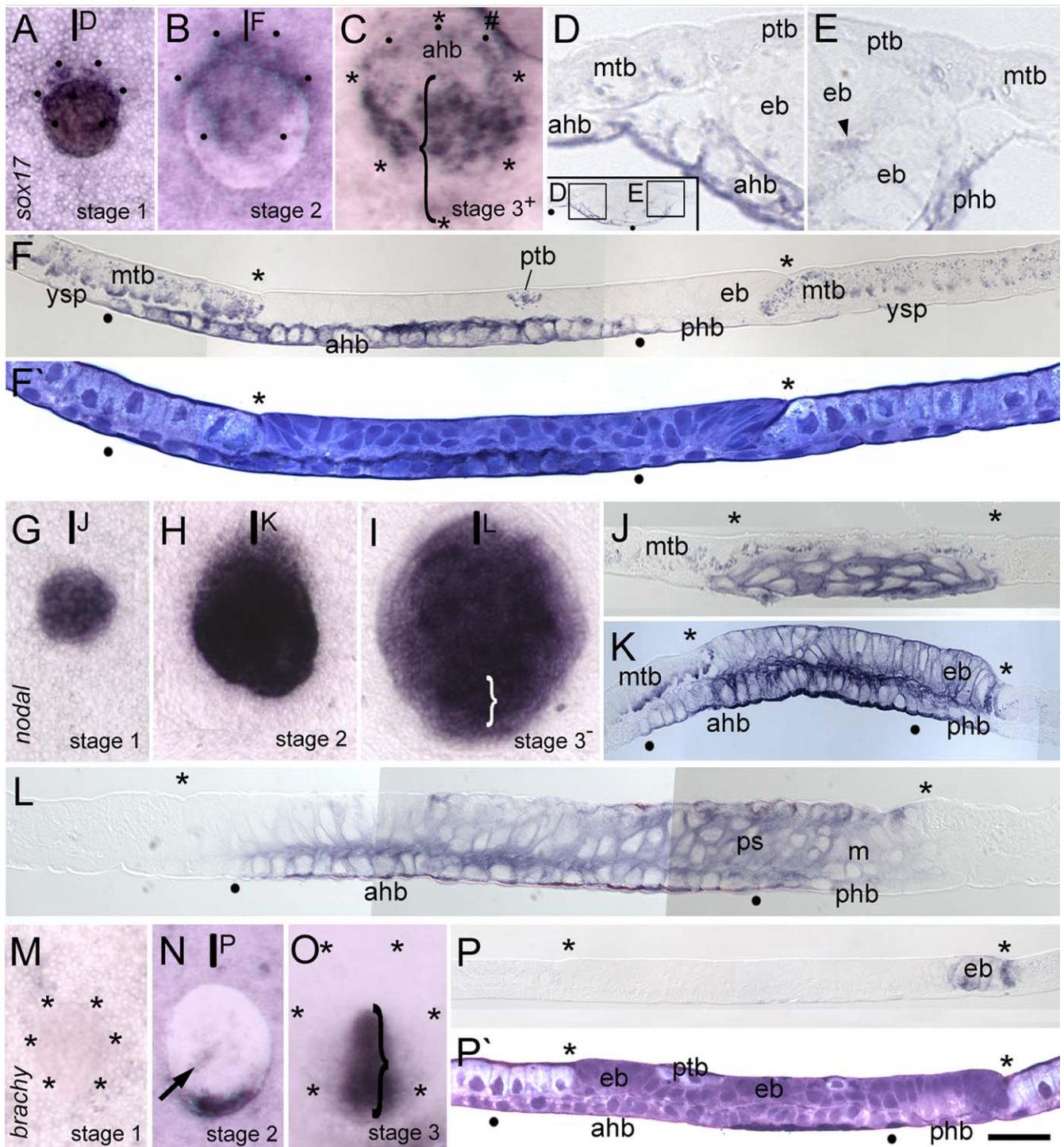


**Fig. 4.** Axial differentiation of *sox17* (A–F), *nodal* (G–L), and *brachyury* (M–P') expression at stage 1 (A, D, E, G, J, M), stage 2 (B, F, F', H, K, N, P, P') and stage 3 (C, I, L, O) pig embryos as seen in overviews (A–C, G–I, M–O) and sagittal sections (D–F', J–L, P, P') of the same specimens, respectively. Embryos shown in A (stage 1), I (stage 3-) and N (stage 2) are also presented in Fig. 1A and B (stage 1), C (stage 2) and D (stage 3-), respectively, prior to in situ hybridisation. The position and orientation of the sections are indicated by bars (in A, B, G–I and N) and boxes in D. F' and P' show methylene blue stained sections to visualise the morphological characteristics of the unstained areas in the neighbouring sections (F and P, respectively). Labeling by asterisks and dots is as in Fig. 1. Brackets mark length of the primitive streak in C (stage 3+), I (stage 3-) and O (stage 3); # marks artifactual fold in C; arrowheads in E mark *sox17* expression in epiblast cells at stage 1; arrow in N marks weakly stained remnants of polar trophoblast also seen in Fig. 1C; mtb, mural trophoblast; ptb, polar trophoblast; eb, epiblast; ahb, anterior hypoblast; phb, posterior hypoblast; ysp, yolk sac precursors; m, mesoderm; ps, primitive streak. Scale bar: (A–C), (G–I), (M–O) 100  $\mu$ m; (D, E) 10  $\mu$ m; (F, F'), (P, P') 25; (J–L) 15  $\mu$ m.

particularly to early stage 2 embryos, which still have a few remnants of polar trophoblast (now also containing granules of *sox17* mRNA, cf. Figs. 2F and 4F). *Nodal* expression is still strong (Fig. 4H) but shows a differential distribution in almost all layers: In the hypoblast its expression coincides with the *sox17* domain in

the AHB and is at its strongest in the posterior two-thirds of the AHB; in the epiblast a small anterior domain has reduced *nodal* expression, and the trophoblast anterior to the anterior margin of the embryonic disc shows patches of *nodal* mRNA confined to its basal compartments (Fig. 4K,  $n = 4$  embryos).

Expression of the mesoderm marker gene *brachyury* is found in a crescent-like area of the embryonic disc at the pole opposite the AHB (Fig. 4N, P and P',  $n = 5$  embryos) and apparently prior to formation of the primitive streak and ingression of mesoderm cells, which occur in this area at stage 3 (cf. Fig. 3). *Brachyury* expression thus marks mesoderm precursors in the epiblast and highlights the embryonic disc change from the circular shape of stage 1 to the oval shape typical for stage 2 in a manner similar to the formation of the posterior gastrula extension (PGE) in the rabbit (Viebahn et al., 2002).

### 3.3. Definitive mesoderm in the primitive streak (stage 3)

The blastocyst at stage 3 ( $n = 7$  serially sectioned embryos) is about twice as long as it is wide in most cases, while the embryonic disc, surrounded by a dense patch of extraembryonic tissue and slightly raised above the blastocyst surface, has elongated to measure between 500 and 700  $\mu\text{m}$  along its anterior–posterior axis (which frequently lies at a right angle to the longest of the blastocyst's three major diameters; Fig. 3A and B). The posterior pole now accommodates the density of the primitive streak, a small round patch within the confines of the posterior border at early stage 3 (Fig. 3A) and a larger oval area spreading anteriorly towards the centre of the embryonic disc, as well as beyond the embryonic disc borders posterolaterally at the late stage 3 (Fig. 3B). The density of the primitive streak is caused by a marked increase in the epiblast's thickness. The latter is covered ventrally by a thick basement membrane seen clearly in the light microscope (cf. arrows in Fig. 3G–J) because additional electron-dense extracellular matrix material has appeared on its hypoblast side (cf. Fig. 3H and M). In isolated patches at the posterior extremity of the primitive streak, the very first definitive mesoderm cells (cf. Fig. 3G) are devoid of basement membrane material and exhibit the typical appearance of a cell “breaking” through the basement membrane in the process of EMT and mesoderm ingression (Fig. 3H, N and O). These “holes” in the basement membrane appear first in the median plane and at late stage 3 also further laterally, but still close to the midline (Fig. 3E and I). No signs of basement membrane discontinuity, EMT or mesoderm ingression are seen further anteriorly or posteriorly at this stage, while free mesoderm cells are, indeed, found to have spread laterally within the confines of the embryonic disc to form intraembryonic mesoderm (Fig. 3F and J), as well as posterolaterally beyond the embryonic disc border to form extraembryonic mesoderm (e.g. cells marked “exm” in Fig. 3F, H–J).

Hypoblast differentiation is principally the same as at stage 2 (Fig. 3K and L), with the exception that all hypoblast regions now contain more cells than at the previous stage; as a result, the high-columnar stretch of the AHB has increased in size, as has the ring of low-columnar hypoblast surrounding the central AHB. At late stage 3, characterised by an enlargement of the primitive streak area (see above), the centre of the AHB lies further posterior to the anterior embryonic disc than at the early streak stage (Fig. 3D). In the periphery just outside of the embryonic disc, yolk sac precursor cells near the embryonic disc have also increased in number (Fig. 3C–F).

Expression patterns of *sox17*, *nodal* and *brachyury* at stage 3 ( $n = 3/2/2$  embryos for *sox17*, *nodal* and *brachyury*, respectively) remain principally unchanged as compared to stage 2, the exception being that *sox17* starts to be expressed in a transverse band of endoderm precursors at the level of the primitive streak's anterior half (Fig. 4C) and that extraembryonic expression of *sox17* and *nodal* is reduced and lost, respectively, both in the trophoblast and in the underlying yolk sac precursors (cf. Fig. 4L). Otherwise, expression patterns mainly follow the morphological

changes observed in the tissue compartments expressing these genes at stage 2: *Sox17* continues to be expressed in the central, high-columnar area of the AHB (Fig. 4C); the anterior epiblast domain lacking *nodal* expression expands in proportion with the overall anterior–posterior elongation of the embryonic disc (Fig. 4I and L); *nodal* expression is reduced bilaterally in two peripheral longitudinally oriented stretches within the embryonic disc borders at early stage 3 (Fig. 4I) and, at late stage 3, it is confined to the anterior two-thirds of the primitive streak (not shown); *brachyury* expression, finally, is transformed from the transverse domain in the PGE-like region at the posterior pole of stage 2 to a longitudinally oriented median domain that covers the primitive streak as it emerges and lengthens anteriorly during stage 3 (Fig. 4O).

## 4. Discussion

### 4.1. Anterior vs. posterior differentiation and the three stages at the start of mammalian gastrulation

The combination of microscopical analysis of dorsal views and serial sections of the same embryo, either after the relatively “strong” glutaraldehyde and  $\text{OsO}_4$  fixation for tissue density and ultrastructural analysis or after the relatively “weak” paraformaldehyde fixation and in situ hybridisation for gene expression analysis, demonstrated how the same tissue (e.g. the hypoblast and its contact area with the epiblast) changed differently according to fixation: Paraformaldehyde apparently led to an instant but mild shrinkage of both layers (Fig. 4F) while glutaraldehyde (with its two aldehyde moieties per molecule) led to a strong shrinkage of the hypoblast (probably due to cross-linking the hypoblast's high content of the cytoskeletal protein cytokeratin, cf. Viebahn et al., 1992), which then forced the epiblast into a dome-shape widely separated from the hypoblast (cf. Fig. 2G, a situation previously described also by Vejlsted et al., 2006, their Fig. 1c). Importantly, the same principal structural characteristics (e.g. overall embryo shape or cellular height and density) could be identified reliably under both fixation conditions (cf. Figs. 2G and 4F): paraformaldehyde led to only small cellular shrinkage artefacts and provided well-preserved tissue (cell layer) integrity whereas glutaraldehyde and  $\text{OsO}_4$  provided excellent fine structural detail (and marked cellular shrinkage), which could then be allocated to the appropriate cell type by comparison with the well-preserved tissue integrity of the paraformaldehyde-fixed specimens of the same stage. Both methods, combined with the gene expression analysis, helped to define three morphogenetic steps at the beginning of mammalian gastrulation, and comparison with the other commonly available mammalian laboratory species, i.e. mouse and rabbit, suggests that these steps apply to mammals in general (see below).

Gastrulation proper starts when the first mesoderm cells break through the basement membrane of the epiblast at the posterior extremity of the emerging primitive streak (see Fig. 3H). The start of gastrulation is preceded (1) by a morphogenetic step in which anterior–posterior axial differentiation is achieved through the appearance of APD (AVE in the mouse, AMC in the rabbit, AHB in the pig) expressing *sox17* (mouse: Pfister et al., 2007; rabbit: Hassoun et al., 2009; pig: this study), and (2) by a more functionally defined step in which epiblast cells start expressing the mesoderm marker gene *brachyury* and accumulate as mesoderm precursors near the posterior pole similar to the situation in the pregastrulation embryo of mouse (Perea-Gomez et al., 2004; Rivera-Perez and Magnuson, 2005) and rabbit (Viebahn et al., 2002). As in the rabbit, this early *brachyury* domain in the pig has a crescent-like shape and turns the

previously spherical embryonic disc into an oval by extending the embryonic disc towards the posterior pole; in the rabbit this crescent-shaped area was indeed shown to be formed as the result of posterior movement of epiblast cells towards the posterior midline and was, therefore, named PGE (for posterior gastrula extension, Viebahn et al., 2002).

In accordance with the staging system for the beginning of gastrulation in chick (Hamburger and Hamilton, 1992) and rabbit (Viebahn, 2004), we would like to designate the three steps mentioned above to define stages 1, 2 and 3 in the pig. Numerically, these three steps coincide with the 3 steps defined by Vejlsted et al. (2006) recently for the early gastrulation of the pig; however, comparison of their specimens with our correlative histological and axial gene expression analysis suggests that their “pre-streak stage 2” (their Fig. 1c) shows, indeed, the pseudostratification of the epiblast typical for the late pre-streak stage defined in the present report (cf. Figs. 1H and 2C and G). Moreover, Vejlsted et al. (2006) described a “pre-streak stage 1” to have an epiblast “fully exposed” (i.e. lacking Rauber’s layer) but to show no signs of polarity, whereas all embryos that lack Rauber’s layer in the present study show clear signs of anterior differentiation (i.e. AHB) in the histological sections. We therefore suggest that the two pre-streak stages of Vejlsted may be useful to subdivide our stage 2 into an early (Rauber’s layer removed) and late (pseudostratified posterior epiblast) stage 2, but that the appearance of the AHB may define stage 1 to stress the role of the hypoblast in defining the anterior–posterior axis prior to primitive streak formation. As a minor point for characterising stage 3, we do not find (R.H. unpublished) that a node forms “during initial development of the primitive streak” (Vejlsted et al., 2006).

Remarkably, these early steps of axial differentiation can be considered to be independent of other morphological specificities, i.e. globe-like (pig) vs. disc-like (rabbit) shape of epiblast at stage 1, or gradual (rabbit) vs. rapid loss (pig) of Rauber’s layer at stage 2; the steps can also be correlated with stages in the mouse (Theiler, 1989; Kaufman, 1992; Downs and Davies, 1993; Tam and Gad, 2004), which presents, again, a different topographical situation (e.g., egg-cylinder shape, polar trophoblast preserved to form the placenta). As it is technically quite challenging to visualise the characteristics of pregastrulation stages in living embryos of pig (Meijer et al., 2000; Fléchon et al., 2004; Vejlsted et al., 2006) and mouse (Downs and Davies, 1993), we suggest that a uniform staging system for early mammalian development should, at the present time, be built on morphogenetic steps whose structural results (e.g. APD, primitive streak, EMT, Hensen’s node, notochordal process) can be defined using histological methods.

In the case of initial mesoderm formation, which is the histologically defined result of primitive streak formation, the pig shows an unusually thick and enduring basement membrane in the vicinity of the primitive streak. Unlike basement membranes of most epithelia it is clearly visible in the light microscope (Fig. 3; cf. Vejlsted et al., 2006, their Fig. 1c). In addition, this thick basement membrane is supported by an as yet undefined dense extracellular matrix on its abepithelial side. As this “reinforced” basement membrane stays intact underlying the primitive streak for a long period of development, the primitive streak of the pig obtains its initial density through pseudostratification of the epiblast (Fig. 3H, previously also described by Vejlsted et al., 2006) rather than through ingression and accumulation of mesoderm cells ventral to the primitive streak as in other mammals (Poelmann, 1981; Viebahn et al., 1995b; for possible functional implications see below). How the apparently “pre-mature” expression of the mesoderm marker vimentin within the whole pre-streak embryonic disc (Prelle et al. 2001) or the

polarised expression of the organizer gene *gooseoid* (Meijer et al., 2000) fits the sequence of axial differentiation described here remains to be clarified in future studies.

#### 4.2. Significance of specific anterior pregastrulation differentiation

The most pronounced species specificity revealed in this study applies to the morphologically and molecularly defined shape of the APD in the pig: it has a disc-like configuration and straddles the anterior embryonic disc border, whereas in mouse and rabbit the APD has a crescent-like configuration and is confined to the embryonic disc (the border of the embryonic disc being defined by the epiblast; Viebahn et al., 1995a). This difference is particularly remarkable because both rabbit and pig go through gastrulation as flat discs, which are integrated into the surface of an expanding blastocyst (see Streeter (1927) and Rabl (1915) for description of complete gastrulation stages in pig and rabbit, respectively); pig and rabbit can, therefore, be expected to have quite similar requirements for the control of the gastrulation process. However, a plausible explanation for the different APD shapes may lie in the different modes of extraembryonic mesoderm formation, which, in turn, reflect specific requirements for nutrition of the embryo and enclosure by a complete amnion. Both these characteristics vary markedly amongst mammals and, not least, between pig and rabbit. Equipped with the vast surface area of a filamentous, unusually long blastocyst (measuring up to 100 centimeters; see Perry et al., 1976), the pig embryo can “afford” to delay attachment and placenta formation to late somite stages; in this situation the blastocyst remains “free-floating” within the uterus for a comparatively long time and this situation requires protection of the developing embryo proper through the formation of the amnion at a much earlier stage than the rabbit embryo, for example. The latter attaches firmly to the endometrium during gastrulation soon after hatching from the zona pellucida and can therefore “afford” to delay amnion formation to the stages following neurulation (Rabl, 1915).

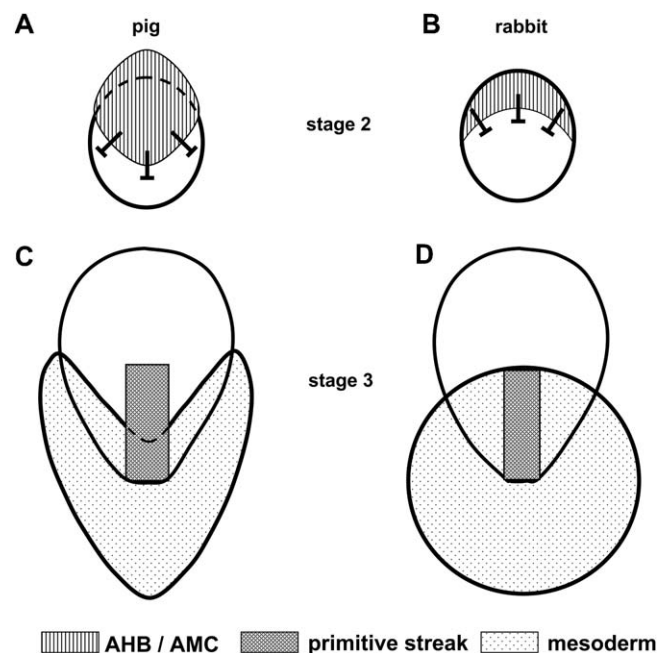


**Fig. 5.** Schematic correlation of shape and presumed inhibitory influence (inverted T-shapes) of APD at stage 2 (A, B) with area covered by mesoderm at stage 3 (C, D) in pig (A, C) and rabbit (B, D) embryos.

The different schedule of amnion formation is presaged at stage 3 by differential growth and spread of extraembryonic mesoderm (Fig. 5C and D), which is needed to support the delicate amnion epithelium on its chorionic side. By extending across the emerging anterior half of the primitive streak, from which most intraembryonic mesoderm derives, and through the signaling molecules typically expressed in the APD (cf. Idkowiak et al., 2004), the large circular AHB of the pig may delay intraembryonic mesoderm formation for a longer period than in species with smaller APD. The signals of the AHB may also inhibit dissolution of the basement membrane required for EMT in this area (Rowe and Weiss, 2008; Nakaya et al., 2008, see also Egea et al., 2008 and Yang and Weinberg, 2008) and may, indeed, be responsible for the deposition of the additional extracellular matrix material on the hypoblast side of the epiblast basement membrane (Fig. 3M–N). Together these activities of the AHB would provide the posterior half of the primitive streak, which is under different molecular control from the anterior half (cf. Martin and Kimelman, 2008) and produces mainly extraembryonic mesoderm, with a distinct growth advantage. The inhibiting, possibly negative, chemotactic influence of the disc-shaped AHB (Fig. 5A) may also force extraembryonic mesoderm to spread anteriorly along the embryonic disc borders only (Fig. 5C). In the rabbit, in contrast, the inhibiting influence of the hypoblast in the (crescent-shaped) AMC (Fig. 5B) may be more limited (e.g. limited to the anterior circumference of the embryonic disc), allowing ingression (and anterolateral migration) of mesoderm cells almost simultaneously along the whole of the primitive streak; consequently, intra- and extraembryonic mesoderm emerge from the primitive streak as a common circular mesodermal plate at stage 3 (Fig. 5D) and migrate “in register” with each other towards the anterior border of the embryonic disc at later stages (cf. Viebahn et al., 1992).

During the developmental period described here, AHB in the pig appears to have moved posteriorly (cf. Fig. 1G for stage 1, Fig. 2G for stage 2 and Fig. 3D for stage 3). This is in contrast to the situation in the mouse where the AVE cells were shown to migrate anteriorly (Thomas and Beddington, 1996) but it correlates, again, with the different structural requirements in these two species. The egg-cylinder shape of the mouse forces the posterior end of the streak to lie unusually close, indeed, to the anterior pole. In this situation, posterior movement of AVE in the mouse would possibly lead to overgrowth of extraembryonic mesoderm anteriorly, which may then interfere with ongoing head induction. Anterior movement of the AVE may, instead, prevent this unwanted influence by acting as a broad median barrier for extraembryonic mesoderm and by channelling thus the extraembryonic mesoderm towards rodent-specific allantoic bud formation (cf. Downs et al., 2009).

Although direct molecular evidence for these functional roles of the AHB is still lacking, the strong *nodal* expression in the hypoblast at the centre of the embryonic disc at stage 2 suggests a critical function of nodal signaling (and activities of its convertases, cf. Ben-Haim et al., 2006) in the differential development of the prospective anterior and posterior halves of the primitive streak.

Taken as a whole, our analysis unravels similarities and discrepancies with regard to axial differentiation between seemingly close relatives of the mammalian phylogenetic tree. This underlines similarities with models of molecular axial differentiation in other vertebrates (Yu et al., 2007) and, at the same time, offers explanations for interspecific variabilities, at least in extraembryonic tissues, possibly due to variations in shape of seemingly simple transient axial organs. These variations may be caused by small variations in proliferative activity and may, in turn, influence subsequent stages, resulting in major changes to the adult body plan. Apart from the necessity to

provide functional proof for a role of APD (and *sox17* expression) in axial and extraembryonic tissue differentiation, questions arise as to how Rauber's layer can be removed so rapidly in the pig, how the anterior pregastrulation differentiation is established at the anterior pole in its specific shape, and what may be the biochemical composition of the thick basement membrane and its extracellular matrix material in the area of the primitive streak.

## Acknowledgements

The excellent technical assistance of Kirsten Falk-Stietenroth, Heike Faust, Irmgard Weiß (Göttingen) and of Antje Frenzel and Birgit Sieg (Mariensee) is gratefully acknowledged. We further thank Dr. Detlef Rath of the Institute of Animal Breeding (Mariensee) for the supply with pregnant gilts and the use of the professional animal facilities. This work was supported by a scholarship grant of the Syrian Government (to R.H. of Tishreen University, Syria), a Ph.D. fellowship from the Boehringer Ingelheim Fonds (to K.F.) and by the Deutsche Forschungsgemeinschaft (to M.B. and C.V.).

## References

- Albazerchi, A., Stern, C.D., 2007. A role for the hypoblast (AVE) in the initiation of neural induction, independent of its ability to position the primitive streak. *Dev. Biol.* 301, 489–503.
- Ang, S.L., Constam, D.B., 2004. A gene network establishing polarity in the early mouse embryo. *Semin. Cell Dev. Biol.* 15, 555–561.
- Arnold, S.J., Robertson, E.J., 2009. Making a commitment: cell lineage allocation and axis patterning in the early mouse embryo. *Nat. Rev. Mol. Cell Biol.* 10, 91–103.
- Barends, P.M.G., Stroband, H.W.J., Taverne, N., te Kronnie, G., Leen, M.P.J.M., Blommers, P.C.J., 1989. Morphology of the preimplantation pig blastocyst during expansion and loss of polar trophectoderm (Rauber cells) and the morphology of the embryoblast as an indicator for developmental stage. *J. Reprod. Fertil.* 87, 715–726.
- Beddington, R.S., Robertson, E.J., 1998. Anterior patterning in mouse. *Trends Genet.* 14, 277–284.
- Behringer, R.R., Eakin, G.S., Renfree, M.B., 2006. Mammalian diversity: gametes, embryos and reproduction. *Reprod. Fertil. Dev.* 18, 99–107.
- Behringer, R.R., Wakamiya, M., Tsang, T.E., Tam, P.P., 2000. A flattened mouse embryo: leveling the playing field. *Genesis* 28, 23–30.
- Ben-Haim, N., Lu, C., Guzman-Ayala, M., Pescatore, L., Mesnard, D., Bischofberger, M., Naef, F., Robertson, E.J., Constam, D.B., 2006. The nodal precursor acting via activin receptors induces mesoderm by maintaining a source of its convertases and BMP4. *Dev. Cell* 11, 313–323.
- Blomberg, L., Hashizume, K., Viebahn, C., 2008. Blastocyst elongation, trophoblastic differentiation, and embryonic pattern formation. *Reproduction* 35, 181–195.
- Chuva de Sousa Lopes, S.M., Hayashi, K., Surani, M.A., 2007. Proximal visceral endoderm and extraembryonic ectoderm regulate the formation of primordial germ cell precursors. *BMC Dev. Biol.* 20, 140.
- del Barco Barrantes, I., Davidson, G., Grone, H.J., Westphal, H., Niehrs, C., 2003. Dkk1 and noggin cooperate in mammalian head induction. *Genes Dev.* 17, 2239–2244.
- Downs, K.M., Davies, T., 1993. Staging of gastrulating mouse embryos by morphological landmarks in the dissecting microscope. *Development* 118, 1255–1266.
- Downs, K.M., Inman, K.E., Jin, D.X., Enders, A.C., 2009. The Allantoic Core Domain: new insights into development of the murine allantois and its relation to the primitive streak. *Dev. Dyn.* 238, 532–553.
- Egea, J., Erlacher, C., Montanez, E., Burtcher, I., Yamagishi, S., Hess, M., Hampel, F., Sanchez, R., Rodriguez-Manzaneque, M.T., Bosl, M.R., Fassler, R., Lickert, H., Klein, R., 2008. Genetic ablation of FLRT3 reveals a novel morphogenetic function for the anterior visceral endoderm in suppressing mesoderm differentiation. *Genes Dev.* 22, 3349–3362.
- Flechon, J.E., 1978. Morphological aspects of the embryonic disc at the time of appearance in the blastocyst of the farm mammals. *Scan. Electron Microsc.* 2, 541–548.
- Flechon, J.E., Laurie, S., Notarianni, E., 1995. Isolation and characterisation of a feeder-dependent, porcine trophoblast cell line isolated from a 9-day blastocyst. *Placenta* 16, 643–658.
- Flechon, J.E., Degrouard, J., Flechon, B., 2004. Gastrulation events in the prestreak pig embryo: ultrastructure and cell markers. *Genesis* 38, 13–25.
- Geisert, R.D., Brookbank, J.W., Roberts, R.M., Bazer, F.W., 1982. Establishment of pregnancy in the pig: II. Cellular remodeling of the porcine blastocyst during elongation on day 12 of pregnancy. *Biol. Reprod.* 27, 941–955.

- Georgiades, P., Rossant, J., 2006. *Ets2* is necessary in trophoblast for normal embryonic anteroposterior axis development. *Development* 133, 1059–1068.
- Hallonet, M., Kaestner, K.H., Martin-Parras, L., Sasaki, H., Betz, U.A., Ang, S.L., 2002. Maintenance of the specification of the anterior definitive endoderm and forebrain depends on the axial mesendoderm: a study using HNF3beta/Foxa2 conditional mutants. *Dev. Biol.* 243, 20–33.
- Hamburger, V., Hamilton, H.L., 1992. A series of normal stages in the development of the chick embryo. *Dev. Dyn.* 195, 231–272.
- Hassoun, R., Püschel, B., Viebahn, C., 2009. *Sox17* expression patterns during gastrulation and early neurulation in the rabbit suggest two sources of endoderm formation. *Cells Tissues Organs*, in press.
- Herrmann, B.G., Labeit, S., Poustka, A., King, T.R., Lehrach, H., 1990. Cloning of the *T* gene required in mesoderm formation in the mouse. *Nature* 343, 617–622.
- Herrmann, B.G., 1991. Expression pattern of the *Brachyury* gene in whole mount TWis/TWis mutant embryos. *Development* 113, 913–917.
- Heuser, C.H., Streeter, G.L., 1929. Early stages in the development of pig embryos, from the period of initial cleavage to the time of appearance of limb-buds. *Carnegie Inst Pub No.* 394. *Contrib. Embryol.* 20, 1–30.
- Idkowiak, J., Weisheit, G., Plitzner, J., Viebahn, C., 2004. Hypoblast controls mesoderm generation and axial patterning in the gastrulating rabbit embryo. *Dev. Genes Evol.* 214, 591–605.
- Kaufman, M.H., 1992. *The Atlas of Mouse Development*. Academic Press, London.
- Kimura, C., Yoshinaga, K., Tian, E., Suzuki, M., Aizawa, S., Matsuo, I., 2000. Visceral endoderm mediates forebrain development by suppressing posteriorizing signals. *Dev. Biol.* 225, 304–321.
- Knoetgen, H., Viebahn, C., Kessel, M., 1999. Head induction in the chick by primitive endoderm of mammalian, but not avian origin. *Development* 126, 815–825.
- Kölliker, A., 1879. *Entwicklungsgeschichte des Menschen und der Höheren Thiere*. Wilhelm Engelmann, Leipzig.
- Liguori, G.L., Borges, A.C., D'Andrea, D., Liguoro, A., Goncalves, L., Salgueiro, A.M., Persico, M.G., Belo, J.A., 2008. Cripto-independent nodal signaling promotes positioning of the A–P axis in the early mouse embryo. *Dev. Biol.* 315, 280–289.
- Lu, C.C., Robertson, E.J., 2004. Multiple roles for nodal in the epiblast of the mouse embryo in the establishment of anterior–posterior patterning. *Dev. Biol.* 273, 149–159.
- Martin, B.L., Kimelman, D., 2008. Regulation of canonical Wnt signaling by *Brachyury* is essential for posterior mesoderm formation. *Dev. Cell* 15, 121–133.
- Meijer, H.A., Van De Pavert, S.A., Stroband, H.W.J., Boerjan, M.L., 2000. Expression of the organizer specific Homeobox gene *Gooseoid* (*gsc*) in porcine embryos. *Mol. Reprod. Dev.* 55, 1–7.
- Mesnard, D., Guzman-Ayala, M., Constam, D.B., 2006. Nodal specifies embryonic visceral endoderm and sustains pluripotent cells in the epiblast before overt axial patterning. *Development* 133, 2497–2505.
- Nakaya, Y., Sukowati, E.W., Wu, Y., Sheng, G., 2008. RhoA and microtubule dynamics control cell–basement membrane interaction in EMT during gastrulation. *Nat. Cell Biol.* 10, 765–775.
- Papaioannou, V.E., Ebert, K.M., 1988. The preimplantation pig embryo: cell number and allocation to trophectoderm and inner cell mass of the blastocyst in vivo and in vitro. *Development* 102, 793–803.
- Patten, B.M., 1948. *Embryology of the Pig*. McGraw-Hill, New York.
- Perry, J.S., Rowlands, I.W., 1962. Early pregnancy in the pig. *J. Reprod. Fertil.* 4, 175–188.
- Perea-Gomez, A., Camus, A., Moreau, A., Grieve, K., Moneron, G., Dubois, A., Cibert, C., Collignon, J., 2004. Initiation of gastrulation in the mouse embryo is preceded by an apparent shift in the orientation of the anterior–posterior axis. *Curr. Biol.* 14, 197–207.
- Perea-Gomez, A., Meilhac, S.M., Piotrowska-Nitsche, K., Gray, D., Collignon, J., Zernicka-Goetz, M., 2007. Regionalization of the mouse visceral endoderm as the blastocyst transforms into the egg cylinder. *BMC Dev. Biol.* 7, 96.
- Perry, J.S., Heap, R.B., Burton, R.D., Gadsby, J.E., 1976. Endocrinology of the blastocyst and its role in the establishment of pregnancy. *J. Reprod. Fertil. Suppl.* , 85–104.
- Pfister, S., Steiner, K.A., Tam, P.P., 2007. Gene expression pattern and progression of embryogenesis in the immediate post-implantation period of mouse development. *Gene Expr. Patterns* 7, 558–573.
- Poelmann, R.E., 1981. The formation of the embryonic mesoderm in the early post-implantation mouse embryo. *Anat. Embryol.* 162, 29–40.
- Prelle, K., Holtz, W., Osborn, M., 2001. Immunocytochemical analysis of vimentin expression patterns in porcine embryos suggests mesodermal differentiation from day 9 after conception. *Anat. Histol. Embryol* 30, 339–344.
- Rabl, C., 1915. Edouard van Beneden und der gegenwärtige Stand der wichtigsten von ihm behandelten Probleme. *Arch. Mikrosk. Anat.* 88, 3–470.
- Reupke, T., Puschel, B., Viebahn, C., 2009. Tracing and ablation of single cells in the mammalian blastocyst using fluorescent DNA staining and multi-photon laser microscopy. *Histochem. Cell Biol.* 131, 521–530.
- Rivera-Perez, J.A., Magnuson, T., 2005. Primitive streak formation in mice is preceded by localized activation of *Brachyury* and *Wnt3*. *Dev. Biol.* 288, 363–371.
- Rosenquist, T.A., Martin, G.R., 1995. Visceral endoderm-1 (VE-1): an antigen marker that distinguishes anterior from posterior embryonic visceral endoderm in the early post-implantation mouse embryo. *Mech. Dev.* 49, 117–121.
- Rossant, J., Tam, P.P., 2009. Blastocyst lineage formation, early embryonic asymmetries and axis patterning in the mouse. *Development* 136, 701–713.
- Rowe, R.G., Weiss, S.J., 2008. Breaching the basement membrane: who, when and how? *Trends Cell Biol.* 18, 560–574.
- Schwartz, P., Piper, H.M., Spahr, R., Spieckermann, P.G., 1984. Ultrastructure of cultured adult myocardial cells during anoxia and reoxygenation. *Am. J. Pathol.* 115, 349–361.
- Selwood, L., Johnson, M.H., 2006. Trophoblast and hypoblast in the monotreme, marsupial and eutherian mammal: evolution and origins. *Bioessays* 28, 128–145.
- Streeter, G.L., 1927. Development of the mesoblast and notochord in pig embryos. *Carnegie Instn Wash Publ* 380. *Contrib. Embryol.* 19, 73–92.
- Tam, P.P.L., Gad, J.M., 2004. Gastrulation in the mouse. In: Stern, C.D. (Ed.), *Gastrulation*. Cold Spring Harbor Laboratory Press, Cold Spring Harbor, NY, USA, pp. 233–262.
- Theiler, K., 1989. *The House Mouse: Atlas of Embryonic Development*. Springer, New York.
- Thomas, P.Q., Beddington, R.S.P., 1996. Anterior primitive endoderm may be responsible for patterning the anterior neural plate in the mouse embryo. *Curr. Biol.* 6, 1487–1496.
- Vejlsted, M., Du, Y., Vajta, G., Maddox-Hyttel, P., 2006. Post-hatching development of the porcine and bovine embryo—defining criteria for expected development in vivo and in vitro. *Theriogenology* 65, 153–165.
- Viebahn, C., 1999. The anterior margin of the mammalian gastrula: comparative and phylogenetic aspects of its role in axis formation and head induction. *Curr. Top. Dev. Biol.* 46, 63–103.
- Viebahn, C., 2004. Gastrulation in the rabbit. In: Stern, C.D.S. (Ed.), *Gastrulation*. Cold Spring Harbor Laboratory Press, Cold Spring Harbor, NY, USA, pp. 263–274.
- Viebahn, C., Lane, E.B., Ramaekers, F.C.S., 1992. Intermediate filament protein expression and mesoderm formation in the rabbit. A double-labelling immunofluorescence study. *Roux's Arch. Dev. Biol.* 201, 45–60.
- Viebahn, C., Mayer, B., Hrabé de Angelis, M., 1995a. Signs of the principal body axes prior to primitive streak formation in the rabbit embryo. *Anat. Embryol.* 192, 159–169.
- Viebahn, C., Mayer, B., Miething, A., 1995b. Morphology of incipient mesoderm formation in the rabbit embryo: a light- and retrospective electron-microscopic study. *Acta Anat.* 154, 99–110.
- Viebahn, C., Stortz, C., Mitchell, S.M., Blum, M., 2002. Low proliferative and high migratory activity in the area of *Brachyury* expressing mesoderm progenitor cells in the gastrulating rabbit embryo. *Development* 129, 2355–2365.
- Voiculescu, O., Bertocchini, F., Wolpert, L., Keller, R.E., Stern, C.D., 2007. The amniote primitive streak is defined by epithelial cell intercalation before gastrulation. *Nature* 449, 1049–1052.
- Weisheit, G., Mertz, K.D., Schilling, K., Viebahn, C., 2002. An efficient in situ hybridization protocol for multiple tissues sections and probes on miniaturized slides. *Dev. Genes Evol* 212, 403–406.
- Wianny, F., Perreau, C., Hochereau de Rieviers, M.T., 1997. Proliferation and differentiation of porcine inner cell mass and epiblast in vitro. *Biol. Reprod.* 57, 756–764.
- Yang, J., Weinberg, R.A., 2008. Epithelial–mesenchymal transition: at the crossroads of development and tumor metastasis. *Dev. Cell* 14, 818–829.
- Yu, J.K., Satou, Y., Holland, N.D., Shin, I.T., Kohara, Y., Satoh, N., Bronner-Fraser, M., Holland, L.Z., 2007. Axial patterning in cephalochordates and the evolution of the organizer. *Nature* 445, 613–617.

## **5.2 The second publication**

Hassoun R, Püschel P, Viebahn C (2009): Sox17 expression patterns during gastrulation and early neurulation in the rabbit suggest two sources of endoderm formation. *Cells Tissues Organs*. In press

# Sox17 Expression Patterns during Gastrulation and Early Neurulation in the Rabbit Suggest Two Sources of Endoderm Formation

Romia Hassoun Bernd Püschel Christoph Viebahn

Abteilung Anatomie und Embryologie, Zentrum Anatomie, Georg-August-Universität, Göttingen, Germany

## Key Words

Primitive streak · Epiblast · Anterior marginal crescent · In situ hybridization · Mammalian embryo · Development

## Abstract

Most gastrointestinal tract and associated gland epithelia originate from the endoderm germ layer discovered by Pander in 1817. The recent surge in stem cell concepts revived interest in the findings of 30 years ago that the endoderm layer itself originates from the epiblast (which since Pander's time had been held to be the forerunner of the ectoderm and mesoderm germ layers only). However, the question as to which parts of the mammalian gastrulation-stage embryonic disc generate endoderm cells is still unresolved. Therefore, the expression of the gene coding for the transcription factor Sox17, a key transcription factor involved in endoderm formation in mouse, chick, frog, and zebrafish, was analyzed in the rabbit, a model organism for mammalian gastrulation morphology, using whole-mount in situ hybridization and high-resolution histological analysis of embryos at gastrulation and early neurulation stages. Sox17 mRNA in the mesoderm and lower layer (hypoblast) compartments within and adjacent to Hensen's node and the anterior segment of the primitive streak confirmed the validity of this approach, as this region had previously been shown to form endoderm in mouse and chick. However, Sox17 expression in central and posterior epiblast at pregastrulation stages together with a

transient expression at the posterior extremity of the primitive streak suggest that endoderm (possibly hindgut) may be formed close to the emerging cloacal membrane, as well.

Copyright © 2009 S. Karger AG, Basel

## Introduction

In the early vertebrate embryo, the endoderm is classically defined as the ventral germ layer which is the precursor of the epithelial lining of the primitive gut tube and which, during organogenesis, regionalizes along its anterior-posterior and dorsal-ventral axes to give rise to the epithelia of the gastrointestinal tract, the respiratory tract and associated organs such as liver and pancreas as well as thyroid gland and thymus. In amniotes, the evi-

## Abbreviations used in this paper

AMC	anterior marginal crescent
AVE	anterior visceral endoderm
d.p.c.	days post coitum
HMG	high mobility group
ISHS	in situ hybridisation signal
PGE	posterior gastrula extension

dence that the endoderm (also called ‘definitive endoderm’) itself is derived from the epiblast and not from the pre-existing primitive endoderm (or hypoblast) of the early embryonic disc is comparatively new (when considering the time that has elapsed since the first description of the endoderm as the ‘Schleimschicht’ in the chick by [Pander, 1817]). This evidence stems from experiments using mouse blastocyst injection chimeras [Gardner and Rossant, 1979], from tissue potency analysis of the epiblast at the primitive streak stage in rat embryos [Levak-Svajger and Svajger, 1974] as well as from the microsurgical grafts of both distal and anterior regions of the mouse embryonic epiblast to ectopic sites at the primitive streak stages [reviewed by Beddington, 1983; Skreb et al., 1976]. Endoderm fate maps were constructed accordingly for mouse [Lawson et al., 1986, 1987, 1991; Tam et al., 2007] and chick [Kimura et al., 2006; Kirby et al., 2003; Lawson and Schoenwolf, 2003] and suggest that extensive cellular movements (similar to those observed in lower vertebrates [frog: Keller, 1975, 1976; Chalmers and Slack, 2000; zebrafish: Warga and Nüsslein-Volhard, 1999] occur in the primitive streak area of the gastrulating embryo and eventually contribute to formation of the endoderm [Lawson and Pedersen, 1992; Parameswaran and Tam, 1995; Quinlan et al., 1995; Lawson, 1999]. These migrating epiblast cells also form the other principal germ layers (ectoderm and mesoderm) and thus establish the whole body plan, which makes for even more complex morphogenetic movements at the cellular level. For example, the progenitors of the gut endoderm are initially localized in the distal regions of the mouse egg cylinder together with mesoderm-forming cells and are, therefore, also called mesendoderm [Beddington, 1981; Tam and Beddington, 1987; Tam, 1989]; these cells are thought to ingress through the anterior segment of the primitive streak 8–10 h after the onset of gastrulation, i.e. at mid-streak stage, and undergo epithelial-mesenchymal transition. Subsequently, some of these cells relocate to the ventral-most layer of the embryo and form an epithelium again while others retain a mesenchymal character and stay in the mesoderm compartment [Kadokawa et al., 1987; Lawson et al., 1987; Tam and Beddington, 1992]. The newly recruited endoderm cells rapidly expand anteriorly and laterally to displace progressively the pre-existing primitive (or visceral) endoderm to extraembryonic sites [Lawson et al., 1986, 1987; Tam et al., 1993; Lin et al., 1994]. Most recently, however, live imaging experiments carried out in the mouse suggest an even more complex but only partial integration of epiblast-derived cells into visceral endoderm, which is then followed by recruitment of vis-

ceral endoderm cells to form endoderm-derived tissues [Kwon et al., 2008].

Basic molecular mechanisms involved in endoderm specification have been elucidated in several vertebrate model animals such as frog (*Xenopus*), zebrafish, chick and mouse. The key zygotic factors in the signaling pathway, which are conserved within these species, are the Nodal-related TGF $\beta$  signaling ligands, the Mix-like family of homeodomain transcription factors, the Gata4/5/6 zinc-finger transcription factors and, finally, the high mobility group (HMG) DNA-binding protein Sox17 [Woodland and Zorn, 2008]. Related to the ‘sex-determining gene on the Y chromosome (*sry*)’ *sox17* belongs to the Sox subgroup F [Lefebvre et al., 2007] and was originally identified as a stage-specific transcriptional regulator during mouse spermatogenesis [Kanai et al., 1996]. *Sox17* was then implicated in endoderm formation when its orthologs *Xsox17 $\alpha$*  (and *Xsox17 $\beta$* ) and *Zsox17* were found to be expressed specifically in the endoderm of *Xenopus* [Hudson et al., 1997] and zebrafish [Alexander and Stainier, 1999], respectively, and when *sox17* was indeed found in the endoderm in a highly dynamic pattern in the mouse [Kinder et al., 2001; Kanai-Azuma et al., 2002]. Interestingly, murine *sox17*-null cells are able to contribute to the early endoderm along the whole intestinal tube; however, from 8.0 days post coitum (d.p.c.) onwards, increased apoptosis in the foregut and failure of mutant cells to differentiate and proliferate in the posterior gut lead to a depletion of endoderm; furthermore, *sox17*-null ES cells are unable to compete with the wild-type cells in colonizing the gut endoderm in the chimeras [Kanai-Azuma et al., 2002]. These functional studies thus made *sox17* known as a key downstream regulatory component of the signaling pathway which is involved in endoderm induction and endoderm differentiation.

Whereas a wealth of information on the cellular fate and on signalling pathways regulating endoderm differentiation is thus available, the topographic distribution of endoderm differentiation signals within the tissue compartments of the early embryo is still little studied, although such knowledge may reveal important clues as to the principles of endoderm formation. To find a location for initial endoderm formation and to differentiate between characteristics of primitive and definitive endoderm, we report here on the tissue distribution of *sox17* in the rabbit embryo throughout gastrulation, i.e. from pre-streak to early somite stages. This may lead to a prospective sequential map for the time and the exact place of origin of the endoderm in mammals. As the endoderm is a central structure around which the body plan is con-



structed, a morphogenetic map for the specification of the mammalian germ layers in general may emerge as well.

## Materials and Methods

### *Animal Tissues*

Uteri of naturally mated New Zealand White rabbits (Lammers, Euskirchen, Germany) were removed through cesarean section after injecting an overdose (320 mg) of Narcoren® (Merial, Halbergmoos, Germany) intravenously. Blastocysts at 6.25–6.75 d.p.c. were flushed using warm sterile phosphate-buffered saline (PBS) and then washed in warm PBS twice to remove blood and cellular residue. Older embryos (7.0–8.0 d.p.c.) were dissected from uteri suspended in sterile PBS using iridectomy scissors after opening the uterine wall antimesometrially. After flushing or primary dissection embryos were fixed in 4% paraformaldehyde (PFA) in phosphate buffer for 1 h at room temperature and dissected using iridectomy scissors or flame-polished tungsten needles to eliminate the coats (zona pellucida equivalents or 'neozona' [Denker, 2000]) and most of the extraembryonic tissue. Embryos were staged using dark-field optics according to the developmental stages 1 to stage 7 as defined in [Viebahn, 2004] and [Blum et al., 2007]. Stages and embryonic age corresponded roughly as follows: 6.25 to 6.75 d.p.c.: stages 1 to 4; 7.0 to 7.6 d.p.c.: stages 5 and 6; 8.0 d.p.c.: stage 7. The dissected embryonic discs were dehydrated and stored in 100% ethanol at –20°C until used for in situ hybridization.

### *In situ Hybridization*

Digoxigenin-labeled mRNA probes were generated using a 707-bp mouse *Sox17* cDNA (kind gift of Dr. H. Lickert, München, Germany), which spans the coding region from nucleotides No. 1102 through to 1808 of the mouse *sox17* cDNA (GenBank accession No. NM\_011441), and chemocompetent cells (DH5alpha *Escherichia coli* cells, Invitrogen, Karlsruhe, Germany) and chemicals (Roche, Mannheim, Germany or Merck, Darmstadt, Germany) as described [Weisheit et al., 2002]. In situ hybridization procedure was carried out using a standard protocol [Lowe et al., 1996; Belo et al., 1997], which had been adapted for the requirements of early rabbit embryonic discs [Weisheit et al., 2002]. As a first step the stored embryonic discs were transferred to nylon baskets under strictly sterile conditions, rehydrated and treated with proteinase K [10 µg/ml proteinase K in PBT (PBS containing 0.1% Tween 20; Sigma, München, Germany)] at room temperature for different periods of time according to their stage of development as follows: 1 min for stage 0; 2 min for stages 1 and 2; 3 min for stage 3; 5 min for stage 4 embryos [Idkowiak et al., 2004]; 10 min for stage 5; 15 min for stage 6 and 20 min for stage 7 embryos; next, all embryos were fixed for 20 min in 0.2% glutaraldehyde/PBT. Hybridization buffer consisted of 50% formamide, 1.4 × SSC (pH 4.5), 0.5 mM EDTA, 50 µg/ml t-RNA, 0.2% Tween 20, 0.5% CHAPS and 50 µg/ml heparin (Sigma). During the pre-hybridization (70°C for 1 h in the hybridization buffer) and hybridization processes (70°C overnight in the hybridization buffer with 1 µl cRNA previously denatured at 95°C for 5 min) the baskets containing the embryonic discs were transferred to sterile screw-top PVC tubes (Bibby-Sterilin, Staffordshire, UK).

To remove the unbound cRNA, the embryos were washed in hybridization buffer and MABT (100 mM maleic acid, 150 mM NaCl, 0.1% Tween 20, pH 7.5). To block nonspecific antibody-binding sites, the embryos were incubated in MABT with 2% Roche blocking reagent and 20% heat-inactivated goat serum; hybridized RNA was visualized using anti-digoxigenin antibody coupled to alkaline phosphatase and BM-purple substrate (both Roche, Mannheim, Germany). Finally, embryos were removed from the nylon baskets and transferred to Petri dishes filled with the substrate to initiate the color reaction, which was then allowed to proceed at room temperature in the dark to exhaustion of the alkaline phosphatase enzyme, i.e. until no further accumulation of the bluish BM-purple reaction product (which started to appear on the second day of BM-purple incubation) was observed in the stereo microscope at high magnification (usually within 4–9 days).

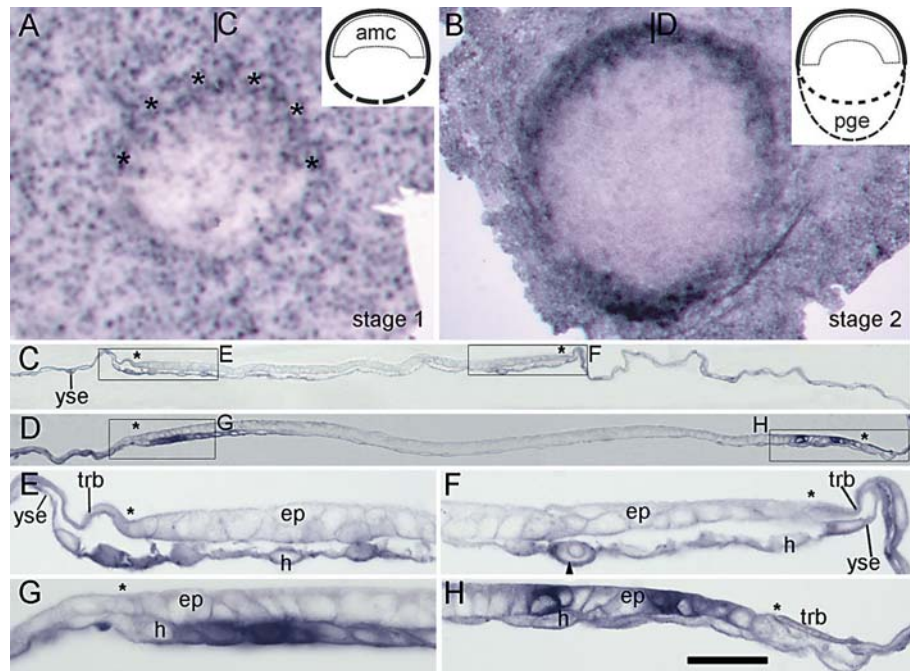
### *Microscopy*

To record the gross morphological distribution of the reaction, the stained embryos were mounted in Mowiol4-88 (Hoechst, Frankfurt, Germany) under a cover glass and photographed prior to dehydrating in ethanol and embedding in Technovit 8100® (Heraeus-Kulzer, Werheim, Germany) at 4°C in tablet moulds as described [Idkowiak et al., 2004]. Polymerized blocks were trimmed and serially sectioned using glass knives at 5 µm thickness in the sagittal or transverse plane. After the position of a given serial section had been verified in the photographs of the gross morphological overview at low magnification, the allocation of *sox17*-expressing cells to the topography of the embryo and, within that location, to tissue layers was determined at high magnification. In most cases, i.e. for sections with tissues which contained strong in situ hybridization reactions, photographs were taken using the differential interference contrast (DIC) setting of the microscope (Axioskop, Zeiss, Göttingen, Germany) to visualize the morphology of the parts of the section where no in situ hybridization reaction had occurred. For tissues with exclusively very weak reactions, DIC was not used; this ensured that the intensity of the reaction was not obscured by the contrast enhancement in the surrounding non-stained cells (fig. 2N, N').

## Results

All in situ hybridization experiments carried out as described above typically produce well-defined BM purple staining reactions in a variety of cell and tissue types at every stage analyzed in this study: In most cases, these in situ hybridization signals (ISHs) start to occur within 1 day after the beginning of the final step of the in situ hybridization procedure and they have a high signal-to-noise ratio, i.e. staining is confined to the cytoplasmic domain of a given cell and strongly stained cells frequently lie next to unstained cells or cell groups. ISHs with a reaction intensity between these extremes also occur frequently and are referred to as weak ISHs in the following

**Fig. 1.** *Sox17* expression patterns in rabbit embryo at stages 1 and 2 (6.25 d.p.c.) as determined by in situ hybridization analyses in en face views (**A, B**) and 5- $\mu$ m sagittal sections at low (**C, D**) and high magnification (**E-H**). The anterior border of the embryonic disc is marked by asterisks in **A**. Insets in **A** and **B** highlight the morphological characteristics of stages 1 and 2, respectively. All sections are orientated with the anterior end to the left and the epiblast to the top. The borders of the embryonic discs in the sections are defined by asterisks. Bars and letters refer to the positions of the sections; boxes in **C** and **D** indicate to the positions of the high magnification details shown in **E-H**. amc = Anterior marginal crescent, ep = epiblast, h = hypoblast, pge = posterior gastrula extension, trb = trophoblast, yse = yolk sac epithelium; arrowhead in **F** points to a labeled hypoblast cell. Scale bar: **A, B** 80  $\mu$ m; **C, D** 50  $\mu$ m; **E-H** 13  $\mu$ m.



description. As reactions occur in a variety of different cells, tissues and organ anlagen, results are presented here stage by stage rather than by following up the development of a particular organ anlage, for example.

#### *Pre-Streak Stages (Stages 1 and 2)*

At stage 1, the embryonic disc can be recognized – if viewed en face under dark-field illumination – on the surface of the blastocyst as an area of high cellular density. One side of the embryonic disc features a stretch with a relatively sharp contour, while the opposite side of the disc displays an irregular, ragged, and therefore indistinct contour; the distinct contour marks the anterior marginal crescent (AMC) as the earliest axial structure at the anterior pole of the mammalian embryonic disc (fig. 1A, inset). Histologically, the AMC is characterized by increased cellular density and cellular height in both the epiblast and the hypoblast – the two cell layers present in the embryonic disc at this stage – if compared with the posterior margin of the disc (fig. 1E, F).

In dorsal views of stage 1, a punctate, salt-and-pepper distribution of strong ISHSs with no apparent asymmetry is found in all extraembryonic areas in the vicinity of, and further away from, the embryonic disc (fig. 1A). The disc itself can be recognized as an area with fewer ISHSs in one half and more numerous ISHSs in the other half of the disc. Denser packing of ISHSs is seen in the area co-

inciding with the AMC (histologically confirmed, see below), while many small patches with weak or no ISHSs appear in that part of the embryonic disc which can be confirmed histologically to be the posterior half.

In sagittal sections many of the single strongly stained cells are seen to belong to the hypoblast layer in the anterior half of the embryonic disc (fig. 1C, E); within the hypoblast cells ISHSs are mainly found to lie close to the nucleus. A few strongly stained hypoblast cells are also found in the posterior half of the embryonic disc (arrowhead in fig. 1F), and these cells are intermingled with weakly or unstained ones. Some cells in the epiblast layer of the AMC are weakly stained, while others are not stained (fig. 1E); in the posterior half of the embryonic disc the epiblast layer is weakly stained near the posterior border (fig. 1F) but it is unstained further anteriorly, i.e. within the central zone of the embryonic disc (fig. 1C). The punctate pattern in the extraembryonic tissue is found to be generated by cells in the lower layer, i.e. by the yolk sac epithelium cells (fig. 1C, F), whereas weak ISHSs are found in both the intervening yolk epithelium cells and in the upper layer, i.e. trophoblast cells (fig. 1C).

At stage 2, a few hours prior to overt primitive streak formation, the anterior contour of the oval-shaped embryonic disc is, in dark-field views, still distinct as before but a sickle-shaped area of low cellular density – called

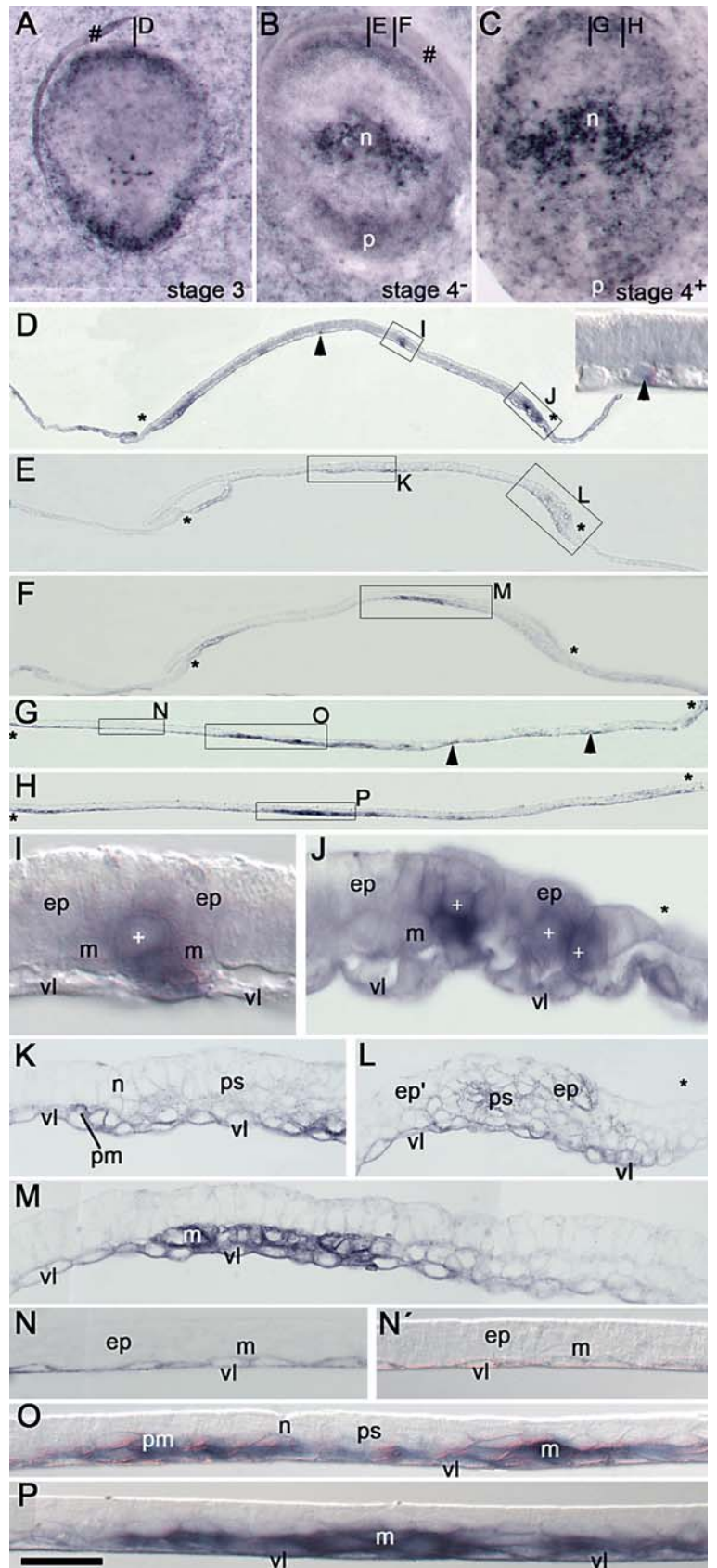


**Fig. 2.** Distribution of *sox17* ISHSs during early gastrulation stages (stages 3–4 at 6.5 – 6.75 d.p.c.) as seen in en face views (A–C) and 5- $\mu$ m sagittal sections at low (D–H) and high magnification (I–P). All sections are orientated with the anterior end to the left and the epiblast to the top. The borders of the embryonic discs in the sections are defined by asterisks. Bars and letters refer to the positions of the sections; boxes in D–H indicate to the positions of the high magnification details shown in I–P. In N' differential interference contrast (DIC) setting of the magnified details seen in N. D, I, O and P are also with DIC setting. ep = Epiblast, ep' = unstained epiblast, m = mesoderm, n = Hensen's node, p = posterior extremity of the primitive streak, ps = primitive streak, pm = prechordal mesoderm, vl = ventral layer; + = mesodermal compartment, arrowheads in D (see also inset in D) and G point to labelled cells in the ventral layer, # refers to tissue processing artefact. Scale bar: C, E, F 108  $\mu$ m; A, B 80  $\mu$ m; D, G, H 50  $\mu$ m; I–P 13  $\mu$ m.

the posterior gastrula extension (PGE) – appears within the posterior half of the embryonic disc and next to the indistinct posterior contour of the embryonic disc (fig. 1B, inset). *Sox17* ISHSs of stage 2 embryos are still strong but produce less of a salt-and-pepper appearance and are confined to the periphery of both the AMC and the PGE (fig. 1B); only close to the posterior pole of the embryonic disc, i.e. in the central segment of the posterior contour, some single strong ISHSs arise. The other parts of the embryonic disc show weak reactions and are devoid of the dispersed strong ISHSs seen at stage 1. In extraembryonic areas *sox17* ISHSs are for the most part evenly distributed at this stage.

In sagittal sections of this stage, strong ISHSs are found in hypoblast cells of the AMC domain, and these cells, which lie now close to each other and are up to twice as high when compared with those at the opposite side (fig. 1G, H), are located posterior and adjacent to 1–3 rows of hypoblast cells with only weak or no reaction within the anterior border of the embryonic disc (fig. 1G). However, the reactions in epiblast cells of this region are similar to those at the previous stage (fig. 1E). The cells with strong reaction seen in en face views in the central segment of the peripheral PGE portion belong to the epiblast layer, which can be distinguished by their cuboidal shape from adjacent (extraembryonic) squamous trophoblast cells (fig. 1F, H); these epiblast cells, in which strong ISHSs fill most of the cytoplasmic rim around the nucleus, lie mainly isolated or in small groups amongst several neighbouring epiblast cells showing no or only weak ISHSs; this produces the mosaic-like staining pattern in the epiblast seen at the posterior pole of the embryonic disc in dorsal views (fig. 1B); hypoblast cells in this area, on the other hand, are only weakly stained (fig. 1H). Other peripheral segments of the PGE show weak ISHSs in both epiblast and hypoblast layers (not shown). The central area of the embryonic disc shows weak ISHSs in the hypoblast layer (fig. 1D); extraembryonic tissues exhibit weak reactions in both the yolk sac epithelium and in the trophoblast layer (fig. 1D, left).

#### *Gastrulation Stages (Stages 3 and 4)*

The gastrulation process becomes apparent at stage 3, when the primitive streak can be seen as a localized cellular density stretching along the posterior half of the midline in en face views under dark-field illumination. Thus, the embryonic disc has elongated towards the posterior pole and its previous oval shape is now transformed into a pear-like shape. The density of the streak is caused by cellular accumulation, following extensive cellular

movements within the epiblast directed towards the posterior midline, and provides the basis for the ingression of epiblast cells through a narrow discontinuity in the basement membrane stretching along the primitive streak. Functional studies in mouse and chick (see ‘Introduction’) suggest that endoderm cells are inserted into the ventral layer of the embryonic disc, which prior to this stage consists of hypoblast cells only. Therefore, from the start of gastrulation onwards, there are likely to be two cell populations in the ventral layer of the embryonic disc. As no reliable markers exist to date to distinguish endoderm from hypoblast, the following description of the cell layers uses ‘ventral layer’ instead of ‘hypoblast’ for most areas of the embryonic disc from stage 3 onwards; only for the AMC, where endoderm is inserted at later stages, is the ventral layer still addressed as hypoblast until stage 4.

In dorsal views of stage 3 embryos, strong *sox17* ISHSs in the AMC and in the posterior parts of PGE lie close to the border of the embryonic disc, similar to those at stage 2 (fig. 2A); however, due to the elongation of the disc these anterior and posterior domains are now more clearly separated by a peripheral band of weakly labeled cells on both sides of the embryonic disc. In addition, single strong ISHSs appear as isolated spots near the anterior midline of the posterior half of the embryonic disc; these spots lie just anterior to the PGE and coincide roughly with the anterior extremity of the emerging primitive streak. Apart from these strongly stained parts of the embryonic disc the remainder of the embryonic disc shows weak reactions only. The extraembryonic tissues exhibit staining patterns similar to those seen at the previous stage.

Sagittal sections of this stage show principally the same staining patterns in the hypoblast found at stage 2 anteriorly and posteriorly (fig. 1G, H, fig. 2D, J, respectively); in addition, single stained cells lie amongst unstained ones in the ventral layer of the anterior half of the embryonic disc (arrowheads in fig. 2D and inset). In the epiblast of the posterior part of PGE, i.e. close to the posterior disc border, the mosaic pattern can be seen similar to that at stage 2, but now ISHSs lie either in the epiblast or in the mesoderm compartments (fig. 2J). The single strongly stained cells seen near the anterior midline of the posterior half of the embryonic disc are also found to lie in the mesoderm compartment, i.e. in the rostral part of the primitive streak (fig. 2I). Generally, there are now weak reactions in the basal parts of the epiblast layer throughout the whole embryonic disc (fig. 2I, J). The ISHSs in the extraembryonic tissues are weak in the tro-

phoblast cells and in the yolk sac epithelium cells (fig. 2D).

As gastrulation proceeds to stage 4, the overview of the whole-mount embryo shows that the embryonic disc elongates further and the Hensen's node appears as a cellular density at the anterior extremity of the primitive streak. As a sign of the establishment of Hensen's node, the prechordal mesoderm cells emerge from Hensen's node ('pm' in fig. 2K) and migrate anteriorly to presage the formation of notochordal process (stage 5, fig. 3A, B).

In dorsal views of early Hensen's node stages (stage 4<sup>-</sup>, fig. 2B), both the AMC domain and the domain near the posterior border of the embryonic disc still present *sox17* ISHSs, but these are weaker than before, and in the area where the single strongly stained spots are seen near the anterior part of the primitive streak at the previous stage (stage 3), a horizontally oriented strongly stained domain arises on either side of the anterior segment of the primitive streak (fig. 2B). In the extraembryonic tissues the intensity of the reactions is only weak or absent at this stage.

Sagittal sections show that the hypoblast layer of the AMC area continues to have ISHSs whereas no ISHSs are found in the epiblast layer (fig. 2E, F). Weak ISHSs can be recognized in the ventral layer covering the primitive streak (fig. 2K, L) and in the ventral layer stretching between Hensen's node and the anterior margin of the embryonic disc (fig. 2E); in fact, in the anterior part of the primitive streak mesoderm cells, including the first prechordal mesoderm cells emanating anteriorly from Hensen's node, are also weakly stained (fig. 2K), whereas in the posterior extremity of the primitive streak they are weakly stained in all three layers (fig. 2L). Lateral to the anterior segment of the expanded primitive streak, the continuous bands of strong ISHSs appear in both mesoderm and ventral layer cells (fig. 2M). The extraembryonic tissues show only weak reactions in the yolk sac epithelium cells at this stage (fig. 2E, F).

In dorsal views of late stage 4 embryos (fig. 2C), the anterior margin of the embryonic disc still carries some ISHSs within a mostly weak anterior *sox17* expression domain. The strongly stained transverse domain seen in the last stage expands anteromedially and posterolaterally thereby now encompassing Hensen's node and more of the anterior segment of the primitive streak than before. Weak *sox17* ISHSs are found in the area located between the anterior margin of the embryonic disc and this strongly stained transverse domain, whereas the area located posterior to the strongly stained transverse domain, in-

cluding the primitive streak, displays weak reactions intermingled with moderately strong ISHSs. The extraembryonic tissues are stained weakly.

Sections of this stage show the strong ISHSs seen in the transverse domain (fig. 2H) to lie in the mesoderm compartment juxtaposed to the ventral layer; these cells intermingle with weakly stained cells located in both the mesoderm and ventral layer compartments and make this transverse expression domain less compact than at the early stage 4. Only few strongly stained cells lie in the ventral layer covering this domain (fig. 2P). In the midline, strong ISHSs are observed in the prechordal mesoderm cells that have emerged from Hensen's node, and weak reactions are found in the ventral layer cells covering these prechordal mesoderm cells (fig. 2O). In the anterior part of the primitive streak, some strongly stained cells in the mesoderm compartments are located adjacent to the ventral layer and are found to lie next to weakly stained cells within the mesoderm and the ventral layers (fig. 2O). Throughout the other parts of the primitive streak, single strongly stained cells are found in the ventral layer (arrowheads in fig. 2G), whereas the posterior extremity of the primitive streak still shows weak ISHSs in all three layers similar to the situation seen at stage 4<sup>-</sup> (fig. 2L). At the anterior margin of the embryonic disc, strong reactions are still present in the hypoblast layer but not in the epiblast layer (fig. 2G, H). The weak reactions located in the region between the anterior margin of the embryonic disc and the strongly stained transverse domain are found to lie in the ventral layer, as can be seen particularly well if no differential interference contrast is used for light microscopic analysis (fig. 2N and N'). Except for the weak reactions found in the epiblast of the posterior extremity of the primitive streak, the epiblast layer throughout the whole embryo shows no ISHSs (fig. 2G, H). Reactions are weak in most of the yolk sac epithelium cells, whereas the upper layer of the extraembryonic tissues (trophoblast) shows no ISHSs.

#### *Neurulation Stages (Stages 5, 6 and 7)*

As a result of gastrulation the notochordal process begins to emerge from Hensen's node along the anterior midline of the embryonic disc (fig. 3A) and, in parallel, the anterior half of embryonic disc begins to elongate along the anterior-posterior axis to accommodate the neural plate as the first step of neurulation. The increasing length of the notochordal process can be determined easily in dorsal views during early neurulation and is, therefore, used here to divide the beginning of neurulation into 3 stages: Stage 5 covers the period after the first

prechordal mesoderm cells leave Hensen's node (end of stage 4) until the notochord acquires the same length as the primitive streak (fig. 3B); during stage 6, the notochordal process elongates further and its posterior part becomes nearly twice as wide as its anterior part; this is in contrast to the posterior half of the embryonic disc which becomes narrower than its anterior half (fig. 4A, B), and at stage 7, the first somites start to form on either side about equidistantly from the two extremities of the notochordal process, i.e. next to the anterior extremity of the posterior, wide part of the notochordal process (fig. 4C, D).

In dorsal views of early stage 5 embryos (fig. 3A), the strongest ISHSs are found on both sides of the (short) notochordal process and both near the anterior margin of the embryonic disc and at the posterior extremity of the primitive streak. The domain next to the notochordal process is similar in shape to the transverse domain observed first at stage 4<sup>-</sup> (fig. 2B) and a little more expanded than at stage 4<sup>+</sup> (fig. 2C); the domain still encompasses the anterior part of the primitive streak and Hensen's node and, therefore, has broadened along the anterior-posterior axis in comparison to earlier stages. In the anterior half of the primitive streak itself, ISHSs are weak; weaker still are ISHSs in Hensen's node and notochordal process and in the posterior third of the embryonic disc. The borders of the embryonic disc encompassing the posterior parts of the primitive streak show, at this stage, also weak ISHSs except for the posterior-most extremity of the primitive streak which is still marked with strong ISHSs. In the extraembryonic tissues, weak ISHSs are distributed and intermingled with small unstained areas.

In sagittal sections of early stage 5 embryos, the strong ISHSs seen in the overview lateral to the notochordal process and primitive streak are found to be located in both the mesoderm compartment and in the ventral layer covering this domain (fig. 3H); towards the anterior margin this domain of strongly stained cells is continuous laterally with the domain of strongly stained cells in the hypoblast and some overlying mesoderm cells (fig. 3D, H). In the midline, the transverse domain is interrupted by the unstained notochordal process (fig. 3F) but it is continuous across the midline anterior to the tip of the notochordal process due to the weak ISHSs in the prechordal mesoderm cells and in the ventral layer covering the prechordal mesoderm (fig. 3F). However, the ventral layer covering the early notochordal process and Hensen's node also shows weak ISHSs (fig. 3F). Along the primitive streak, weak ISHSs are found in some cells located in the mesoderm and ventral layers (fig. 3C, F), but the poste-

rior extremity of the primitive streak shows weak reactions in a continuous oblique band of cells lying across all three layers, and this band touches anteroventrally several more strongly stained cells in the ventral layer underlying the primitive streak (fig. 3G). The reactions in the extraembryonic tissues are found to be weak in most yolk sac epithelium cells and absent in the trophoblast cells (not shown).

In dorsal views of late stage 5 embryos (fig. 3B), two bands of strong reactions are found to run parallel on each side of the elongating notochordal process. At the level coinciding roughly with Hensen's node, these bands extend posterolaterally to contact the posterolateral margins of the embryonic disc. Strong ISHSs are found along almost all margins of the embryonic disc except for the posterior pole where the margin shows only weak ISHSs. Weak ISHSs are found in an arch-like region located between the strongly stained parallel bands and the anterior and lateral strongly stained margins (crosses in fig. 3B). No ISHSs are found in Hensen's node and notochordal process. In the primitive streak, weak reactions are found in the anterior segment and in the posterior extremity, whereas most of the posterior half shows no reactions. In the extraembryonic tissues most *Sox17* ISHSs are found next to the embryonic disc, while the remaining extraembryonic areas have weak or no ISHSs.

Sections analyzed for this stage show that in the band-like domains of ISHSs located next to the notochordal process reactions are strongest in the ventral layer, but weaker in the mesoderm and weaker still in the neural

**Fig. 3.** *Sox17* expression patterns during early neurulation stages (stages 5<sup>-</sup> at 7.0 d.p.c. and 5<sup>+</sup> at 7.6 d.p.c.) as seen in en face views (A, B) and 5- $\mu$ m sections at low (C, D) and high magnification (E-N). All sections are orientated with the epiblast to the top and the sagittal ones are orientated with the anterior end to the left and the epiblast to the top. The borders of the embryonic discs in the sections are defined by asterisks. Bars and letters in A refer to the positions of the sagittal sections and in B according to the length of the transverse sections shown in I-N; boxes in C, D indicate to the positions of the high magnification details shown in E-H. I-N are with differential interference contrast (DIC) settings. h = Hypoblast, m = mesoderm, n = Hensen's node, nc = notochordal process, np = neural plate, pm = prechordal mesoderm, ps = primitive streak, trb = trophoblast, vl = ventral layer, yse = yolk sac epithelium; arrowheads in J indicate to unstained cells in the ventral layer located closed to the notochordal process, # refers to tissue fold artefact, brackets in A and B mark the length of the notochordal process, x marks arch-like weakly stained areas. Scale bar: A, B 108  $\mu$ m; C, D 50  $\mu$ m; E-N 13  $\mu$ m.

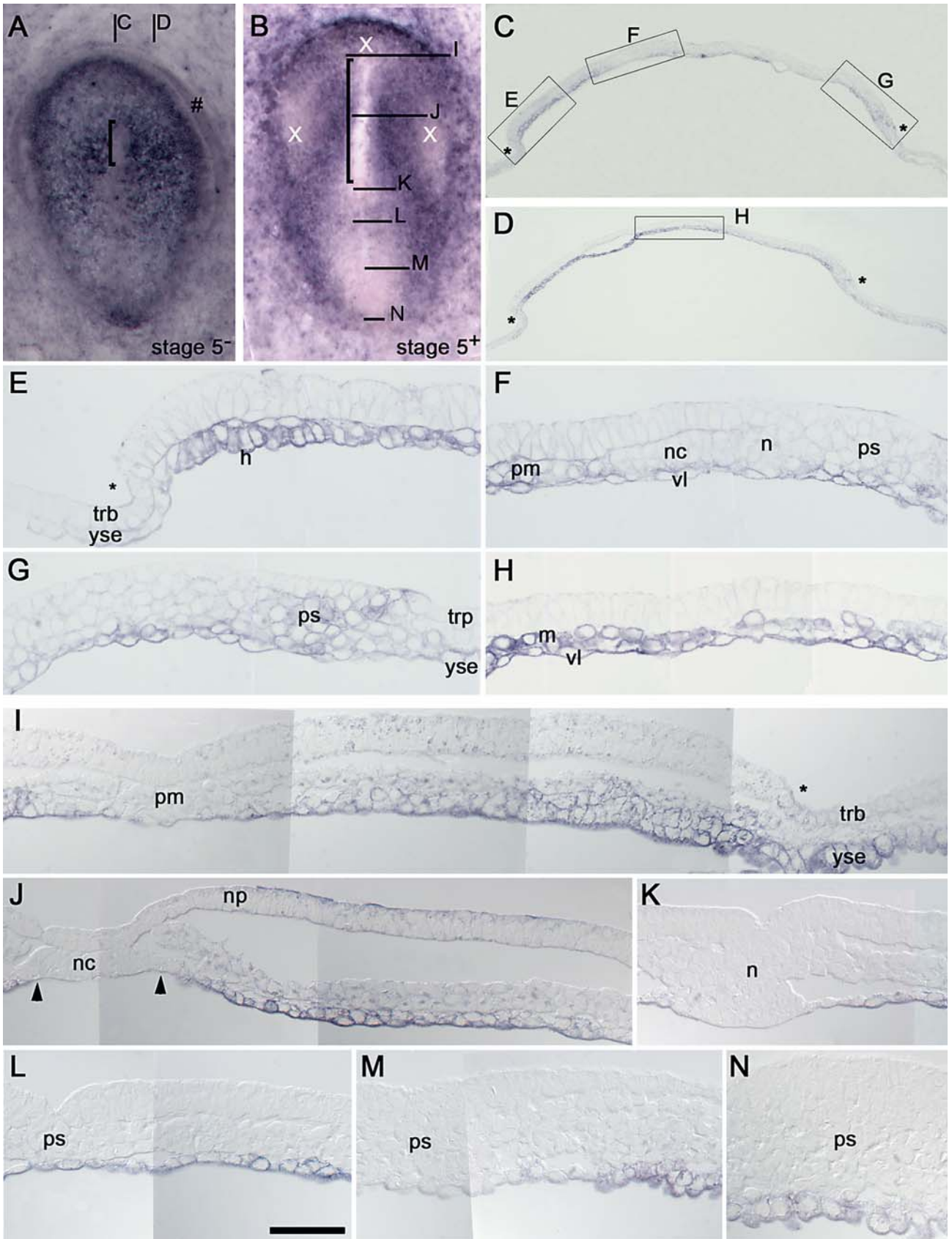


plate overlying them (fig. 3J). In the oblique bands located laterally at the level of Hensen's node and most of the primitive streak, reactions are confined to the ventral layer (fig. 3K–M). Cells of the notochordal process do not show ISHSs and they are separated from the strongly stained ventral layer cells laterally by a few cells which are unstained and difficult to allocate either to the notochordal process or the ventral layer laterally (arrowheads in fig. 3J). No ISHSs are found in the prechordal mesoderm cells next to weak reactions in the mesoderm and ectoderm (fig. 3I). Similarly, Hensen's node and the primitive streak are devoid of ISHSs, while the ventral layer covering these parts has no ISHSs at the level of Hensen's node (fig. 3K) and also the level of the most posterior half of the primitive streak (fig. 3M), whereas stronger ISHSs in this layer are found at both levels of the anterior part and posterior extremity of the primitive streak (fig. 3L and N, respectively). At the margins of the embryo including the posterolateral margins encompassing the posterior half of the embryonic disc, which are strongly stained at this stage, strong ISHSs are found in the ventral layer and weak ones in mesoderm cells (fig. 3I). In the arch-like area located between the lateral border of the embryo and the band-like domain (area marked 'x' in fig. 3B), the ISHSs are weak to absent in the mesoderm and in the ventral layer posteriorly (fig. 3J, right) and are weak in the mesoderm but stronger in the ventral layer more anteriorly (fig. 3I). Strong ISHSs are found in the yolk sac epithelium of the extraembryonic tissues adjacent to the embryo while in these cells further away from the embryo the reactions are weak or absent, the trophoblast of the extraembryonic tissues shows no ISHSs (fig. 3I).

In dorsal views of early stage 6 embryos (fig. 4A), the two oblique bands of strong ISHSs are found again at each side of the most anterior part of the wide, posterior region of the notochord and these bands extend posterolaterally to contact the margins of the embryo, a situation very similar to that found at stage 5<sup>+</sup> (fig. 3B). However, distinctly weaker ISHSs are found in two longitudinal band-like domains on either side of the anterior, narrow part of the notochordal process and extend the oblique bands of strong ISHSs towards the anterior pole of the embryo. Strong ISHSs are found in most of the embryonic margins except for the border encompassing the posterior pole of the embryonic disc, which shows no reactions. In an arch-like area located between the strongly stained anterior margin of the embryo and the weakly stained two bands, which run along the anterior narrow part of the notochordal process, no or weak ISHSs are

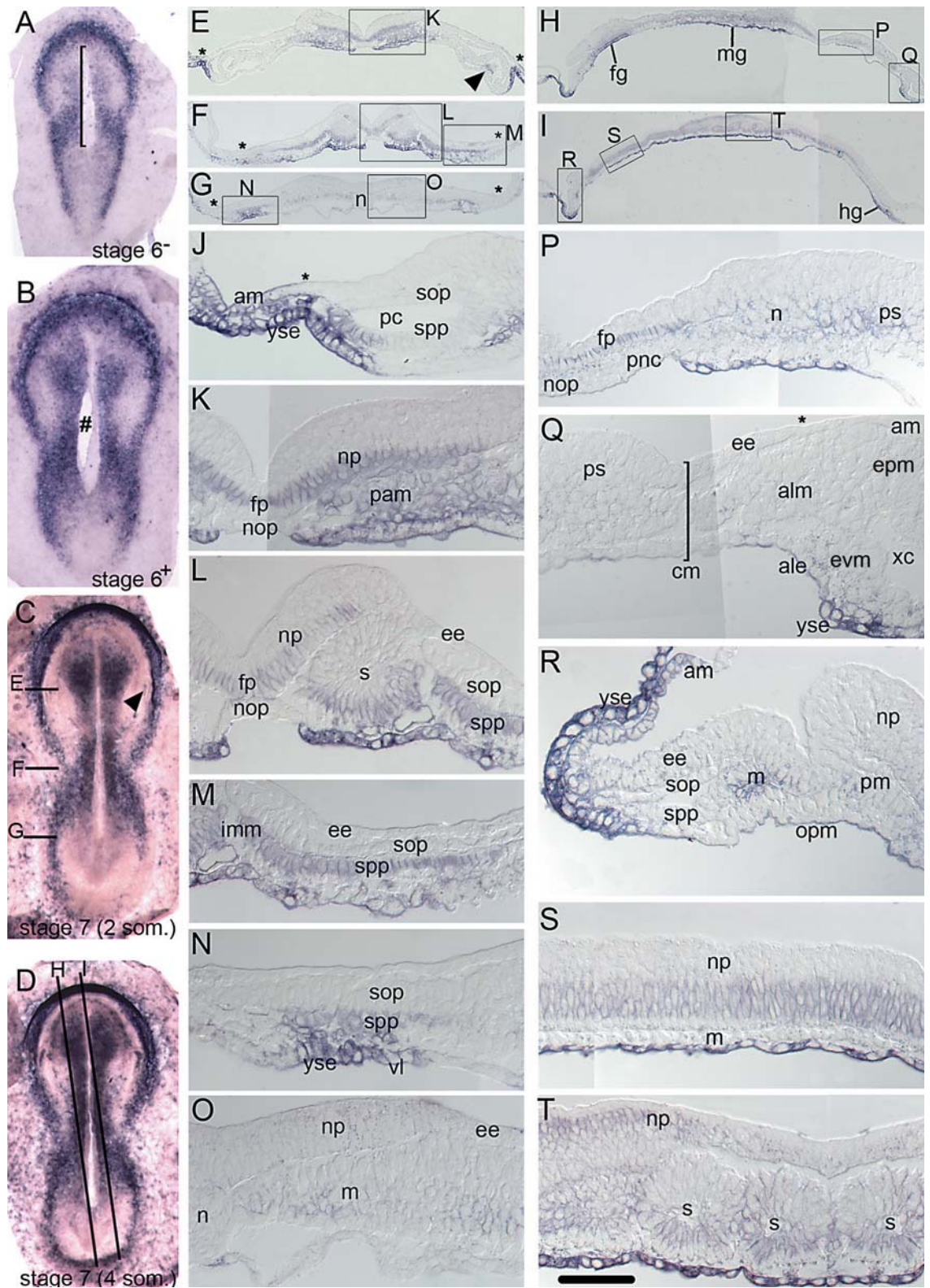
found. No ISHSs are found in Hensen's node and notochordal process. Weak ISHSs can be seen in most of the anterior part of the primitive streak. In the extraembryonic tissues, strong ISHSs are restricted to a narrow band located next to the anterior circumference of the embryonic disc.

In the sections (data not shown), distribution of ISHSs in the strongly stained oblique band-like domains to the germ layers is similar to that of stage 5 (fig. 3J). However, in the weakly stained band-like domains on either side of the anterior, narrow part of the notochord, the ISHSs are found to be weak and in the ventral layer only. The expression pattern in the margins of the embryo is similar to the pattern found at the previous stage (fig. 3I), and – as also found in the last stage – the prechordal mesoderm cells, notochordal process and node show no reactions. The weak reaction found in the overview in most of the anterior part of the primitive streak is found to be confined to the ventral layer (fig. 3L). Strong ISHSs are found in the yolk sac epithelium cells of the extraembryonic tissues adjacent to the embryo, while in the cells further away from the embryo the *sox17* ISHSs are absent; in the trophoblast layer no ISHSs are seen.

At late stage 6, i.e. in the late presomite stage (fig. 4B), the patterns of *sox17* ISHSs are found to be similar in form to that of early stage 6; however, the two weakly

**Fig. 4.** *Sox17* expression patterns during neurulation stages (stages 6<sup>-</sup> to 7 at 8.0 d.p.c.) as seen in en face views (A–D) and 5- $\mu$ m sections at low (E–I) and high magnification (J–T). All sections are orientated with the epiblast to the top and the sagittal ones are orientated with the anterior end to the left and the epiblast to the top. Asterisks indicate the borders of the embryonic discs. Bars and letters in C and D refer to the positions of transverse and sagittal sections, respectively; boxes in E–I indicate the positions of the high magnification details shown in K–T, but J was taken from a section anterior to E. K–T are with differential interference contrast (DIC) settings. ale = Allantoic endoderm, alm = allantoic mesoderm, am = amnion, cm = emerging cloacal membrane, ee = epidermal ectoderm, epm = extraembryonic parietal mesoderm, evm = extraembryonic visceral mesoderm, fg = foregut anlage, fp = floor plate, hg = hindgut anlage, imm = intermedial mesoderm, m = mesoderm, mg = midgut anlage, n = Hensen's node, np = neural plate, nop = notochordal plate, opm = oropharyngeal membrane, pc = pericardial cavity, pam = paraxial mesoderm, pm = prechordal mesoderm, pnc = posterior notochord, ps = primitive streak, s = somite, spp = splanchnopleuric mesoderm, sop = somatopleuric mesoderm, vl = ventral layer, xc = extraembryonic cavity, yse = yolk sac epithelium; bracket in A indicates the length of the notochordal process, # in B refers to tissue damage artefact, arrowheads in C and E point to the heart anlage. Scale bar: A–D 156  $\mu$ m; H, I 108  $\mu$ m; E–G 50  $\mu$ m; J–T 13  $\mu$ m.





stained band-like domains on either side of the anterior narrow part of the notochordal process now have strong ISHSs in the ventral layer and weaker ones in the mesoderm layer (see below stage 7; fig. 4K) and are slightly wider than at early stage 6, while the anterior weakly or non-stained arch-like domain has acquired the shape of an inverted U at this stage. Here, too, the reactions are confined to the mesoderm and the ventral layer. Other than that the distribution of ISHSs is similar to that found at early stage 6.

At stage 7, when 2–4 somite pairs have formed, the distribution of ISHSs has, again, changed only little as compared to stage 6. However, the two posterior extremities of the inverted U-shaped anterior domain have widened posteriorly, so that two lateral oval-like areas appear containing a short and narrow longitudinal band of weak ISHSs which coincide with the bilateral heart anlagen just anterior to the level of the most anterior somite (arrowhead in fig. 4C, fig. 4D). Also, the posterior area without ISHSs overlying the posterior half of the primitive streak has turned into an arch-like shape encompassing the weakly stained anterior half of the primitive streak (fig. 4C, D). In the extraembryonic tissues, scattered ISHSs are found again at this stage.

The sections obtained at this stage show that the two oblique band-like domains on either side of the posterior notochordal process contain strong ISHSs in the ventral layer (the future midgut at this level, fig. 4H, I). Weak expression is found in the splanchnopleuric mesoderm, which is now separated from the somatopleuric mesoderm by a narrow intraembryonic coelom (fig. 4M, N). At more anterior levels (somite levels: fig. 4F; narrow part of notochordal process: fig. 4E), the somites (fig. 4L, T) and the neural plate (fig. 4K, S), but not the epidermal ectoderm (fig. 4L, M), show weak ISHSs in the ventral half of the epithelium and in the underlying mesoderm; however, strong ISHSs are found in the ventral layer covering these structures (the future foregut, fig. 4E, K, H, I). Within the two lateral oval-shaped areas located just anterior to the level of the somites between the strongly stained embryonic disc margins and the strongly stained longitudinal band-like domains, ISHSs are found to lie in the splanchnopleuric mesoderm of the heart anlage and in the underlying ventral layer (future foregut; fig. 4J).

Along the anterior margin, strong reactions are found in the lower layer (hypoblast and yolk sac epithelium) and weak ones in the ectoderm (fig. 4R, J). The two layers of the oropharyngeal membrane show weak or no ISHSs, whereas some splanchnopleuric mesoderm cells anterior and next to this membrane show weak reactions; the pre-

chordal mesoderm which lies posterior to the oropharyngeal membrane has no or only weak ISHSs (fig. 4R). No ISHSs are found in the notochordal plate (and the posterior notochord), whereas the floor plate of the neuroectoderm directly overlying the notochord shows weak reactions ventrally similar to the weak ISHSs in the ventral parts of neural plate laterally (fig. 4K, P). Only weak reactions are found in the centre of Hensen's node, whereas in the cells of the ventral layer underlying Hensen's node and the next small part of the primitive streak strong reactions are seen as at earlier stages (fig. 4P). Weak reactions are found in the ectoderm and mesoderm cells lateral to Hensen's node (fig. 4O), whereas the posterior part of the primitive streak located next to the posterior margin of the embryonic disc shows no reactions at this stage (fig. 4Q). Near the posterior margin of the embryonic disc, ISHSs are found in the ventral layer (the future hindgut, fig. 4I, Q), in the allantoic endoderm which is continuous posteriorly with the (strongly stained) yolk sac epithelium (see below) and in the ventral part of the allantoic mesoderm which is continuous posteriorly with the visceral extraembryonic mesoderm. No reactions are found in the amnion and in the parietal extraembryonic mesoderm (fig. 4Q). In the extraembryonic tissues located next to the anterior margin of the embryonic disc, strong ISHSs are found in the yolk sac epithelium and weak ones in the amniotic epithelium (fig. 4I, J, R), whereas the remaining parts of the extraembryonic tissues show weak or strong ISHSs in the yolk sac epithelium intermingled with unstained areas (fig. 4F, G).

## Discussion

This gene expression study shows that the *Sox17*, as a key transcription factor for vertebrate endoderm formation, displays specific expression patterns which are consistently found throughout the early phases of laying down the body plan from pre- and early gastrulation through to early neurulation stages. *Sox17* mRNA is found: (1) in prospective endoderm cells of the central epiblast at the early streak stage, (2) adjacent to the anterior segment of the stage 3 and 4 primitive streak in mesoderm cells and, adjacent to these mesoderm cells, in prospective endoderm cells inserted into the ventral layer, and (3) bilateral to the notochordal process during early neurulation (stage 5), again in both mesoderm and the ventral layer. In addition, and described for the first time in a mammalian embryo, *sox17* mRNA is found in a mosaic-like distribution in the epiblast at the posterior pole

of the embryonic disc immediately prior to the appearance of mesoderm cells in the primitive streak; this posterior expression domain finds its continuation in all three cell layers at the posterior extremity of the primitive streak as gastrulation proceeds up to early neurulation stages. Possibly indirectly connected with endoderm formation, *sox17* mRNA is also found during early neurulation stages in some mesodermal and neural components lying next to the endoderm as well as in extraembryonic tissues. Apparently without direct connection to locations of endoderm formation, *sox17* mRNA appears in the emerging anterior marginal crescent (AMC), the axis defining structure in the anterior half of the embryonic disc immediately prior to gastrulation, and thereby serves as an additional molecular marker for anterior-posterior axis definition.

The fact that the cRNA probe used in this study was generated from a mouse *sox17* cDNA may be regarded as a methodological limitation, but the distinct expression patterns found here at enhanced stringency conditions (1.4×SSC compared to 5×SSC generally used in ISH; see Materials and Methods) coincide with the known topography of endoderm formation in mouse and chick on the one hand [Lawson et al., 1986; Lawson and Pedersen 1992; Kinder et al., 2001; Kanai-Azuma et al., 2002; Lawson and Schoenwolf, 2003; Pfister et al., 2007] and with hypothetical but topographically plausible additional sites of endoderm formation such as the posterior extremity of the primitive streak, on the other. Together, these two considerations may be taken as providing sufficient support for our main conclusion about the topography of endoderm formation, while further reaching conclusions, e.g. whether other members of the Sox-subgroup F are involved in either of the two endoderm sources suggested here, will require RT-PCR amplification and cloning of a *sox17* cDNA from rabbit using predicted exon sequences from the genomic sequence which became available in the ENSEMBL database only after the experimental part of the study was completed. At present, the positive evidence of the *sox17* knock-out mouse [Kanai-Azuma et al., 2002] and the high homology when comparing *sox17* sequences of mouse, rabbit and human (GenBank Accession Nos. NM\_011441 [mouse], NM\_022454 [human] and ENSEMBL-ID ENSOCUT00000012645 [rabbit]) on the one hand, and the negative evidence that *sox18* is most likely not involved in the endoderm cell lineage [Pennisi et al., 2000] on the other, have to be weighed against the probability that our riboprobe (spanning the *sox17* coding region with the high mobility group) recognizes

other members of the Sox subgroup F (*sox7* and *sox18*) as well.

The mosaic-like expression pattern seen in the posterior epiblast cells prior to the appearance of the primitive streak has not been found in other mammalian embryos analyzed so far [Kinder et al., 2001; Kanai-Azuma et al., 2002; Pfister et al., 2007] but it is reminiscent of the onset of mesoderm formation, which starts with the specific expression of the key regulatory gene *brachyury* in single epiblast cells dispersed in a mosaic-like pattern at the posterior pole of the embryonic disc [Viebahn et al., 2002]. Indeed, the consistent finding of this early expression may be an indication for the possibility that the epiblast contains progenitor cells which are primed for endoderm formation simultaneously with, or prior to, mesoderm formation, but extensive experimentation will be needed to find out which of the two progenitor types is a subgroup of the other (in the true sense of the mesendoderm coined for amphibian and fish development), or whether there are, indeed, two separate progenitor populations for endoderm and mesoderm, respectively.

Before the primitive streak acquires the maximal length, another small population of endoderm progenitors seems to appear at its rostral extremity and is in prime position to insert directly into the lower layer, as was observed in the chick at early primitive streak stages and using a newly developed labeling method [Kimura et al., 2007]. However, the relatively low number of early endoderm cells [Tam and Beddington, 1992] may be explained by the second region of endoderm recruitment as defined by posterior *sox17* expression. This interpretation is also supported by the phenotype of the *sox17* knock-out mouse: In this mutant, the severity of the gut phenotype was most pronounced in the posterior gut and *sox17*-deficient cells were unable to colonize the mid- and hindgut of the chimeras whereas the prospective foregut developed quite normally until the late neural plate stage [Kanai-Azuma et al., 2002]. However, the posterior *sox17* expression in the rabbit contrasts with results in mouse and chick, where no *sox17* expression has so far been described at the posterior extremity of the streak [Kanai-Azuma et al., 2002; Chapman et al., 2007; Pfister et al., 2007; Tam et al., 2007]. A solution to this discrepancy may lie in a mere difference in the interspecific timing of posterior endoderm commitment and recruitment; this posterior domain may, indeed, contribute precursors of the extraembryonic endoderm (allantoic endoderm and posterior yolk sac endoderm [Tam et al., 2007]), and this process differs profoundly even between closely related mammalian species [Mossman, 1937].

As gastrulation proceeds, increased *sox17* expression appears around Hensen's node and the anterior segment of the primitive streak. This coincides with an increasing endoderm contribution described in the same region in the mouse [Kanai-Azuma et al., 2002; Pfister et al., 2007]. In these areas almost all newly recruited cells seem to migrate peripherally some distance within the middle layer and then insert into the ventral layer, probably to form foregut endoderm, a finding also obtained in the chick embryo at similar stages [Kimura et al., 2007]. However, the *sox17* expression domains of the rabbit appear to support differences in endoderm precursor cell movement observed between avian and mammalian embryos, which concern anterior definitive endoderm moving in step with the mesoderm layer [Kimura et al., 2006] in the chick, whereas in the mouse dorsal foregut endoderm moves independently of the mesoderm [Tam et al., 2007].

Not directly related to the endoderm sources described so far, *sox17* expression is found in early prechordal mesoderm cells, which indicates that – similar to the situation in the chick [Kimura et al., 2007] – these cells may contribute, after migration anteriorly and laterally, to the foregut. Further anterior to the prechordal mesoderm, there is an expression domain just anterior to the oropharyngeal membrane, and this may be related to the induction process of the very early pancreas primordium because loss of *sox17* function leads to the lack of *Pdx1* expression (a gene related to pancreas differentiation) while *Hex* (required for liver differentiation [Bogue et al., 2000]) is still expressed in this area [Stainier, 2002].

Several neural structures such as the neural plate and the floor plate and some mesodermal structures such as somites and splanchnopleuric mesoderm express *sox17* mRNA at early neurulation stages (fig. 4), which may be an indication of *sox17* activity partially overlapping (and co-operating) with *sox2* and *sox3* activity in early neural tissues [Wood and Episkopou, 1999] and, possibly, in the differentiation of the foregut: *sox2* is expressed in the gut endoderm in the chick and mouse, whereas *sox3* transcripts are detected in the posterior region of the foregut in mouse early somite-stage embryos [Wood and Episkopou, 1999] but not in chick embryos [Kimura et al., 2007]. *Sox17* is also expressed in developing blood vessels and the heart (fig. 4) [Matsui et al., 2006; Sakamoto et al., 2007] and is therefore likely to play an important role in the development of tissues other than the endoderm. On the other hand, *sox17* knockout mutant data suggest that the morphogenetic defects outside the en-

doderm are secondary to defects in the endoderm [Kanai-Azuma et al., 2002].

At pre-streak stages (stage 1 and 2), *sox17* expression is present either in embryonic and extraembryonic tissues of the rabbit, whereas in the mouse egg cylinder, the expression of *sox17* was first found at pre-streak stages in the extraembryonic visceral endoderm nearest to the ectoplacental cone and then to expand progressively to the whole extraembryonic visceral endoderm [Kanai-Azuma et al., 2002; Pfister et al., 2007]. Interestingly, in the chick embryo, *sox17* is expressed before streak formation in early populations of posterior cells including the lower layer of Koller's sickle (KS) and in the middle layer of the posterior marginal zone (PMZ), whereas no expression was found in the epiblast layer of KS and of the PMZ and in the caudal germ wall (CGW) [Chapman et al., 2007]. In the chick, endoderm precursor cells may, thus, have descended from epiblast at a much earlier stage than in the mammalian embryo. In any case, with its early expression in the hypoblast of the AMC and the colocalization with several other anteriorizing genes such as *DKK1* and *Cer1* [Idkowiak et al., 2004], *sox17* serves to identify anterior-posterior polarity early in the pre-gastrulating rabbit embryos. Moreover, the hypoblast in the AMC could share properties with the extraembryonic endoderm of the mouse which is essential in the establishment of the body plan [Beddington and Robertson, 1999; Brennan et al., 2001; Hoodless et al., 2001; Yamamoto et al., 2001]. The expression of *sox17* in the anterior hypoblast of the AMC at pre-primitive streak formation, if compared with *sox17* [Kanai-Azuma et al., 2002; Pfister et al., 2007] and *hex* expression in the AVE in the mouse organism [Keng et al., 1998], supports a potential role of *sox17* in development of anterior structures.

In summary, the rabbit provides the tissue resolution of gene expression necessary for the analysis of the complex topography of initial endoderm formation. The current study thus extends our knowledge of mammalian germ layer generation; moreover, the rabbit's morphological similarity with most other mammalian groups during this phase of development makes the integration of the results into the concepts of early human development an intriguing proposition. Whether the identity of different parts of gut endoderm is defined by the two expression domains in the pregastrulation epiblast is now open for discussion. As a first step towards revealing the answer to this question, fate map studies should now be designed to compare directly the tissue potency in the anterior and posterior extremities of the primitive streak.

## Acknowledgements

We express our grateful acknowledgement to Kirsten Falk-Stietenroth, Heike Faust and Irmgard Weiss for their technical assistance and to Dr. Heiko Lickert of the Institute of Stem Cell

Research, München, Germany, for supplying the *sox17* cDNA probe. This work was supported by a scholarship grant of the Syrian Government (to R.H.) and by the Deutsche Forschungsgemeinschaft (Vi 151/8-1).

## References

- Alexander, J., D.Y. Stainier (1999) A molecular pathway leading to endoderm formation in zebrafish. *Curr Biol* 9: 1147–1157.
- Beddington, R.S.P. (1981) An autoradiographic analysis of the potency of embryonic ectoderm in the 8th day postimplantation mouse embryo. *J Embryol Exp Morphol* 64: 87–104.
- Beddington, R.S.P. (1983) The origin of the foetal tissues during gastrulation in the rodent; in Johnson, M.H. (ed): *Development in Mammals*, vol. 5. Amsterdam, Elsevier, pp 1–32.
- Beddington, R.S.P., E.J. Robertson (1999) Axis development and early asymmetry in mammals. *Cell* 96: 195–209.
- Belo, J.A., T. Bouwmeester, L. Leyns, N. Kertesz, M. Gallo, M. Follettie, E.M. De Robertis (1997) Cerberus-like is a secreted factor with neutralizing activity expressed in the anterior primitive endoderm of the mouse gastrula. *Mech Dev* 68: 45–57.
- Blum, M., P. Andre, K. Muters, A. Schweickert, A. Fischer, E. Bitzer, S. Bogusch, T. Beyer, H.W.M. van Straaten, C. Viebahn (2007) Ciliation and gene expression distinguish between node and posterior notochord in the mammalian embryo. *Differentiation* 75: 133–146.
- Bogue, C.W., G.R. Ganea, E. Sturm, R. Ianucci, H.C. Jacobs (2000) Hex expression suggests a role in the development and function of organs derived from foregut endoderm. *Dev Dyn* 219: 84–89.
- Brennan, J., C.C. Lu, D.P. Norris, T.A. Rodriguez, R.S. Beddington, E.J. Robertson (2001) Nodal signalling in the epiblast patterns the early mouse embryo. *Nature* 411: 965–969.
- Chalmers, A.D., J.M. Slack (2000) The *Xenopus* tadpole gut: fate maps and morphogenetic movements. *Development* 127: 381–392.
- Chapman, S.C., F.R. Schubert, G.C. Schoenwolf, A. Lumsden (2003) Anterior identity is established in chick epiblast by hypoblast and anterior definitive endoderm. *Development* 130: 5091–5101.
- Chapman, S.C., K. Matsumoto, Q. Cai, G.C. Schoenwolf (2007) Specification of germ layer identity in the chick gastrula. *BMC Dev Biol* 30: 91.
- Denker, H.-W. (2000) Structural dynamics and function of early embryonic coats. *Cells Tissues Organs* 166: 180–207.
- Gardner, R.L., J. Rossant (1979) Investigation of the fate of 4.5 day post-coitum mouse inner cell mass cells by blastocyst injection. *J Embryol Exp Morphol* 52: 141–152.
- Hoodless, P.A., M. Pye, C. Chazaud, E. Labbe, L. Attisano, J. Rossant, J.L. Wrana (2001) FoxH1 (Fast) functions to specify the anterior primitive streak in the mouse. *Genes Dev* 15: 1257–1271.
- Hudson, C., D. Clements, R.V. Friday, D. Stott, H.R. Woodland (1997) Xsox17alpha and -beta mediate endoderm formation in *Xenopus*. *Cell* 91: 397–405.
- Idkowiak, J., G. Weisheit, J. Piltzner, C. Viebahn (2004) Hypoblast controls mesoderm generation and axial patterning in the gastrulating rabbit embryo. *Dev Genes Evol* 214: 591–605.
- Kadokawa, Y., Y. Kato, G. Eguchi (1987) Cell lineage analysis of the primitive and visceral endoderm of mouse embryos cultured in vitro. *Cell Diff* 21: 69–76.
- Kanai, Y., M. Kanai-Azuma, T. Noce, T.C. Saido, T. Shiroishi, Y. Hayashi, K. Yazaki (1996) Identification of two Sox17 messenger RNA isoforms, with and without the high mobility group box region, and their differential expression in mouse spermatogenesis. *J Cell Biol* 133: 667–681.
- Kanai-Azuma, M., Y. Kanai, J.M. Gad, Y. Tajima, C. Taya, M. Kurohmaru, Y. Sanai, H. Yonekawa, K. Yazaki, P.P. Tam, Y. Hayashi (2002) Depletion of definitive gut endoderm in Sox17-null mutant mice. *Development* 129: 2367–2379.
- Keller, R.E. (1975) Vital dye mapping of the gastrula and neurula of *Xenopus laevis*. I. Prospective areas and morphogenetic movements of the superficial layer. *Dev Biol* 42: 222–241.
- Keller, R.E. (1976) Vital dye mapping of the gastrula and neurula of *Xenopus laevis*. II. Prospective areas and morphogenetic movements of the deep layer. *Dev Biol* 51: 118–137.
- Keng, V.W., K.E. Fujimori, Z. Myint, N. Tamamaki, Y. Nojyo, T. Noguchi (1998) Expression of Hex mRNA in early murine postimplantation embryo development. *FEBS Lett* 426: 183–186.
- Kimura, W., S. Yasugi, C.D. Stern, K. Fukuda (2006) Fate and plasticity of the endoderm in the early chick embryo. *Dev Biol* 289: 283–295.
- Kimura, W., S. Yasugi, K. Fukuda (2007) Regional specification of the endoderm in the early chick embryo. *Dev Growth Differ* 49: 365–372.
- Kinder, S.J., T.E. Tsang, S.L. Ang, R.R. Behringer, P.P. Tam (2001) Defects of the body plan of mutant embryos lacking Lim1, Otx2 or Hnf3beta activity. *Int J Dev Biol* 45: 347–355.
- Kirby, M.L., A. Lawson, H.A. Stadt, D.H. Kumiski, K.T. Wallis, E. McCraney, K.L. Waldo, Y.X. Li, G.C. Schoenwolf (2003) Hensen's node gives rise to the ventral midline of the foregut: implications for organizing head and heart development. *Dev Biol* 253: 175–188.
- Kubo, A., K. Shinozaki, J.M. Shannon, V. Kouskoff, M. Kennedy, S. Woo, H.J. Fehling, G. Keller (2004) Development of definitive endoderm from embryonic stem cells in culture. *Development* 131: 1651–1662.
- Kwon, G.S., M. Viotti, A.K. Hadjantonakis (2008) The endoderm of the mouse embryo arises by dynamic widespread intercalation of embryonic and extraembryonic lineages. *Dev Cell* 15: 509–520.
- Lawson, K.A. (1999) Fate mapping the mouse embryo. *Int J Dev Biol* 43: 773–775.
- Lawson, K.A., J.J. Meneses, R.A. Pedersen (1986) Cell fate and cell lineage in the endoderm of the presomite mouse embryo, studied with an intracellular tracer. *Dev Biol* 115: 325–339.
- Lawson, K.A., J.J. Meneses, R.A. Pedersen (1991) Clonal analysis of epiblast fate during germ layer formation in the mouse embryo. *Development* 113: 891–911.
- Lawson, K.A., R.A. Pedersen, S. Van de Geer (1987) Cell fate, morphogenetic movement and population kinetics of embryonic endoderm at the time of germ layer formation in the mouse. *Development* 101: 627–652.
- Lawson, K.A., R.A. Pedersen (1992) Clonal analysis of cell fate during gastrulation and early neurulation in the mouse; in Chadwick, D.J., J. Marsh (eds) *Postimplantation Development in the Mouse*. Wiley, Chichester (CIBA Foundation Symp 165), pp 3–26.
- Lawson, K.A., G.C. Schoenwolf (2003) Epiblast and primitive-streak origins of the endoderm in the gastrulating chick embryo. *Development* 130: 3491–3501.

- Lefebvre, V., B. Dumitriu, A. Penzo-Mendez, Y. Han, B. Pallavi (2007) Control of cell fate and differentiation by Sry-related high-mobility-group box (Sox) transcription factors. *Int J Biochem Cell Biol* 39: 2195–2214.
- Levak-Svajger, B., A. Svajger (1974) Investigation on the origin of the definitive endoderm in the rat embryo. *J Embryol Exp Morphol* 32: 445–459.
- Lin, T.P., P.A. Labosky, L.B. Grabel, C.A. Kozak, J.L. Pitman, J. Kleeman, C.L. MacLeod (1994) The *Pem* homeobox gene is X-linked and exclusively expressed in extraembryonic tissues during early murine development. *Dev Biol* 166: 170–179.
- Lowe, L.A., D.M. Supp, K. Sampath, T. Yokoyama, C.V.E. Wright, S.S. Potter, P. Overbeek, M.R. Kuehn (1996) Conserved left-right asymmetry of nodal expression and alterations in murine situs inversus. *Nature* 381: 158–161.
- Matsui, T., M. Kanai-Azuma, K. Hara, S. Matoba, R. Hiramatsu, H. Kawakami, M. Kurohmaru, P. Koopman, Y. Kanai (2006) Redundant roles of Sox17 and Sox18 in postnatal angiogenesis in mice. *J Cell Sci* 119: 3513–3526.
- Mossman, H.W. (1937) Comparative morphogenesis of the fetal membranes and accessory uterine structures. *Contrib Embryol Carnegie Inst* 26: 129–246.
- Pander, C.H. (1817) Beiträge zur Entwicklungsgeschichte des Hühnchens im Eye. Brönnner, Würzburg.
- Parameswaran, M., P.P.L. Tam (1995) Regionalisation of cell fate and morphogenetic movement of the mesoderm during mouse gastrulation. *Dev Genet* 17: 16–28.
- Pennisi, D., J. Gardner, D. Chambers, B. Hosking, J. Peters, G. Muscat, C. Abbott, P. Koopman (2000) Mutations in Sox18 underlie cardiovascular and hair follicle defects in ragged mice. *Nat Genet* 24: 434–437.
- Pfister, S., K.A. Steiner, P.P.L. Tam (2007) Gene expression pattern and progression of embryogenesis in the immediate post-implantation period of mouse development. *Gene Expr Patterns* 7: 558–573.
- Quinlan, G.A., E.A. Williams, S.S. Tan, P.P.L. Tam (1995) Neuroectodermal fate of epiblast cells in the distal region of the mouse egg cylinder: implication for body plan organization during early embryogenesis. *Development* 121: 87–98.
- Sakamoto, Y., K. Hara, M. Kanai-Azuma, T. Matsui, Y. Miura, N. Tsunekawa, M. Kurohmaru, Y. Saijoh, P. Koopman, Y. Kanai (2007) Redundant roles of Sox17 and Sox18 in early cardiovascular development of mouse embryos. *Biochem Biophys Res Commun* 360: 539–544.
- Skreb, N., A. Svajger, B. Svajger (1976) Developmental potentialities of the germ layers in the mammals. CIBA Found Symp 40. Chichester, Wiley, pp 27–39.
- Stainier, D.Y. (2002) A glimpse into the molecular entrails of endoderm formation. *Genes Dev* 16: 893–907.
- Tam, P.P.L. (1989) Regionalisation of the mouse embryonic ectoderm: allocation of prospective ectodermal tissues during gastrulation. *Development* 107: 55–67.
- Tam, P.P.L., R.S.P. Beddington (1987) The formation of mesodermal tissues in the mouse embryo during gastrulation and early organogenesis. *Development* 99: 109–126.
- Tam, P.P.L., R.S.P. Beddington (1992) Establishment and organization of germ layers in the gastrulating mouse embryo; in Chadwick, D.J., J. Marsh (eds): *Postimplantation Development in the Mouse*. CIBA Foundation Symp 165. Chichester, Wiley, pp 27–49.
- Tam, P.P., P.L. Khoo, S.L. Lewis, H. Bildsoe, N. Wong, T.E. Tsang, J.M. Gad, L. Robb (2007) Sequential allocation and global pattern of movement of the definitive endoderm in the mouse embryo during gastrulation. *Development* 134: 251–260.
- Tam, P.P., E.A. Williams, W.Y. Chan (1993) Gastrulation in the mouse embryo: ultrastructural and molecular aspects of germ layer morphogenesis. *Microsc Res Tech* 26: 301–328.
- Viebahn, C. (2004) Gastrulation in the rabbit; in Stern, C.D.S. (ed): *Gastrulation*. Cold Spring Harbor, Cold Spring Harbor Laboratory Press, pp 263–274.
- Viebahn, C., C. Stortz, S.M. Mitchell, M. Blum (2002) Low proliferative and high migratory activity in the area of *Brachyury* expressing mesoderm progenitor cells in the gastrulating rabbit embryo. *Development* 129: 2355–2365.
- Warga, R.M., C. Nüsslein-Volhard (1999) Origin and development of the zebrafish endoderm. *Development* 126: 827–838.
- Weisheit, G., K.D. Mertz, K. Schilling, C. Viebahn (2002) An efficient in situ hybridisation protocol for multiple tissues sections and probes on miniaturized slides. *Dev Genes Evol* 212: 403–406.
- Wood, H.B., V. Episkopou (1999) Comparative expression of the mouse Sox1, Sox2 and Sox3 genes from pre-gastrulation to early somite stages. *Mech Dev* 86: 197–201.
- Woodland, H.R., A.M. Zorn (2008) The core endodermal gene network of vertebrates: combining developmental precision with evolutionary flexibility. *Bioessays* 30: 757–765.
- Yamamoto, M., C. Meno, Y. Sakai, H. Shiratori, K. Mochida, Y. Ikawa, Y. Saijoh, H. Hamada (2001) The transcription factor FoxH1 (FAST) mediates Nodal signaling during anterior-posterior patterning and node formation in the mouse. *Genes Dev* 15: 1242–1256.

## **6. The manuscript**

Hassoun R, Schwartz P, Rath D, Viebahn C, Maenner J: Germ layer differentiation during early hindgut formation in the rabbit and pig embryo.

For submission to J Anat (receiving editor: Karl Zilles, Forschungszentrum Jülich, Germany  
E-mail: [k.zilles@fz-juelich.de](mailto:k.zilles@fz-juelich.de))

**Germ layer differentiation during early hindgut formation in the rabbit and pig embryo.**

Romia Hassoun<sup>1</sup>, Peter Schwartz<sup>1</sup>, Detlef Rath<sup>2</sup>, Christoph Viebahn<sup>1</sup>, Jörg Männer<sup>1</sup>

<sup>1</sup>Department of Anatomy and Embryology, Göttingen University, Göttingen, Germany

<sup>2</sup> .... Institute of Animal Science and Behaviour, Mariensee, Germany

Corresponding author:

Jörg Männer, Department of Anatomy and Embryology, Kreuzbergring 36, 37075 Göttingen, Germany.

Tel.: +49-551-39-7032, Fax: +49-551-39-7043,

E-mail: [jmaenne@gwdg.de](mailto:jmaenne@gwdg.de)



## Summary

Compared to recent advances in understanding molecular aspects of endoderm differentiation, the morphology of germ layer formation and, therefore the topographical arrangement of molecular factors leading to endoderm formation, is still poorly defined; this is particularly true during the transition from primary to secondary neurulation, the latter of which starts at the posterior pole of the embryonic disc. To find common principles of germ layer development in mammals, pig and rabbit embryos were analysed as two mammalian species with human-like embryonic disc morphology using a comparative light and electron microscopical approach. With regard to endoderm development intimate intercellular contact between posterior primitive streak mesoderm and the posterior endoderm is found but there is no ultrastructural evidence for a cellular contribution of primitive streak mesoderm to the posterior endoderm. However, a two-step process emerges for the formation of the cloacal membrane, which is closely related to posterior germ layer differentiation: At first, there is a continuous mesoderm layer and numerous patches of electron-dense flocculent extracellular matrix in the prospective region of cloacal membrane formation. In a second step, the cloacal membrane is formed after disappearance of mesoderm and the establishment of intercellular contacts between the endoderm and ectoderm. This involves single cells at first and then gradually spreads to form a seam-like area of intimate contact between the two epithelial cell layers. This process follows different timing schedules in the two species analysed: It runs in parallel from gastrulation to early somite stages in the pig while in the rabbit, the process starts at early somite stages and is accomplished at around the 18 somite stage. In both species, however, cloacal membrane formation is complete prior to the start of secondary neurulation (and therefore of secondary development). These results highlight the special requirements for endoderm formation during development of the hindgut and suggests new mechanisms for the pathogenesis of human urogenital and anorectal malformations.

**Key words:** mammalian morphogenesis, posterior pole, cloacal membrane, extracellular matrix, urogenital and anorectal malformations

## **Introduction**

Formation and differentiation of the endoderm germ layer moved into the centre of attention recently due to the advances in finding molecular tools for generating endodermal derivative replacements such as insulin producing pancreatic islands in vitro (Murry and Keller 2008; Zaret and Grompe 2008; Collombat et al. 2009). The endoderm is the ventral-most epithelial cell layer of the tri-laminar embryonic disc of gastrulation-stage amniote embryos. It derives from the epiblast layer of the bi-laminar pre-gastrulation embryonic disc (Gardner and Rossant 1979), and is gradually inserted into the hypoblast (primitive endoderm) layer (Tam et al. 2007; Kwon et al. 2008; Burtscher and Lickert 2009). Morphologically, this process is thought to be combined with mesoderm and notochord formation at the anterior end of the primitive streak (cf. (Kinder et al. 2001; Kirby et al. 2003; Lewis and Tam 2006) and molecular factors driving this process are beginning to be understood (Lewis and Tam 2006). However, cellular mechanisms separating prospective endoderm cells from epiblast and inserting them into hypoblast remain enigmatic and recent molecular data from rabbits, suggest that the posterior end of the primitive streak might be a second field of endoderm formation during early neurulation stages (Hassoun et al. 2009).

Several developmental processes at the anterior end of the primitive streak are quite well understood (Charrier et al. 1999; Joubin and Stern 1999), not least, due to the seminal and long-standing concept of the amphibian organizer (Spemann and Mangold 1924) and its equivalent structure, Hensen's node, in amniotes (Waddington and Schmidt 1933); but similar organizer activities or potencies have not been identified at the posterior end of the primitive streak except that – as a more global morphogenetic process – the whole of the primitive streak is in its late phase of development considered to be transformed into the tail bud (Knezevic et al. 1998), which then completes caudal body formation by a process known as secondary neurulation or secondary development (Müller and O'Rahilly 2004). Analyses of mutant mice identified a couple of genes involved in secondary development (Holland et al. 1995; Gofflot et al. 1997; Wilson and Beddington 1997) but many functional interactions of these genes as well as cellular mechanisms driving this process are not well understood. In addition, a relatively detailed description of the dynamically changing morphology of the posterior pole of the embryo during gastrulation and neurulation is available for the human embryo, only (Müller and O'Rahilly 2004), and may not be applicable to amniote and mammalian embryos in general. However, understanding the dynamic changes in the topographical relationship between the three germ layers at the posterior pole of the

mammalian embryo and the identification of a possible second field of endoderm formation as a contributor to the epithelial lining of the hindgut might be important, not least, for understanding the pathogenesis of anorectal and urogenital malformations, which are frequent in some domestic animals and man (Kluth and Lambrecht 1997; Favre et al. 1999; Papapetrou C 1999; Mo et al. 2001).

The present study was carried out to document the development of germ layer morphology and topography at the posterior pole of the mammalian embryonic disc during gastrulation and neurulation with a special focus on endoderm formation. For this purpose, light and electron microscopical characteristics of cells, tissues and the extracellular matrix were analysed in two mammalian species with similar flat (non-rodent) embryonic discs (pig, rabbit) but different timing of germ layer formation (cf. (Rabl 1915) and (Streeter 1927)). The study discloses morphological principles of early caudal body formation, which might be common to mammals as well as non-mammalian amniotes and significant for understanding normal and abnormal development of the mammalian hindgut.

## **Material and Methods**

### **Embryos**

For collecting porcine embryos, late pre-pubertal gilts (Landrace x Large White, Institute of Animal Science and Behaviour, Mariensee, Germany) were stimulated (1) using 5ml of a synthetic progestagen (2,2 mg Regumate®/ml, Intervet, Unterschleißheim, Germany) per os once daily for 10-18 days, and (2) using 1500 IU pregnant mare serum gonadotropin (Integonan®, Intervet) i.m. 72 h, prior to starting the mating schedule with Piétrain boars; on the day before mating, gilts were superovulated using 500 IU human chorionic gonadotropin (hCG, Ovogest®, Intervet) intravenously. Each gilt was mated (or artificially inseminated) twice, the first time 24 h after hCG treatment and a second time 36 or 48 h after hCG treatment. The time of the first mating was taken to be the time of conception from which embryonic age was calculated, i.e. embryos designated to be recovered at 11.0 days post coitum (d.p.c.) had an embryonic age of minimally 10.0 and maximally 11.0 days. Uteri were removed after slaughter carried out between 11.0 and 13.0 d.p.c. and were flushed twice with 20 ml warm (37° C) phosphate buffered saline (PBS) containing 2% polyvinyl alcohol (PVA). Blastocysts were collected in large petri dishes, washed in warm PBS twice to remove blood or cellular residue and stored in PBS at room temperature for not more than 1 h until microdissection.

For collecting rabbit embryos, young adult New Zealand White rabbits (Lammers, Euskirchen, Germany) were superovulated by single injections of pregnant-mareserum-gonadotropin (100 I.E. i.m.; Intergonan®, Intervet, Unterschleißheim, Germany) and human choriogonadotropin (180 I.E. i.m.; Predalon®, Organon, Oberschleißheim, Germany) 72 h in advance and immediately before natural mating, respectively. Uteri were removed between 8.0 and 9.5 d.p.c. through cesarean section after injecting a lethal dose (320 mg) of Narcoren® (Merial, Halbergmoos, Germany) intravenously. Uterine segments containing the implantation chambers were separated using scissors and suspended in PBS at room temperature to open the uterine wall antimesometrially using iridectomy scissors. Using dark field illumination and a stereomicroscope, embryos were freed at their endometrial attachment sites and most of their extraembryonic tissues were removed, again using iridectomy scissors.

For both light and transmission electron-microscopical analysis blastocysts were further microdissected using iridectomy scissors and tungsten needles to eliminate extraembryonic tissue that may obscure morphological features critical for staging specimens after fixation. Tissues were prefixed for 2-3 h in a mixture of 1,5% paraformaldehyde (PFA) and 1,5% glutaraldehyde (GA) in phosphate buffer followed by postfixation in 1% OsO<sub>4</sub> in phosphate buffer and embedding in araldite® (Plano, Wetzlar, Germany; cf. Schwartz et al., 1984).

### **Morphological analysis**

Fixed embryos including adjacent extraembryonic regions were photographed as whole mounts both prior to, and following, embedding in Araldite® for staging purposes (s. below) and for correlation of morphological findings obtained in sections with those observable in whole mount views of the same specimen. Subsequently, complete series of semithin (1 µm) sections were cut either in the transverse or sagittal plane using a diamond knife and stained with methylene blue (Schwartz et al. 1984). The positions of serial sections were recorded in photographs of the gross-morphological (whole mount) overviews taken at low magnification in each specimen, emphasis being placed on the midline region of, and posteriorly and laterally adjacent to, the primitive streak. At suitable intervals 70 nm sections were cut for transmission-electron-microscopical analysis of regions previously defined in semithin sections and whole mount views. If necessary, selected semithin sections were re-embedded in Araldite® (Viebahn et al., 1995b) and sectioned at 70 nm.

## **Staging**

Gastrulation and early neurulation stages defined by (Blum et al. 2007) for the rabbit embryo in accordance with Hamburger and Hamilton stages for the chick (Hamburger and Hamilton 1992) were applied here to the pig, also. Calculated embryonic age in pig embryos ranged from 11.0 d.p.c. (stage 4) to 13.0 d.p.c. (stage 8 = 4-6 somite pairs), whereby due to the double-mating-scheme employed these stages may be reached also at 10.0 or 12.0 d.p.c., respectively. In the rabbit, posterior differentiation analogous to the features found in these pig stages occurred at older stages (s. below) and coincided with the stages 5 through to the 18-somite stage, which corresponded to embryonic ages of 8.0 to 9.5 d.p.c., respectively. Four to eight serially sectioned embryos were analysed for each developmental stage in both species.

## **Results**

### **Posterior development in the pig embryo**

As in most amniotes, the posterior pole of the embryonic disc in the pig is dominated by the longitudinally oriented primitive streak for a comparative long phase of development, i.e. from the time of appearance of the first mesoderm cells at stage 3 (Hassoun et al. 2009) through stage 4 (Hensen's node stage, Fig. 1A) and 5 (notochordal process stage, Fig. 1B) until early (Fig. 1C) and late (Streeter 1927) somite stages. Beginning with stage 3, mesoderm cells start to leave the primitive streak epiblast through wide gaps in the epiblast basement membrane and spread out within the space between epiblast and hypoblast. As a result, a continuous, more or less dense cellular sheet of mesoderm bridges the posterior border of the embryonic disc at stage 4 (Fig. 1G). This newly formed sheet of mesoderm cells thus separates epiblast and hypoblast as well as trophoblast and yolk sac epithelium (extraembryonic endoderm). Mesoderm cells themselves, too, frequently lie separated by wide extracellular spaces, in particular at the extraembryonic periphery where a continuous mesodermal lining of the chorionic cavity is found (not shown). Within the embryonic disc, several epiblast cells at the posterior pole of the primitive streak region have a distinct basement membrane, which is continuous with the basement membrane of the trophoblast lying posteriorly adjacent to the embryonic disc (Fig. 1G). These epiblast cells do not show morphological signs of epithelio-mesenchymal transition (lack of basement membrane, bottle-shaped cells) typical of primitive streak epiblast (cf. Fig. 1G, left) and are, therefore, addressed as prospective surface ectoderm cells of the region where tail, cloacal membrane and the infraumbilical abdominal wall will form (cf. Fig. 1H). In close proximity to these posterior prospective surface ectoderm cells,

numerous patches of electron-dense floccular extracellular material lie on the mesodermal side of the basement membrane and frequently fill the intercellular space between individual ectoderm and mesoderm cells (Fig. 1J). In the dorsal cell layer (extraembryonic) trophoblast cells with their numerous microvilli, a rather dense cytoplasmic consistency and numerous apoptotic bodies can be distinguished easily from (intraembryonic) prospective surface ectoderm cells, which have only few microvilli, a lighter cytoplasm (electron microscopic data not shown) and very few apoptotic bodies. In the ventral cell layer, however, the border between the (intraembryonic) hypoblast and the (extraembryonic) yolk sac epithelium is indistinct although the hypoblast has generally a higher number of cells lying closer together than the yolk sac epithelium (posterior). Although both these parts of the ventral layer clearly have an apicobasally polarised epithelial nature, a basement membrane is missing on their (basal) surface facing the mesodermal compartment, within and outside the embryonic disc, at this stage (not shown).

At stage 5, when the neural plate is induced and rises in the anterior half of the embryonic disc (at around 12.0 d.p.c.), extraembryonic tissues, in particular the amnion, start to fold up with the effect that (1) the surface ectoderm, now for its main part high-columnar and pseudostratified, is increasingly separated from the ventral layer and folded onto the posterior part of the primitive streak, and that (2) the border between the embryonic surface ectoderm, here more isoprismatic than high-columnar, and the emerging, squamous amniotic epithelium is brought to lie dorsal to the primitive streak as well. The posterior embryonic disc border between surface ectoderm and primitive streak epiblast is also marked by a distinct change in epithelial height (primitive streak epiblast being pseudostratified and even higher than surface ectoderm), however, this border now coincides with a short stretch of close apposition between a few cells each from surface ectoderm and the ventral layer (Fig. 1H). The ventral layer now consists of a pseudostratified high-columnar epithelium on both sides of the posterior embryonic disc border. Inside the embryo it is now addressed as endoderm, outside it represents the epithelium of the allantoic diverticulum; as true epithelia both layers have a thin basement membrane on their surface facing the mesoderm compartment (not shown). Anterior to the area of contact with the ectoderm, i.e. towards the mesoderm near the primitive streak, there are areas of close contact with mesoderm cells (Fig. 1K) and a basement membrane is missing as at later stages (cf. Fig. 1N). Further posteriorly, mesoderm cells are lacking between ectoderm and endoderm in the limited area of contact between ectoderm and endoderm. At young stages of this phase of development this contact area measures about 10  $\mu\text{m}$  in all direction (anterioposteriorly and to both sides of the midline) and is, thus, the first

sign of a definitive cloacal membrane consisting of ectoderm and endoderm only. The size of the contact area is limited by the presence of mesoderm cells which are densely packed anteriorly (in the area of the primitive streak) and loosely packed posteriorly and laterally with the effect that the contact area is surrounded completely by mesoderm in both embryonic and extraembryonic regions (Fig. 1H). Patches of electron-dense flocculent extracellular material on the mesodermal side of the basement membrane are still found between surface ectoderm and endoderm in this contact area (Fig. 1L) but the space between surface ectoderm and endoderm has become narrower in most places as compared to the previous stage.

As neurulation proceeds to stage 8 (four somite pairs) and is accompanied by forward bending of the neural plate at the anterior pole (at around 13.0 d.p.c.), the area of the cloacal membrane broadens to measure 40 – 50  $\mu\text{m}$  in the longitudinal plane and 75 $\mu\text{m}$  in the transverse plane. Both ectoderm and endoderm are now high-columnar pseudostratified epithelia; mesoderm cells are still excluded from the area of the cloacal membrane and have come to lie anterior (as mesoderm of the primitive streak), posterior and lateral (as mesoderm of the infraumbilical abdominal wall and extraembryonic allantoic mesoderm) to the cloacal membrane. The surface ectoderm has hardly changed in position, contains fewer apoptotic bodies as compared to the previous stage and is now supported by a dense mesodermal layer which itself shows a distinct and smooth surface towards the chorionic cavity (Fig. 1K). Both layers, surface ectoderm and extraembryonic (allantoic) mesoderm show a gradually decreasing height at the border with the amnion. The endoderm layer, on the other hand, has generally increased in height further when compared to the previous stage and this is now also true for the ventral side of the narrow allantoic diverticulum, which has developed in connection with the folding of the ventral layer. Both ectoderm and endoderm are supported by a broad and continuous basement membrane except for the area of the cloacal membrane, where stretches with close ectodermal-endodermal contact without basement membrane interchange with stretches of distinct intercellular spaces between the two epithelia; the latter frequently contains small patches of electron-dense flocculent extracellular material (Fig. 1M).

To sum up formal germ layer development in the pig, a two-step process emerges: the first step is characterised by (1) the presence of a continuous mesoderm layer, (2) numerous patches of electron-dense flocculent extracellular matrix, and (3) intimate contact between primitive streak mesoderm and endoderm within, or near the anterior border of, the prospective region of cloacal membrane formation; the second step is defined by direct intercellular contact between endoderm and surface ectoderm cells which involves single cells

at first and then gradually spreads to form the definitive cloacal membrane consisting of a roundish, plate-like area of intimate contact between several rows of cells within stretches of pseudostratified surface ectoderm and endoderm.

### **Posterior development in the rabbit embryo**

In the rabbit embryo, the phase of a complete mesoderm cell layer bridging the posterior border of the embryonic disc and thereby separating the dorsal from the ventral cell layers (i.e. epiblast and trophoblast from hypoblast and yolk sac epithelium, respectively) lasts through stage 5 up to the 8- somite stage (Fig. 2A, B, E, F) and early somite stages (not shown). Principally similar topographical and cytological characteristics prevail throughout: A couple of epiblast cells immediately posterior to the primitive streak do not show morphological signs of epithelio-mesenchymal transition (Fig. 2E). The ventral layer consists of a squamous to isoprismatic hypoblast lying underneath the primitive streak and of an isoprismatic yolk sac epithelium lying underneath the trophoblast region. Both these cell layers have an apico-basal polarity as in the pig (of earlier stages, cf. Fig. 1A and G). In the more distal extraembryonic mesoderm, though, there are wide spaces between mesoderm cells heralding chorionic cavity formation. The main structural distinction as compared to the pig at this stage are the greater height (isoprismatic to low-columnar) of trophoblast epithelium (which – as in the pig – also carries numerous microvilli as opposed to epiblast or ectoderm, data not shown) and the relative density of embryonic and extraembryonic mesoderm (Fig. 2E), which makes distinguishing the posterior border of the embryonic disc more difficult than in the pig.

The next phase in germ layer differentiation, namely folding of surface ectoderm and endoderm as well as formation of the cloacal membrane, occurs at about the same speed (between 8 and 9 d.p.c.) as in the pig (between 11 and 12 d.p.c., cf. Fig. 1G and H) but has a more complex topographical arrangement in the ventral cell layer: Rather than being a stretch of isoprismatic to high-columnar (endoderm) epithelium, the ventral layer is still squamous and, in an area measuring about 50  $\mu\text{m}$  in diameter, forms multiple invaginations. These are, at first (at the 8 somite stage), separated from the surface ectoderm by a few mesoderm cells (Fig. 1F), while at later stages (13 somite pairs), the epithelium of the invaginations is increasingly dense and isoprismatic and its basal surface is in direct contact with the basement membrane of the surface ectoderm (Fig. 2K). Frequently there is, also, close contact between mesoderm and endoderm cells near the tips of these invaginations (Fig. 2J). The surface ectoderm layer immediately posterior to the primitive streak is isoprismatic, at first (Fig. 2F),



but is later high-columnar (Fig. 2G). Similar to the situation in pig, however, numerous patches of electron-dense flocculent extracellular material are now found on the mesodermal side of the basement membrane of the surface ectoderm, too (Fig. 2I and K). Further posteriorly, the surface ectoderm has enlarged as compared to the previous stage, bends dorsally and brings the border between surface ectoderm and amnion epithelium to a position dorsal to the primitive streak (Fig. 2G) as in the pig (cf. Fig. 1H). Extraembryonic mesoderm appears denser than in the pig and contains numerous capillary blood vessels already (Fig. 1G, to the left).

At more advanced somite stages (18 pairs of somites; 9.5 d.p.c. Fig. 3D), the multiple endoderm invaginations are replaced by a patch of high-columnar pseudostratified epithelium which forms a continuous stretch of close contact with the overlying surface ectoderm (Fig. 3H). This definitive anlage of the cloacal membrane measures about 100  $\mu\text{m}$  along the anterior-posterior axis (cf. Fig. 3G, H) and about 25  $\mu\text{m}$  along the transverse axis. The surface ectoderm has slightly increased in height as compared to the last stage and shows only few apoptotic bodies. At the anterior end of the cloacal membrane area and next to the posterior end of the primitive streak, mesoderm cells are in close contact with endoderm cells without intervening basement membrane (Fig. 3H). In the area of the cloacal membrane there is a discontinuous basement membrane and areas of intimate intercellular contact between endoderm and surface ectoderm, but there are also and still a few patches of electron-dense flocculent extracellular material in the space between basement membrane and the basal surface of the endoderm epithelium (Fig. 3L and M).

## **Discussion**

### **Early hindgut development in the mammalian embryo**

The comparative light and electron microscopic analysis of germ layer development at the posterior pole of the embryonic disc in two mammalian species with a similar disc morphology uncovered the same principles of germ layer differentiation and relocation but different schedules of development in relation to the gastrulation and neurulation process (Fig. 3): Mesoderm emerging from the primitive streak (s. asterisks in Fig. 3B) is spread widely in all directions by mid-gastrulation with the effect that the dorsal and ventral layers at the posterior pole – present since the late blastocyst stage (Fig. 3A) – are completely separated by a more or less dense mesoderm cell layer (Fig. 3B). This is accompanied by differentiation (1) of the dorsal layer of the embryo into surface ectoderm posterior to the primitive streak and

amnion epithelium adjacent to the embryonic disc border and (2) of the ventral layer into endoderm which is fated to line the hindgut and the allantoic diverticulum; here, contact with the mesoderm emerging from the posterior pole of the primitive streak may be of functional significance (Fig. 3B). As the next distinct step, both dorsal and ventral layers fold back onto the embryonic disc thereby forming the amniotic cavity and the allantoic diverticulum, respectively (Fig. 3C). During this process posterior surface ectoderm is carried dorsally and hindgut endoderm is carried ventrally. At the hinge point of these folding processes both epithelia come into close contact and this is the beginning of cloacal membrane formation (Fig. 3C). For establishing this contact, mesoderm cells present between the two layers at the presumed position of the cloacal membrane (cf. Fig. 3B) need to disappear locally. As soon as the cloacal membrane is formed secondary neurulation starts with the rise of the posterior pole of the primitive streak to form the tail bud (also called caudal eminence in human development), which is the organizer of secondary neurulation and, hence, of secondary development (Müller and O'Rahilly 2004); cf. Fig. 3C and D). As secondary development proceeds, mainly through lengthening of the tail bud, the fates and relative positions of the different stretches developing within the plane of any one germ layer gradually find their final position from which organogenesis can start as the next step (Fig. 3D). Remarkably, the differentiation process described here starts at mid-gastrulation (stage 4) and is accomplished by early neurulation (stage 8 with 3 somite pairs) in the pig, whereas in the rabbit this start is delayed at least to soon after the same early neurulation stage (stage 8) and is accomplished not before mid-neurulation (18 somite pairs) taking, though, roughly the same amount of absolute developmental time (approx. 48 h).

Comparison of both morphology and timing schedules with the equivalent features of other mammals including man is difficult as only limited data are available. Early stages of the mouse show ample mesoderm at the posterior end of the primitive streak and beyond thus clearly separating surface ectoderm and endoderm at the posterior pole of the egg cylinder (Downs and Bertler 2000; Downs et al. 2009) while mid-neurulation stages (9 – 11 somite pairs, Theiler stage 13) appear to have typically folded extraembryonic membranes (amnion and yolk sac) and a complete bona fide cloacal membrane (cf. Fig. 13a, panels c and d in (Kaufman 1992); the intermediate phase, though, has not yet been studied using high resolution light microscopy or ultrastructural analysis. Human development, on the other hand is quite well described (cf. (Müller and O'Rahilly 2004) and even shows the feature of a continuous mesoderm layer separating early ectoderm and endoderm prior to cloacal membrane formation (Pohlman 1911) and s. below); however, due to the notoriously

inadequate tissue preservation at the appropriate stages required (stage 7 to 10, i.e. 15 to 21 d.p.c. (O'Rahilly and Müller 1987) transmission electron microscopical evidence is not available (and probably never will be) to analyse the appearance of the extracellular matrix between the germ layers at the posterior pole of the human embryonic disc.

At least, the interspecific comparison suggests that the differentiation and relocation of the germ layers at the posterior pole of the mammalian embryonic disc may be morphologically similar in all mammals despite striking differences in (extraembryonic) differentiation of the allantoic mesoderm (the “connecting stalk”) adjacent to the posterior pole of the embryonic disc. On the other hand, similarities in the position of amnion formation amongst pig, rabbit (this study) and mouse (Kaufman 1992) raises the intriguing possibility that amnion in higher primates (Heuser and Streeter 1941) and man (cf. (Luckett 1978) may originate from trophoblast (rather than from epiblast) in these species, too.

### **Is there a second (posterior) field of endoderm formation?**

The high-columnar pseudostratified stretch of endoderm (and its precursors in the endoderm invaginations in the rabbit) correlates in its relative position with the expression of the transcription factor gene *sox17* at the posterior pole of the stage 5 rabbit embryo, which raised the possibility of a second field of endoderm formation (Hassoun et al. 2009). However, no morphological signs of a *mesenchymal-to-epithelial* transition (from primitive streak mesoderm to posterior endoderm) were found at the comparatively late stages investigated here. Only a close apposition of mesoderm and endoderm just anterior to the region of cloacal membrane formation is regularly found (Figs. 1K and 2J) and may suggest – particularly in the light of hindgut defects in *sox17* knock-out mice and in chimeras with *sox17*-null-cells (Kanai-Azuma et al. 2002) – that at least intimate cell-to-cell contact may be necessary for endoderm differentiation in hindgut and tailgut formation. Eventually, secondary development will bring a putative posterior source of endoderm formation into close proximity to (and to fuse with) the source of endoderm at the anterior end of the primitive streak (Fig. 3D). From then onwards, endoderm differentiation is likely to proceed depending on the expression of *sox17*, only (Kanai-Azuma et al. 2002), and this may then be independent of endoderm originating from the anterior or posterior ends of the primitive streak. However, classical fate map studies (cf. (Franklin et al. 2008) could clarify whether or not the posterior end of the primitive streak may be a source of endoderm formation.

### **Cloacal membrane formation**

Possibly due to the paucity of data from well-preserved specimens of early human embryos (Florian 1933), textbooks of human embryology usually give only vague information on early development of the cloacal membrane and suggest that it represents an area of the embryonic disc that remains in its initial bi-laminar state throughout gastrulation and neurulation. Indeed, such a view seemed to be in accordance with observations from (Wyburn 1937) who described the cloacal membrane as an initially large area of ectodermal-endodermal contact that becomes reduced in size by the immigration of mesoderm from the posterior end of the primitive streak. Our present data from pig and rabbit embryos show that, during the early stages of gastrulation, a continuous layer of mesoderm is formed at the posterior pole of the embryonic disc which connects the posterior end of the primitive streak with the extra-embryonic mesoderm. An area of direct contact between the ectoderm and endoderm that could be interpreted as cloacal membrane becomes apparent only at advanced stages of gastrulation and must, therefore, be established by the disappearance of mesodermal cells from the prospective cloacal membrane region (cf. Fig. 3B and C). Interestingly, these data correspond to the situation described for human embryos (Pohlman 1911) and, thus, suggest that the cloacal membrane should no longer be seen as a remnant of the two-layered embryonic disc, at least during mammalian development. Rather, the cloacal membrane appears to be a newly developing structure whose size depends on the disappearance of mesodermal cells and is followed by establishment of direct contact between the posterior ectoderm and endoderm. The latter may vary in morphological detail (cf. endodermal invaginations in the rabbit) or in its timing relative to gastrulation and neurulation.

### **Role of the extracellular matrix**

The appearance of an interrupted basement membrane and patches of flocculent electron-dense extracellular material between the ectoderm and endoderm of the forming cloacal membrane is reminiscent of data obtained in the oropharyngeal membrane of the golden hamster (Waterman RE 1977) and the chick (Waterman and Schoenwolf 1980), where fibronectin was found to be a functional component of the extracellular matrix (Waterman RE 1980). The oropharyngeal membrane plays an equally pivotal role near the anterior pole of the embryonic disc to ascertain proper arrangement of anterior organ anlagen such as the prechordal plate, preoral gut (Seessel's pocket: (Seessel A 1877) and Rathke's pouch, to name but a few. Analysis of early stages may reveal a hitherto unexpected initial phase of oropharyngeal membrane formation in which mesoderm needs to be removed in the midline to establish the necessary ectodermal-endodermal cell contact, As a further parallel to posterior

development described in the present study, foregut endoderm formation (possibly originating from the prechordal plate as it is inserted into the endoderm (Müller and O'Rahilly 2003) may also depend on the vicinity of formal apposition between ectoderm and endoderm.

### **Implications for the pathogenesis of urogenital and anorectal malformations**

For a long time, several urogenital (e.g. exstrophy-epispadias complex) and anorectal malformations (e.g. imperforate anus; “persistent” cloaca) were suspected to result from abnormal development of the cloacal membrane (for reviews see (Kluth and Lambrecht 1997), and (Männer and Kluth 2005). In recent years, this idea was supported by observations made in animal models which suggest that anorectal malformations might result from abnormal processes mainly affecting the caudal (anal) part of the cloacal membrane (Kluth et al. 1995; Mo et al. 2001; Qi et al. 2002), whereas urogenital malformations might result from abnormal processes mainly affecting the cranial (urogenital) part of the cloacal membrane (Männer and Kluth 2003; Männer and Kluth 2005). Knowledge about the normal and abnormal formation of the cloacal membrane, therefore, might be the key to the understanding of the pathogenesis of anorectal and urogenital malformations. Our present study is well suited to close the information gap on initial cloacal membrane formation and might be of interest for the elucidation of the morphogenesis of hindgut malformations: Domestic pigs, for example, have a high spontaneous incidence of anorectal malformations (0.2-0.3%) and are therefore used as an animal model for human anorectal malformation (Van der Putte and Neeteson 1984). If formation of the cloacal membrane, indeed, were to depend on the disappearance of mesodermal cells, abnormalities in cell removal (e.g. apoptosis, directed migration) or disturbance in extracellular matrix composition may present relatively simple testable models which may answer the question as to how aberrant development of the cloacal membrane leads to congenital malformations.

### **Acknowledgements**

The excellent technical assistance of Kirsten Falk-Stietenroth, Heike Faust, Irmgard Weiß (Göttingen) and of Antje Frenzel and Birgit Sieg (Mariensee) are gratefully acknowledged. This work was supported by a scholarship grant of the Syrian Government (to R.H. of Tishreen University, Syria), a grant by the Deutsche Forschungsgemeinschaft (to C.V.).

## Figure Legends

**Fig. 1.** Light and electron microscopy of germ layer differentiation in the pig as seen in dorsal views of whole embryonic discs (A-C), in median sagittal semithin (1 $\mu$ m) sections (D-I, K) and in ultrathin sections (J, L-N) taken from the same embryos at stage 4 (A, D, G, J), stage 5 (B, E, H, K, L) and stage 8 (C, F, I, M, N), respectively. The position of the areas shown in (G, H, I and K) is indicated with boxes in the lower magnification shown. The electron microscopic images were taken from the same or from the neighbouring section analysed with light microscopy. Asterisks mark the embryonic-extraembryonic border in the dorsal layer of the embryonic disc, arrowheads point to the basement membrane, arrows point to patches of electron-dense material in the extracellular space next to the basement membrane. Brackets in K point to the mesoderm-endoderm contact area. am amnion epithelium, end endoderm. exm extraembryonic mesoderm, m mesoderm, n node, ps primitive streak, se surface ectoderm, tb trophoblast, vl ventral layer, yse yolk sac epithelium. Scale bar: 400  $\mu$ m in A-C, 30  $\mu$ m in G-I, 10  $\mu$ m in K, 1.5  $\mu$ m in J, L, M, N.

**Fig. 2.** Light and electron microscopy of germ layer differentiation in the rabbit as seen in dorsal views of whole embryonic discs (A, B) or embryos (C-D), in semithin (1 $\mu$ m) sections (E-H, J) and in ultrathin sections (I, K-M) taken from the same or similar embryos at various stages, respectively: stage 5 (A, E), 8-somite-stage (B, F, I), 13-somite stage (C, G, J, K) and 18-somite-stage (D, H, L, M). The position of the sections within the embryo is marked in A-C, the position of the areas selected for high magnification is indicated with boxes in the lower magnification shown. The electron microscopic images were taken from the same or from the neighbouring section analysed with light microscopy. Asterisks mark the embryonic-extraembryonic border in the dorsal layer of the embryonic disc, arrowheads point to the basement membrane, arrows point to patches of electron-dense material in the extracellular space next to the basement membrane. inv invagination of endoderm layer, all other labelling as for Fig. 1. Scale bar: 800  $\mu$ m in A-D, 30  $\mu$ m in E-H, 6.5  $\mu$ m in J, 1.5  $\mu$ m in I, K-M.

**Fig. 3.** Schematic representation of germ layer differentiation and fate at the posterior pole of the mammalian embryo from late blastocyst stage (A), through gastrulation and neurulation (B and C) until early organogenesis. The stages shown in B and C were investigated in this study; A and D are shown to illustrate the topography of the origin and the fate of the germ layers involved. To avoid confusion, the thickness of germ layers is not drawn to scale.

## References

- Blum M et al. (2007) Ciliation and gene expression distinguish between node and posterior notochord in the mammalian embryo. **Differentiation 75: 133–146.**
- Burtscher I and Lickert H (2009) Foxa2 regulates polarity and epithelialization in the endoderm germ layer of the mouse embryo. **Development 136: 1029-38.**
- Charrier J et al. (1999) Defining subregions of Hensen's node essential for caudalward movement, midline development and cell survival. **Development 126: 4771-4783.**
- Collombat P et al. (2009) The ectopic expression of Pax4 in the mouse pancreas converts progenitor cells into alpha and subsequently beta cells. **Cell 138: 449-62.**
- Downs KM and Bertler C (2000) Growth in the pre-fusion murine allantois. **Anat Embryol (Berl) 202: 323-31.**
- Downs KM et al. (2009) The Allantoic Core Domain: new insights into development of the murine allantois and its relation to the primitive streak. **Dev Dyn 238: 532-53.**
- Favre A et al. (1999) Anorectal malformations associated with enteric dysganglionosis in Danforth's short tail (Sd) mice. **J Pediatr Surg 34: 1818-21.**
- Florian J (1933) The early development of man, with special reference to the development of the mesoderm and the cloacal membrane. **J Anat 67: 263-276.**
- Franklin V et al. (2008) Regionalisation of the endoderm progenitors and morphogenesis of the gut portals of the mouse embryo. **Mech Dev 125: 587-600**
- Gardner RL and Rossant J (1979) Investigation of the fate of 4.5 day post-coitum mouse inner cell mass cells by blastocyst injection. **J Embryol Exp Morphol 52: 141-152.**
- Gofflot F et al. (1997) Genetic patterning of the developing mouse tail at the time of posterior neuropore closure. **Dev Dyn 210: 431-45.**
- Hamburger V and Hamilton HL (1992) A series of normal stages in the development of the chick embryo. **Dev Dynam 195: 231-272.**

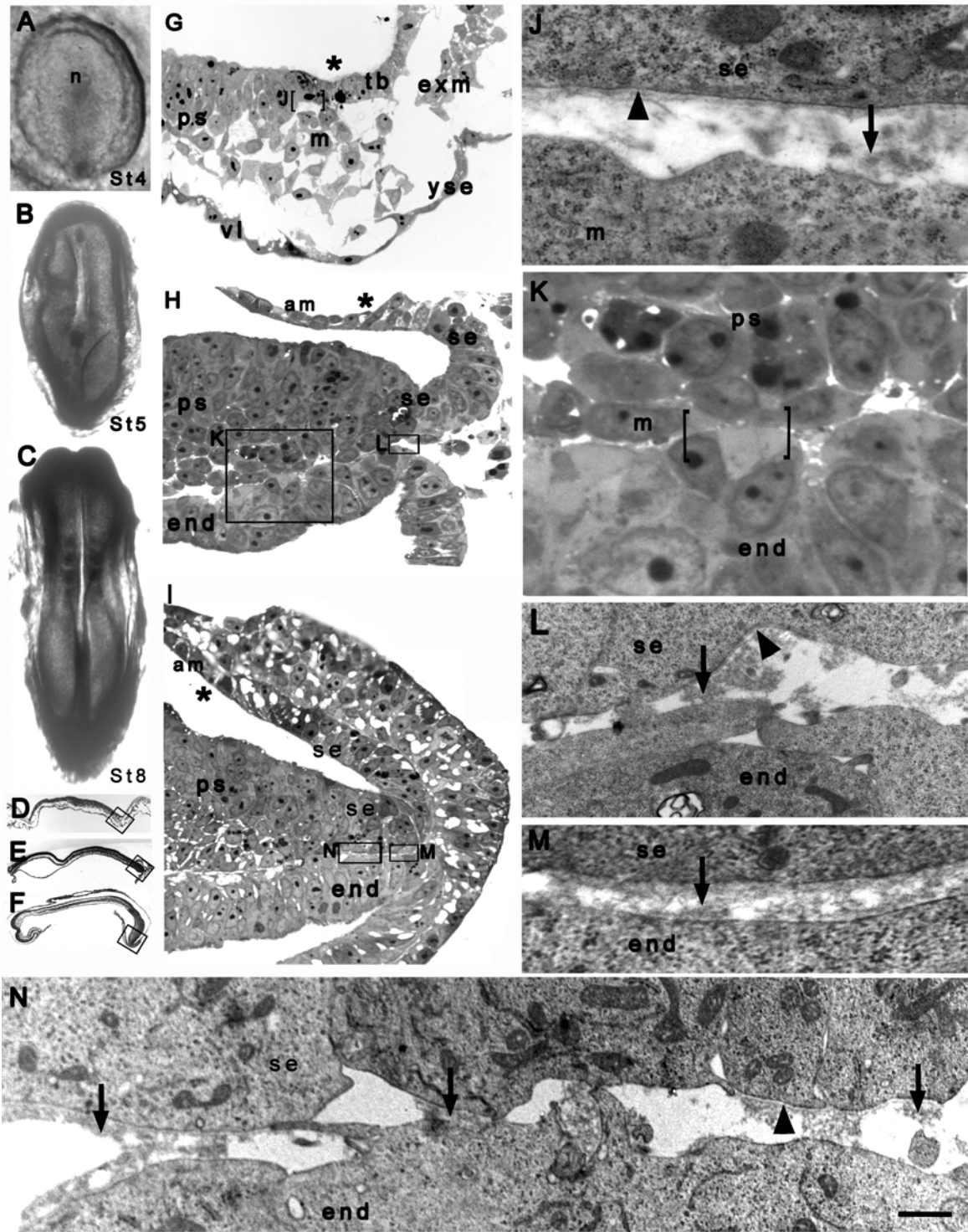
- Hassoun R et al. (2009) Sox17 expression patterns during gastrulation and early neurulation in the rabbit suggest two sources of endoderm formation. **Cells Tissues Organs (in press)**.
- Heuser CH and Streeter GL (1941) Development of the macaque embryo. **Contrib Embryol Carnegie Instn 29: 15-55**.
- Holland PWH et al. (1995) Conservation of *brachyury(t)* genes in amphioxus and vertebrates: developmental and evolutionary implications. **Development 121: 4283-4291**.
- Joubin K and Stern CD (1999) Molecular interactions continuously define the organizer during the cell movements of gastrulation. **Cell 98: 559-571**.
- Kanai-Azuma M et al. (2002) Depletion of definitive gut endoderm in Sox17-null mutant mice. **Development 129: 2367-79**.
- Kaufman MH (1992) The atlas of mouse development. **Acad Press, London**.
- Kinder SJ et al. (2001) The organizer of the mouse gastrula is composed of a dynamic population of progenitor cells for the axial mesoderm. **Development 128: 3623-3634**.
- Kirby ML et al. (2003) Hensen's node gives rise to the ventral midline of the foregut: implications for organizing head and heart development. **Dev Biol 253: 175-88**.
- Kluth D and Lambrecht W (1997) Current concepts in the embryology of anorectal malformations. **Semin Pediatr Surg 6: 180-6**.
- Knezevic V et al. (1998) Continuing organizer function during chick tail development. **Development 125: 1791-1801**.
- Kwon GS et al. (2008) The endoderm of the mouse embryo arises by dynamic widespread intercalation of embryonic and extraembryonic lineages. **Dev Cell 15: 509-20**.
- Lewis SL and Tam PP (2006) Definitive endoderm of the mouse embryo: Formation, cell fates, and morphogenetic function. **Dev Dyn 235: 2315-2329**.
- Luckett WP (1978) Origin and differentiation of the yolk sac and extraembryonic mesoderm in presomite human and Rhesus monkey embryos. **Am J Anat 152: 59-98**.



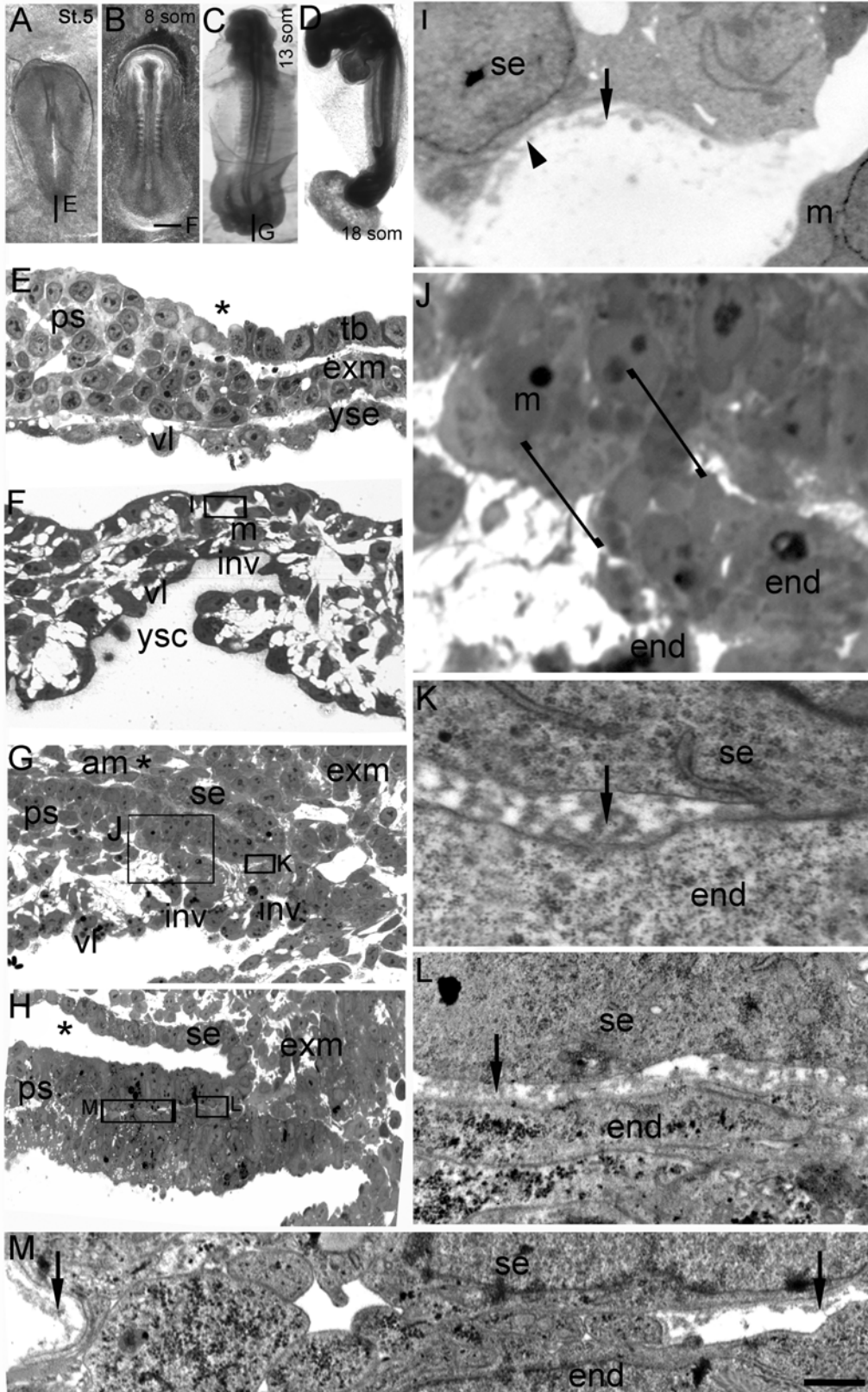
- Männer J and Kluth D (2003) A chicken model to study the embryology of cloacal exstrophy. **J Pediatr Surg 38: 678-81.**
- Männer J and Kluth D (2005) The morphogenesis of the exstrophy-epispadias complex: a new concept based on observations made in early embryonic cases of cloacal exstrophy. **Anat Embryol (Berl) 210: 51-7.**
- Mo R et al. (2001) Anorectal malformations caused by defects in sonic hedgehog signaling. **Am J Pathol 159: 765-74.**
- Müller F and O'Rahilly R (2003) The prechordal plate, the rostral end of the notochord and nearby median features in staged human embryos. **Cells Tissues Organs 173: 1-20.**
- Müller F and O'Rahilly R (2004) The primitive streak, the caudal eminence and related structures in staged human embryos. **Cells Tissues Organs 177: 2-20.**
- Murry CE and Keller G (2008) Differentiation of embryonic stem cells to clinically relevant populations: lessons from embryonic development. **Cell 132: 661-80.**
- O'Rahilly R and Müller F (1987) Developmental stages in human embryos. **Carnegie Inst Washington Publication 637.**
- Papapetrou C DF, Reardon W, Winter R, Spitz L, Edwards YH, (1999) A genetic study of the human T gene and its exclusion as a major candidate gene for sacral agenesis with anorectal atresia. **J Med Genet 36: 208-13.**
- Pohlman AG (1911) The development of the cloaca in human embryos. **Am J Anat 12:1-26.**
- Rabl C (1915) Edouard van Beneden und der gegenwärtige Stand der wichtigsten von ihm behandelten Probleme. **Arch Mikr Anat 88: 3-470.**
- Schwartz P et al. (1984) Ultrastructure of cultured adult myocardial cells during anoxia and reoxygenation. **Am J Pathol 115: 349-361.**
- Seessel A (1877) Zur Entwicklungsgeschichte des Vorderdarms. **Arch Anat Phys Anat Abt p449-467.**

- Spemann H and Mangold H (1924) Über Induktion von Embryonalanlagen durch Implantation artfremder Organisatoren. **Arch Mikr Anat Entwicklungsmech 100: 599-638.**
- Streeter GL (1927) Development of the mesoblast and notochord in pig embryos. **Carnegie Instn Wash Publ 380, Contrib Embryol 19: 73-92.**
- Tam PP et al. (2007) Sequential allocation and global pattern of movement of the definitive endoderm in the mouse embryo during gastrulation. **Development 134: 251-60**
- Van der Putte SC and Neeteson FA (1984) The pathogenesis of hereditary congenital malformations of the anorectum in the pig. **Acta Morphol Neerl Scand 22: 17-40.**
- Waddington CH and Schmidt GA (1933) Induction by heteroplastic grafts of the primitive streak in birds. **Wilhelm Roux Arch Entwicklungsmech Org 128: 522-563.**
- Waterman RE (1977) Ultrastructure of oral (buccopharyngeal) membrane formation and rupture in the hamster embryo. **Dev Biol 58: 219-229.**
- Waterman RE BG (1980) Indirect immunofluorescent staining of fibronectin associated with the floor of the foregut during formation and rupture of the oral membrane in the chick embryo. **Anat Rec 198: 619-635.**
- Waterman RE and Schoenwolf GC (1980) The ultrastructure of oral (buccopharyngeal) membrane formation and rupture in the chick embryo. **Anat Rec 197: 441-70.**
- Wilson V and Beddington RSP (1997) Expression of T protein in the primitive streak is necessary and sufficient for posterior mesoderm movement and somite differentiation. **Dev Biol 192: 45-58.**
- Wyburn GM (1937) The development of the infra-umbilical portion of the abdominal wall, with remarks on the aetiology of ectopic vesicae. **J Anat 71:201-231.**
- Zaret KS and Grompe M (2008) Generation and regeneration of cells of the liver and pancreas. **Science 322: 1490-4.**

Hassoun et al., Fig. 1



Hassoun et al., Fig. 2



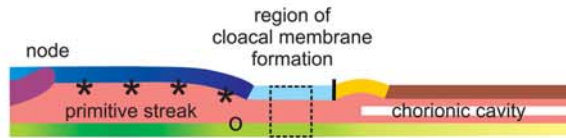
**Hassoun et al., Fig. 3**

Germ layer differentiation at the posterior pole of the mammalian embryo

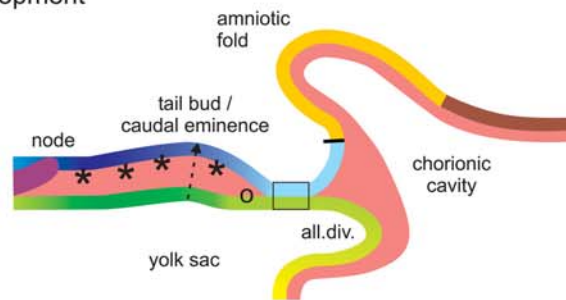
A late blastocyst



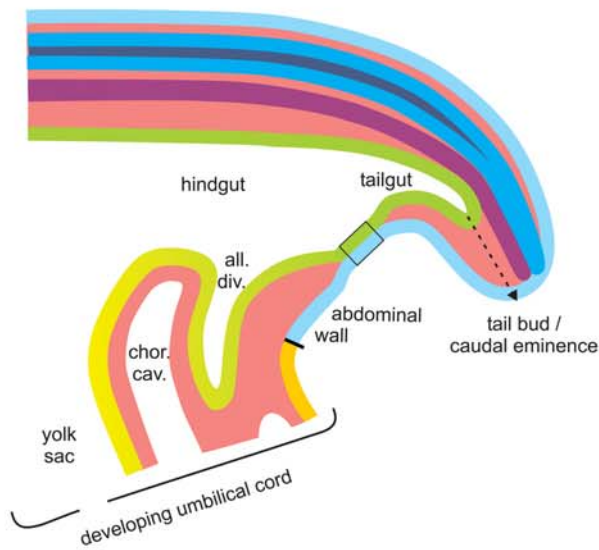
B gastrulation / neurulation













C secondary development



D organogenesis



**Legend:**

- |   |   |                                     |
|---|---|-------------------------------------|
|  epiblast                |  mesoderm          | embryonic-extraembryonic border     |
|  hypoblast               |  endoderm          | * epithelial-mesenchymal transition |
|  trophoblast             |  amnion epithelium | O mesoderm-endoderm contact area    |
|  extraembryonic endoderm |  neuroectoderm     | □ cloacal membrane                  |
|  surface ectoderm        |  notochord         |                                     |

## **7. Acknowledgements**

A journey is easier when you travel together. Interdependence is certainly more valuable than independence. This work has been accompanied and supported by many people and it is a pleasant aspect that I have now the opportunity to express my gratitude to all of them

First, my deepest gratitude is to my supervisor, Prof. Dr. Christoph Viebahn. I have been amazingly fortunate to have an advisor who gave me the guidance and provided a motivating enthusiastic and critical atmosphere during the many discussions we had. Herr Viebahn taught me how to question thoughts and express ideas. His wisdom, patience and support helped me to finish this dissertation. I am also thankful to him for encouraging the use of correct grammar and consistent notation in my writings and for carefully reading and commenting on countless revisions of this work. Herr Viebahn has been always there to listen and give advice. I hope that one day I would become as good an advisor to my students as Herr Viebahn has been to me

Many other people have helped me during this work. I would like to express my heart-felt gratitude to the members of our group in the department of anatomy and embryology of Georg-August University in Goettingen, Dr. Peter Schwartz, Dr. Bernd Püschel, Kirsten Falk-Stietenroth, Heike Faust, Irmgard Weiß and Hannes Sydow for their continuous support especially in the lab-related work. I am also thankful to the secretary Heike Altmann who helped me to overcome many crisis situations and made the life in the institute a lot more enjoyable.

## **8. Curriculum Vitae**

### **Contact information**

Name: Romia Hassoun  
Address: Center of anatomy  
Department of Anatomy and Embryology  
Kreuzbergring 36, 37075 Göttingen  
Country: Germany  
Telephone: 05512760027  
Cell Phone: 017664622325  
Email: diamant29@hotmail.de

### **Personal information**

Romia Hassoun was born on June, 01, 1975 in Latakia, Syria.  
I am female and have a Syrian citizenship. I married and have two children.

### **Education and employment history**

I did at 1993 the final secondary school examination in Latakia/Syria. Then I studied for 6 years (1993 – 1999) human medicine in the Tishreen University in Syria and at 1999 I did the medical graduate examination.

Thereafter (between 1999 and 2002), I followed postgraduate training in the paediatric department in an academic clinical centre in Syria

In Mai/ 2002: I got a scholarship from Syrian government to make doctoral project in Germany. Since 2009 I am working on the embryological researches in the department of anatomy and embryology of Georg August University in Goettingen. Germany

### **Publications**

Hassoun R, Schwartz P, Feistel K, Blum M, Viebahn C (2009a): Axial differentiation and early gastrulation stages of the pig embryo. Differentiation. In press

Hassoun R, Püschel P, Viebahn C (2009b): Sox17 expression patterns during gastrulation and early neurulation in the rabbit suggest two sources of endoderm formation. Cells Tissues Organs. In press